Chemical Reactors in Porous Media

Pablo Castañeda Rivera
castaneda@impa.br

Advisor: Dan Marchesin
Co-advisor: Johannes Bruining

Prefácio e agradecimentos

*A*ntes de qualquer agradecimento ou apresentação, gostaria de me desculpar por usar a língua inglesa neste trabalho em vez do harmonioso português. Neste país, Brasil, fui bem recebido e fico grato pelo tempo que temos compartilhado juntos. Gostaria de homenageá-lo com uma dissertação no seu idioma oriundo, porém não o domino e a vantagem que guarda o inglês por sua difusão é desta vez, para mim importante.

Este trabalho é o fechamento de um ciclo, espero porém que seja também o ínicio de tantos outros. No entanto, acharia prudente dar uma retrospectiva desse ciclo inicial, que como qualquer outro teve tanto seus lampejos e brilhos quanto quase sua própria extinção.

Cheguei ao IMPA seis anos atrás farejando a geometria que Do Carmo exala até o *outro lado da dobra do mapa*, lá no México. Porém, pensava ficar pouco tempo e quis aprender um pouco de matemática computacional, assim conheci a Dan e pouco soube de Mafredo.

Dan atua no campo das matemáticas que contém o meu fascínio, a matemática aplicada, onde não só a intuição geométrica guia nossos sentidos mas também é munida da experiência do que acreditamos que se passa no mundo. É aqui onde nossa imaginação é menos mirabolante e contudo os resultados são carregados pelas nossas mirações.

Esta tese abrange um pouco disto tudo... minhas viagens por territórios para mim desconhecidos e o conhecimento e experiência de Dan que não permitiu que eu ficasse divagando. Não é só por isso que eu fico grato Dan, senão também pela paciência que você teve nas lidas e revisões e com elas tantas sugestões, assim como as inúmeras contribuições suas neste trabalho. Obrigado também por ser um grande amigo.

O trabalho desenvolvido decorre de um problema estruturado por Hans, que me ajudou muito na compreensão das raízes físicas e químicas do estudo contido aqui. Sempre será um prazer poder trabalhar ao seu lado e, mesmo que tendo análises na matemática abstrata, as discussões e conversas serão, como de costume ricas em conhecimentos e divertimentos, obrigado também por se fazer presente.

Permitam-me agradecer antes de mais nada à completa banca que revisou este trabalho, e seus comentários dos quais surgiram grandes melhoras no texto escrito. Obrigado André e Sarkis pela ajuda em momentos difíceis, pelas excelentes aulas e a paciência na leitura do primeiro manuscrito. Agradeço a Zubelli pelas aulas de EDOs, pela confiança no exame e pelas sugestões para melhorar este trabalho. Fred, muito obrigado pelo apoio ao longo deste último período e os comentários sempre estimulantes. Cido, muito obrigado mesmo pela leitura detalhada e as grandes sugestões. E a Wanderson meus mais respeitosos agradecimentos, não só pela leitura minuciosa, senão por ser às vezes um segundo orientador e quase uma guia no mundo da matemática.

Antes de mais delongas, gostaria de voltar minha atenção ao México e agradecer à minha *alma matter*, a UNAM e aos professores que aí trabalham, em especial à gente do Departamento de Matemáticas (Julieta, Oscar e Luis) e aos pesquisadores do IIMAS (Pablo, Clara, Arturo Olvera e Vargas, Tim e Gilberto), que me formaram em primeira instância e que de alguma forma me levaram a conhecer o IMPA. E sempre antes de tudo a Martín Cañas que no segundo grau me deu a primeira dica sobre o mundo das matemáticas.

Mas, "cadê a curta temporada no IMPA?" Bom, não era tão curta assim, mas era para ser de dois anos só. Dois anos no Brasil é tempo demais para conhecer um mundo, ou vários, cada um mais charmoso do que o outro. O mundo mesmo do IMPA deixou-me cativo!

Aqui conheci um paraíso utópico (ou talvez tropical) da matemática, onde alunos e pesquisadores são colegas, onde cada um tem uma voz, onde as perguntas, e as conversas "fiadas" têm como resultado uma colaboração contínua. Muito obrigado a todos:

Aos alunos por compartilharem comigo as aulas e os estudos, por serem parte deste contínuo aprendizado e mesmo assim conseguindo tempos vagos para curtir esta cidade!

A todos os professores do IMPA, pelo que ensinam fora e dentro de aula, fazendo desta instituição um excelente lugar para as matemáticas. Obrigado Enrique por nos mostrar como *Sacarle el Diablo*.

Aos funcionários e a galera por estarem aí sorridentes sempre e conversar conosco deixando-nos voltar à realidade, puxando-nos as orelhas quando estamos perdendo os prazos, mas especialmente por mostrar-nos o verdadeiro estilo brasileiro.

Dos amigos gostaria de agradecer em especial a Juan, Dalia, Pancho e Pedro por serem parte deste ciclo, cada um com suas peculiaridades e ajudas, de conversas de resultados nos campos de cada um e da pareceria que sempre foi proporcionada.

O Dan teve a idéia de criar um seminário para seus alunos, com o fim de discutir e comentar os avanços (ou não) de cada um. Este espaço foi primordial no trabalho de muitos e quero agradecer a todos pela constante participação. Mais que um especial reconhecimento seria merecido para o *Mestre dos Magos*, JD, por apontar o ponto de quebra; Julio por toda a ajuda com aquele refinamento nos argumentos eu serei eternamente grato.

Não poderia esquecer nunca a Gustavo Hime pela ajuda, as conversas e a paciência que ele teve no início desta tese nas correções do inglês, muito obrigado. O *Guerrillero* Sérgio também sempre esteve em "pé de luta" para ajudar e passar tempos bons, valeu!

Muita gente passou e compartilhou o tempo e falta de tempo comigo. Espero que todos se sintam inclusos nestes agradecimentos: Jimmy, Freddy, Cristián, Damián, Vanessa, Crica, Pablote, Guarino, ...

Eu disse vários mundos. Mesmo o IMPA estando na floresta, nas montanhas, tem um concorrente, Santa Teresa, a vila que mora do lado da *Cidade*. Quando cheguei ao Rio, o segundo ponto de referência foi aqui em *Santeré* onde aprendi a viver em paz e longe do tumulto da metrópole.

Aqui achei uma nova família que me fez sentir em casa. Obrigado pelo tempo que me concederam como parte de vocês. Nem falta dizer a Fernando, Carmen, Luiz, Denise, Jorge, Naoko, Hiro, Sandrinha, Valentina, Fernanda, Stefano, Silvia, Pipoca, Christiane ... o quanto estou feliz em tê-los encontrado!

Ao espaço do *Castelinho38* e ao pessoal que ali trabalha quero dizer também muito obrigado pelo período que me proporcionaram para trabalhar nos últimos resultados deste trabalho, a harmonia e a tranqüilidade de lá deram um toque especial às idéias.

Mmhm, mundos diversos e famílias múltiplas. Celso José, Lucas e todo o pessoal da *Escola Nacional de Circo* merecem não só o reconhecimento do trabalho deles, senão minha maior alegria de ter participado da animação que imprimem na vida.

Com a minha família sempre estarei grato por tudo o que eles representam em qualquer dos meus mundos, por serem eles quem me alentam cada vez que preciso ajuda e me fazem ser quem sou nas ocasiões que devo me pôr em pé, é a todos vocês desde a *Legión extranjera del norte* até cada um dos *chapines*, como aqueles foragidos que deixaram o eixo Guatemala-México-Estados Unidos, a quem agradeço por me darem a felicidade de todos os anos e a intuição de cada instante.

Meus pais e meus irmãos sabem que sempre serão parte importante de mim, que formam o elo onde todas as melhores realidades se fundem, meu tio Sergio sabe também o seu lugar no meu desenvolvimento, mas acredito que *La Carmela* merece um especial reconhecimento, pois suas palavras quando criança "Cualquier cosas que imgainés alguien más ya lo habrá pensado" curiosamente me inspiraram procurando no quê minha imaginação poderia dar um diferencial naquilo tudo que pensamos no coletivo. Espero que isso seja refletido nas abordagens pouco tradicionais ao longo deste trabalho.

Assim, só espero que esta tese lhes seja interessante. Provavelmente está carregada de análise e aguardo que seja a primeira parcela da minha sina nesta área; toda queda que já tive na minha vida matemática esteve ligada à análise. De fato, a penúltima vez me deixou fora do IMPA e pensei em voltar ao México...

Todavia tive alguém que confiou, ela me ajudou a lutar para voltar, e sendo assim, a luta continuou para conseguir fazer um doutorado aqui e ganhar outros quatro anos neste país, a teu lado Chris, que sem você esta tese não seria escrita. Todo meu amor está aqui e este trabalho é dedicado a você.

Finalmente, quero agradecer ao CNPq e a CAPES pelo apoio financieiro ao longo do doutorado atravez da bolsa da PEC-PG.

Pablo Castañeda Rivera
8 de Janeiro de 2010
Rio de Janeiro, Brasil

RESUMO. Estamos interassados em reações químicas exotérmicas que ocorrem no ar em uma pequena região de um meio poroso sólido condutor. O ar é injetado no centro da esfera. O calor é gerado perto do centro e conduzido através da parede da esfera. O objetivo é determinar quando haverá ignição ou extinção, dependendo do equilíbrio entre reação e condução. Simplificamos a descrição matemática do sistema, imaginando que a reação ocorre somente na região próxima ao centro da esfera com temperatura uniforme, enquanto que a condução do calor ocorre no resto da esfera, uma casca esférica. O sistema de equações de reação-difusão reduz-se à equação do calor na casca, acoplada na fronteira interior com uma equação diferencial ordinária para a região de reação. Esta EDO pode ser considerada como uma condição de contorno não-linear para a equação do calor na casca.

Esta simplificação permite uma análise completa para a evolução temporal do sistema. Mostramos que, dependendo dos parâmetros físicos, o sistema admite um ou três equilíbrios. Este último caso tem importança física: dois dos equilíbrios representam atratores ("extinção" ou "ignição") com bacias de atração separadas pela variedade estável da terceira singularidade. Utilizamos teoria de operadores para a análise da estabilidade linear e teoria de ponto fixo em uma equação de Volterra não-linear para provar a existência e unicidade de soluções para todos os tempos. Aplicamos uma decomposição espectral para descrever a evolução por meio de um sistema infinito de equações diferenciais ordinárias acopladas, provando a regularidade de soluções para dados de Cauchy gerais, assim como o comportamento assintótico para tempos grandes.

Uma conclusão prática de interesse é que para esferas de dimensões maiores as chances de extinção são maiores. Outra conclusão é que o sistema completo é muito bem aproximado por uma única EDO, a qual provém de um tipo de modelo "reduzido" para o reator.

PALAVRAS CHAVE. Reator químico, meios porosos, perdas de calor, combustão *in-situ*, condição de contorno não-linear, sistema infinito de EDOs.

ABSTRACT. We are interested in an exothermic chemical reaction occurring in air within a small region of a conductive spherical solid porous medium. The air is injected at the center of the sphere. Heat is generated near the center, and conducted to the wall of the sphere. The issue is to determine if there is ignition or extinction, depending on the predominance of reaction or conduction. We simplify the mathematical description of the system by imagining that the reaction occurs only in a region with uniform temperature located around the center of the sphere, while conduction occurs in the rest of the sphere, a surrounding shell. The system of reaction-diffusion equations reduces to a linear heat equation in the shell, coupled at the internal boundary to a nonlinear ordinary differential equation in the reaction region. This ODE can be regarded as a (nonlinear) boundary condition for the heat equation in the shell.

This simplification allows making a complete analysis of the time evolution of the system. We show that, depending on physical parameters, the system admits one or three equilibria. The latter case has physical interest: the two equilibria represent attractors ("extinction" or "ignition") with basins of attraction separated by the stable manifold for the third equilibrium. We utilize operator theory for the linear stability analysis, as well as fixed point theory of a nonlinear Volterra equation for the existence and uniqueness of solutions for all times. We also use a spectral decomposition to describe the evolution by means of an infinite number of coupled nonlinear ordinary differential equations, providing regularity of the solutions for general Cauchy data, as well as the nonlinear asymptotic behavior for long times.

One interesting practical conclusion is that higher dimensionality of the sphere increases the probability of extinction. Another interesting conclusion is that the whole system is quite well described by a single ODE, which is a kind of "reduced" model for the reactor.

KEYWORDS. Chemical reactor, porous media, heat losses, *in-situ* combustion, nonlinear boundary value problem, infinite ODE system.

Contents

Introduction

If oxygen is in intimate contact with fuel Arrhenius law says that reaction will occur, even at low temperatures. However, in a porous medium heat losses can equalize the small reaction heat generated, so that the system remains trapped in a very slow reaction mode. Such a mode is indistinguishable from extinction. On the other hand, if heat losses initially remain smaller than the heat generated by the reaction, temperature increases and spontaneous ignition occurs. Heat losses are strongly dependent on the geometry of the heat dissipating region. Therefore we distinguish three idealized geometries, *viz.* linear, cylindrical and spherical. We analyze a basic heat diffusion equation model, which incorporates an Arrhenius heat generation term.

Our goal is to establish under which conditions either the heat losses or the heat reaction govern the global behavior in a chemical reactor. The reactor is idealized as a sphere or an infinitely long cylinder, with a surrounding heat dissipating region. It will be useful to study first an idealized situation where the reactor is planar and bounded between two infinite planes, one thermally isolated and the other one in thermal contact with a heat conducting medium.

The first attempts to solve the problem of "extinction" or "combustion" in porous media are contained in the article [6], where earlier references can be found such as the pioneering work of Tadema and Weijdema, see [35].

We idealize the reactor by assuming that it is in a time dependent spatially homogeneous state in the reaction region. For the conductive region we assume that it is in a time dependent state with symmetry induced by the geometry considered. It is assumed that in the reaction region we can control the amounts of fuel and oxygen so as to keep them constant. This is the case when we inject fresh reactants at a fixed rate in the porous reactor and expel the combustion products. Thus, we study only the dependence of the reaction rate on the temperature.

Chemical engineers assume that this setup can only lead to extinction or ignition. We prove that this is indeed true for most practical cases. Depending on physical parameters, the system admits one or three equilibria. The latter case has physical interest: the two equilibria represent attractors ("extinction" or "ignition") with basins of attraction separated by the stable manifold for the third equilibrium.

We find out that the nature of the solutions for the reactor problem with heat losses is determined in each geometry by two parameters, namely, the temperature of the external boundary and the Damköhler number that relates the physico-chemical magnitudes.

The mathematical analysis of the system is greatly simplified by the assumption that the reaction occurs only in a region with uniform temperature located around the injection area, while conduction occurs in the surrounding region. The system of reaction-diffusion equations reduces to a linear heat equation in the shell with boundary condition governed by a nonlinear ordinary differential equation.

Such boundary conditions are treated by Goldstein *et al.* in [11] and [17], and by Vitillaro in [38]. Nonetheless, both groups are interested in regularity, existence and uniqueness. We only consider a specific boundary condition; therefore, we are able to determine the global behavior of the solution.

One interesting practical conclusion is that higher dimensionality of the domain increases the probability of extinction. Another interesting conclusion is that the whole system is quite well approximated by a single ODE provided by a *reduced model* for the reactor, which possesses kind of "quasi-steady state solution".

In classical reaction-diffusion systems the idea of quasi-steady state solutions is well known. If it is assumed that the diffusion term acts in a slower fashion than the reaction term then a simplified system can be analyzed. However, this simplification does not always lead to nice approximations of the whole reaction-diffusion equation, see [12]. It is inappropriate for our case.

Quite contrary, we take advantage that the reaction governs one region while the diffusion governs in the other region. Then, the growth of the exothermic reaction is bounded by the heat flux at the interfase, so essentially every solution converges to one of the two stable equilibria. This is the core of the reduced model.

Reaction-diffusion equations have been studied for a long time. Applications include chemical reactions, physics, biology. Problems related to combustion can be attacked naturally as reaction-diffusion systems, as it has been done by Matkowsky *et al.*, see for example [26] and [28]. However, the complexity of the equations restricts the results; and a complete description of the solution is not easy to obtain. For the study of reaction-diffusion systems, we recommend the classical book of Smoller (1994) and the celebrated essay from Fife (1979), which has biological applications.

We explain briefly how this work is organized. In Chapter 1 we construct the physical model that can be used for different reaction heats, reactor geometries and sizes. We nondimensionalize the equations, giving rise to the Damköhler number γ, which includes most of the chemical phenomena, as pointed out to us by J. Bruining.

In Chapter 2 we identify the stationary solutions of the problem. Here we give the first glimpse of a very simple model, called the reduced model, which provides a simplified picture of the behavior of the full nonlinear system.

In Chapter 3 we ensure that there exist three equilibria; linear analysis shows that two of them behave as attractors. The third one behaves as a repeller that separates the attracting basins of the two stable equilibria, verifying the Chemical Engineering picture. Appendix A contains the technical part for Chapter 3, namely, the explicit solutions of the linearized model around each one of the equilibria.

In Chapter 4 we prove the existence, uniqueness and regularity for all times of solutions of the nonlinear Cauchy problem for the reactor. As Appendix B contains technical material for Chapter 4, we recommend to skip it initially. Nevertheless, the last section consists of a brief self-contained summary of the whole Appendix B.

In Chapter 5 we rewrite the complete problem as a system with an infinite number of ODE's. This system provides a complete and intuitive picture of the global dynamics, which agrees with the simplified picture obtained earlier; the repeller is actually analogous to a saddle, with a stable manifold separating the attracting basins of the two attractors. Our proofs, however, require technical restrictions on the initial data.

Finally, in Chapter 6 we present conclusions and mention applications to physical reality.

We close this work with six appendices containing material that can be skipped in a first reading. In Appendix A we obtain bases of eigenvectors for the linearized models near the equilibria. Appendix C contains the Bessel function theory used to handle the cylindrical case studied in Appendices A and B. Appendix D explains why the boundary conditions chosen are the interesting ones. In Appendix E we describe the numerical methods used for our simulations. In our problem, simulations were fundamental to gain intuition. In Appendix F, we present the physico-chemical background, and we show how to estimate the Damköhler number γ.

Chapter 1

The reactor model for heat flow

This chapter describes the class of models to be solved. First we construct the physical model. Then, we reduce the complexity of the model equation by taking advantage of geometrical symmetries. Finally, we nondimensionalize the equations for $\mathcal{N}$ spatial dimensions.

1.1 Physical model: equation for conservation of energy

We derive a set of equations that describe the conservation of energy in a medium where heat generation and thermal flow occurs. Fick's law describes the transport of energy by conduction, and Arrhenius' law describes the rate of energy generated by the exothermic reaction between oxygen and the fuel.

Then the rate of change of the heat energy in each domain is equal to the reaction rate, which is governed by Arrhenius' law inside the domain, plus Fick's law that governs the heat flow at the boundary of the domain. For a general domain Ω we have:

$$\frac{d}{dt}\int_\Omega Q dV \;=\; \int_\Omega \Delta H\, c_o\, c_c\, A \exp\left(-\frac{E}{RT}\right) dV + \int_{\partial\Omega} \kappa\, \nabla T \cdot \hat{n}\, dS, \tag{1.1}$$

where $Q = Q(\mathbf{x}, t)$ is the thermal energy density and $T = T(\mathbf{x}, t)$ the temperature distribution in Kelvin (here $\mathbf{x}$ means position in $\mathbb{R}^{\mathcal{N}}$ with $\mathcal{N} = 1, 2, 3$, dV and dS the respective elements of volume and area with $\hat{n}$ the normal vector to the surface $\partial\Omega$), the constant ΔH denotes the reaction enthalpy per unit mass of oxygen consumed, c_o and c_c are the concentrations of the reacting oxygen and fuel, A is the pre-exponential factor, E is the activation energy of the reaction, R is the universal constant of ideal gases and κ is the homogeneous thermal conductivity in the porous medium. The Table 1 in Appendix F contains notations, definitions and typical physical values for these and other quantities.

Given that the focus of the study is to evaluate the three geometric domains (namely linear, cylindrical and spherical), the general case is formulated irrespectively of dimension. Radial symmetry is of primary importance; therefore, the entire domain will be studied as the $\mathcal{N}$-dimensional solid sphere $B_L := B[0; L]$, centered on the origin with radius L. The domain B_L is further divided in two parts. Part 1 is the internal subdomain, namely the $\mathcal{N}$-dimensional solid sphere $B_a := B[0; a]$ representing the subregion where the reaction occurs. Typically B_a will be a 3D solid sphere, a cylindrical column or a top

layer. Part two is the external subregion, namely an interval, a ring or the generic $\mathcal{N}$-dimensional solid shell $S := B_L \backslash B_a$ (open at $r = a$ and closed at $r = L$), which represents the subregion where no reaction occurs but the heat is dissipated.

The region of interest must be described prior to defining the boundary and initial conditions for (1.1). The reactor is shown schematically in Fig. 1.1, and consists of a solid porous medium, both in the reaction region B_a and the conduction region S. We consider two scenarios for our reactor: the petroleum reservoir and the catalytic heater.

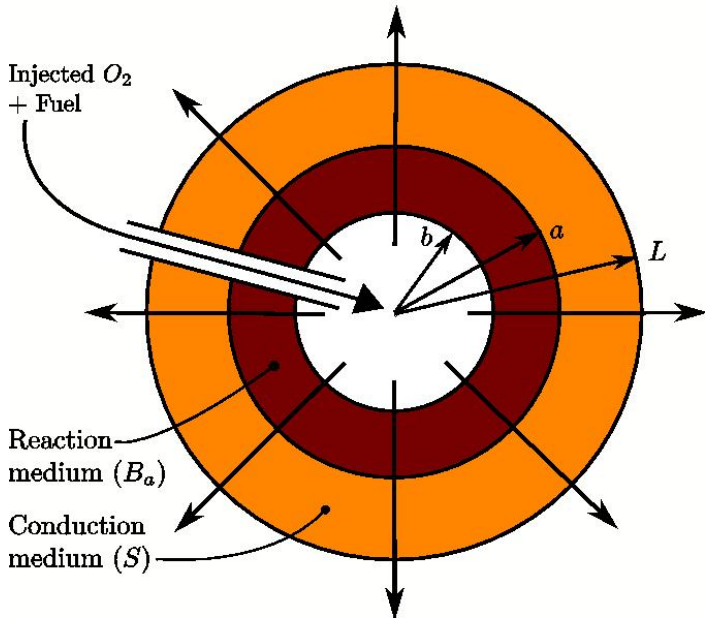

Figure 1.1: Schematic reactor. The temperature outside the ball B_L is fixed. The arrows represent the direction in which the injected gas moves.

The model discussed as part of this work was originally conceived as an oil reservoir, however, the application of our model is illustrated better in the catalytic heater, which we will describe later in this report.

The petroleum reservoir. Air injection into the reservoir is accomplished through a bore hole (drill hole or well); air (oxygen) injected into the well will initially displaces in all directions, generating an expanding sphere centered at the injection point. The injected air will be forced upward by buoyancy forces, thereby changing its geometry into a cylinder around the well, ultimately spreading into a horizontal layer neat the cap rock. Each of the three transient conditions described above will have a corresponding idealized domain.

The well is shown on Fig. 1.1 by the inner region of radius b, which is assumed to be small as compared to the radii a and L. However a is also small as compared with L, this ratio is fundamental for the analysis. The reaction occurs as a result of the injected air in the presence of coke contained within the porous medium. The coke results from previous chemical processes and typically it is a solid chain of carbons trapped in the porous medium. We assume that concentrations of coke and oxygen are kept constant because it is expected that an ignition in the reaction occurs very fast, so these concentrations are important as initial data. (This assumption is invalid for long times in an oil reservoir.)

The catalytic heater. We assume that a fixed proportion mixture of air or O_2 and gaseous hydrocarbon (the "fuel") is injected at a constant rate. We assume that the gas reacts with oxygen only in the presence of a catalytic converter (located only within the porous medium B_a), so that no reaction occurs either in the injection region or in the conduction region. The arrows leaving the reactor in Fig. 1.1 show the direction in which the residual gases are expelled. In this scenario, all radii a, b and L are comparable. However, since b can be accounted for through small modifications of the equations coefficients (and the conclusions are similar), we use the assumption $b = 0$ to simplify the formulae.

Therefore, for the analysis of this work we consider the scenario of the catalytic heater. However, we have to keep in mind that under certain restrictions our conclusions are still valid for the petroleum reservoir.

In the next subsections we construct the physical equations for the reaction region B_a and the conduction region S assuming radial symmetry in the entire domain B_L.

1.1.1 Balance of energy in the internal region

We explain our motivation for taking a homogeneous temperature in the internal region. Recall that we have assumed that there is radial symmetry in the whole domain.

We will also assume that in the interior region B_a the thermal conductivity is much larger than the conductivity in the external region S. We will now explain why we assume that the temperature is homogeneous in B_a.

Indeed, notice that if we assume that Q remains finite when $\kappa \to \infty$, then for any domain Ω in B_a

$$\lim_{\kappa\to\infty} \frac{1}{\kappa}\left\{ \int_\Omega \Delta H\, c_o\, c_c\, A \exp\left(-\frac{E}{RT}\right) dV - \frac{d}{dt}\int_\Omega Q\, dV \right\} = 0, \tag{1.2}$$

so, dividing Eq. (1.1) by κ, in a region $\Omega \subset B_a$, and taking the limit as $\kappa \to \infty$, we obtain that

$$\int_{\partial\Omega} \nabla T \cdot \hat{n}\, dS, \tag{1.3}$$

must vanish. But using Gauss formula in (1.3) this is the same as

$$\int_\Omega \Delta T\, dV = 0. \tag{1.4}$$

This holds for all regions Ω inside B_a; therefore the Laplace equation $\Delta T = 0$ holds in B_a pointwise for smooth temperature spatial distributions.

For the 1D case we have that $\partial^2 T/\partial x^2 = 0$, *i.e.*, the temperature profile is

$$T(x,\, t) = \alpha(t)\, x + \beta(t), \qquad x \in [0,\, a],\, t \geq 0, \tag{1.5}$$

where $\alpha(t)$ and $\beta(t)$ vary with time. Because x is a radial variable we have the symmetry condition $T_x(0,\, t) = 0$, which implies that $\alpha(t) \equiv 0$, so that the temperature remains homogeneous in the interval. Therefore the temperature will be determined by continuity on

the right boundary, *i.e.*, $T(x,\,t) = T(a,\,t)$ for all $x \in [0,\,a)$. At any rate, the temperature is homogeneous.

For the $\mathcal{N}$ dimensional cases with $\mathcal{N} \geq 2$, the interior region B_a has the $(\mathcal{N}-1)$-sphere surface as its boundary ∂B_a. For radially symmetric temperature distributions the argument is natural, because

$$\left\{ \begin{array}{rcll} \Delta T & = & 0, & \mathbf{x} \in B_a,\, t \geq 0 \\ T & = & f(t), & \mathbf{x} \in \partial B_a,\, t \geq 0 \end{array} \right. \tag{1.6}$$

for an homogeneous temperature $f(t)$ on the sphere surface, which implies $T(\mathbf{x},\,t) = f(t)$ for all $\mathbf{x} \in B_a$. Therefore, the temperature will be determined by continuity at the boundary, *i.e.*, $T(\mathbf{x},\,t) = T(\mathbf{a},\,t)$ for all $\mathbf{x} \in B_a$ and where $\mathbf{a} \in \partial B_a$. Again, the temperature is homogeneous in B_a.

From now on, we will assume that the temperature is homogeneous in B_a, and that in S it depends only on the distance from the origin. We notice that the volume $V_{\mathcal{N}}$ of B_a and the area $S_{\mathcal{N}}$ of ∂B_a are given by

$$V_{\mathcal{N}} = C_{\mathcal{N}} a^{\mathcal{N}}, \quad S_{\mathcal{N}} = \mathcal{N} C_{\mathcal{N}} a^{\mathcal{N}-1}; \quad \text{where} \quad C_1 = 1,\, C_2 = \pi \text{ and } C_3 = 2\pi/3. \tag{1.7}$$

Notice that we take $\kappa \to \infty$ in the internal region, where $\nabla T \equiv 0$, so the last term in (1.1) gives no information when the Ω domain is strictly inside the region B_a. In order to understand the contribution of this term, we integrate (1.1) on $B[0;\,a+\epsilon]$ and take the limit when $\epsilon \to 0+$; in this way $\nabla T \cdot \hat{n}$ is computed immediately outside of B_a. We get

$$V_{\mathcal{N}} \frac{\partial Q}{\partial t} = V_{\mathcal{N}}\, \Delta H\, c_o\, c_c\, A \exp\left(-\frac{E}{RT} \right) + S_{\mathcal{N}} \kappa \big(\nabla T \cdot \hat{n} \big) \Big|_{\partial B_a +}, \tag{1.8}$$

where ∂B_a+ stands for the "outside" boundary of B_a.

The thermal energy density Q is related to the temperature T by the heat capacity per unit mass $(\rho c)_i$ (the subindex i represents the internal region B_a) through

$$\frac{\partial Q}{\partial t} = \frac{dQ}{dT} \frac{\partial T}{\partial t} = (\rho c)_i \frac{\partial T}{\partial t}. \tag{1.9}$$

and therefore Q is also homogeneous in B_a.

In the domains we study (linear, cylindrical and spherical), we have that at the boundary ∂B_a the normal derivative $\nabla T \cdot \hat{n}$ is equal to the radial derivative $\partial T/\partial r$ always; so using this identity in (1.8), and the relationship (1.9), we get

$$V_{\mathcal{N}}\, (\rho c)_i \frac{\partial T}{\partial t} = V_{\mathcal{N}}\, \Delta H\, c_o\, c_c\, A \exp\left(-\frac{E}{RT} \right) + S_{\mathcal{N}} \kappa \frac{\partial T}{\partial r} \Big|_{\partial B_a +}, \tag{1.10}$$

which is the final form of the equation of conservation of energy in B_a. We will analyze how the thermal flow in the external region with no reaction S affects the reaction in B_a, for each geometry.

1.1.2 Heat transport in the external region

For the external sub-domain S, using the divergence theorem in any subregion Ω of S, we derive analogously to Eq. (1.1):

$$\frac{d}{dt}\int_\Omega Q\,dV \;=\; \int_{\partial\Omega} \kappa\,\nabla T\cdot\hat{n}\,dS \;=\; \int_\Omega \operatorname{div}\left(\kappa\,\nabla T\right) dV. \tag{1.11}$$

This is valid for all sub-domains of S, therefore it is valid locally. With κ constant and the heat capacity per unit mass $(\rho c)_e$ also constant (the subindex e represents the external region S), this leads to

$$(\rho c)_e \frac{\partial T}{\partial t} = \kappa\,\Delta T. \tag{1.12}$$

1.1.3 The reactor model for the complete domain

We summarize Eqs. (1.10) and (1.12) for $T = T(\mathbf{x},\, t)$:

$$\begin{cases} (\rho c)_e \dfrac{\partial T}{\partial t} &= \kappa\,\Delta T & \mathbf{x}\in S,\, t\geq 0 \\[2ex] V_{\mathcal{N}}\,(\rho c)_i \dfrac{\partial T}{\partial t} &= V_{\mathcal{N}}\,\Delta H\,c_o\,c_c\,A\exp\left(-\dfrac{E}{RT}\right) + S_{\mathcal{N}}\kappa \left.\dfrac{\partial T}{\partial r}\right|_{\partial B_a+} & \mathbf{x}\in B_a,\, t\geq 0 \end{cases} \tag{1.13}$$

The second equation matches the heat flux between the exterior and the interior regions. We will work only with external limits of derivatives on the boundary ∂B_a+ of the interior region B_a, since the temperature T is homogeneous in B_a (spatial derivatives within B_a vanish and convey no information, as we explained in the derivation of (1.8)).

We have formulated the equations for conservation of energy. In the following section we introduce the radially symmetric version of Eq. (1.13) and we construct the corresponding nondimensional equations that are the object of this work.

1.2 The complete nondimensional equations

The radial domain stretches in r from 0 to L. The reaction takes place inside B_a, centered at the origin with a fixed radius $a < L$. The reactor zone stretches radially from $r = 0$ to $r = a$.

Noticing from Eq. (1.7) that the ratio $S_{\mathcal{N}}/V_{\mathcal{N}} = \mathcal{N}/a$, the radially symmetric equations (1.13) for the temperature in the $\mathcal{N}$-dimensional ball in $\mathbb{R}^{\mathcal{N}}$ with radius L:

$$(\rho c)_e \frac{\partial T}{\partial t} \;=\; \kappa \frac{1}{r^{\mathcal{N}-1}}\frac{\partial}{\partial r}\left(r^{\mathcal{N}-1}\frac{\partial T}{\partial r}\right) \qquad r\in[a,\,L],\, t\geq 0 \tag{1.14}$$

$$(\rho c)_i \left.\frac{\partial T}{\partial t}\right|_{r=a} \;=\; \Delta H\,c_o c_c\,A\exp\left(-\frac{E}{RT}\right)\Big|_{r=a} + \frac{\mathcal{N}\kappa}{a}\left.\frac{\partial T}{\partial r}\right|_{r=a+} \qquad r\in[0,\,a],\, t\geq 0. \tag{1.15}$$

In Eqs. (1.14)-(1.15) we took advantage of the radial symmetry to drop the angular terms in the Laplacian.

Remark 1.1 *In Eq.* (1.14) *we implicitly define the spatial first and second derivatives at the boundaries* $r = a$, L *in the following sense, the limits* $\lim_{r\to a+} \partial^n T/\partial r^n$ *for* $r = a$ *and* $\lim_{r\to L-} \partial^n T/\partial r^n$ *for* $r = L$ *exist for* $n = 1, 2$. *We will look for solutions that are "regular" at the boundaries of* S *in this sense.*

In order to close the system, we will need boundary and initial conditions, namely,

$$\begin{aligned} T(r,\,t) &= T_L, \qquad r = L,\, t \geq 0 \quad (1.16)\\ T(r,\,0) &= T_i(r), \qquad r \in [a,\,L], \quad (1.17)\end{aligned}$$

where T_L stands for the reactor temperature at the exterior surface, which is kept fixed, and $T_i(r)$ the initial temperature profile in the reactor. Notice that the radially symmetric initial profile must be extended for the whole domain, *i.e.*, $T_i : [0,\,L] \to \mathbb{R}$, with $T_i(r) = T_i(a)$ for $r \in [0,\,a]$.

We nondimensionalize the physical magnitudes with

$$r := a\tilde{x}, \qquad L := a\tilde{L}, \qquad t_R := (\rho c)_i a^2/\kappa, \qquad t := t_R\tilde{t},$$

$$\theta := TR/E, \qquad \theta_L := T_L R/E \qquad \text{and} \qquad \theta_i(\tilde{x}) := T_i(r)R/E,$$

obtaining for (1.14) and (1.15)

$$\begin{aligned} \frac{(\rho c)_e a^2}{\kappa t_R}\frac{\partial\theta}{\partial\tilde{t}} &= \frac{1}{\tilde{x}^{\mathcal{N}-1}}\frac{\partial}{\partial\tilde{x}}\left(\tilde{x}^{\mathcal{N}-1}\frac{\partial\theta}{\partial\tilde{x}}\right) \qquad \tilde{x} \in [1,\,\tilde{L}],\, t \geq 0 \quad (1.18)\\ \frac{(\rho c)_i a^2}{\kappa t_R}\frac{\partial\theta}{\partial\tilde{t}}\bigg|_{\tilde{x}=1} &= \frac{\Delta H\, c_o c_c A a^2 R}{\kappa E}\exp\left(-\frac{1}{\theta}\right)\bigg|_{\tilde{x}=1} + \mathcal{N}\frac{\partial\theta}{\partial\tilde{x}}\bigg|_{\tilde{x}=1+} \quad \tilde{x} \in [0,\,1],\, t \geq 0, \quad (1.19)\end{aligned}$$

and for (1.16) and (1.17)

$$\begin{aligned} \theta(\tilde{x},\,t) &= \theta_L, \qquad t \geq 0,\, \tilde{x} = \tilde{L} \quad (1.20)\\ \theta(\tilde{x},\,0) &= \theta_i(\tilde{x}), \qquad \tilde{x} \in [1,\,\tilde{L}]. \quad (1.21)\end{aligned}$$

Introducing the ratio $\mathcal{E}$ of heat capacities per unit mass and the number γ (the *Damköhler group IV*, see [4])

$$\mathcal{E} = \frac{(\rho c)_e}{(\rho c)_i} \qquad \text{and} \qquad \gamma = \frac{\Delta H\, c_o\, c_c\, A\, a^2 R}{\kappa\, E}, \quad (1.22)$$

and dropping the tildes, we rewrite the system (1.18)-(1.21) in the form:

$$\begin{cases} \mathcal{E}\dfrac{\partial\theta}{\partial t} = \dfrac{1}{x^{\mathcal{N}-1}}\dfrac{\partial}{\partial x}\left(x^{\mathcal{N}-1}\dfrac{\partial\theta}{\partial x}\right) & x \in [1,\,L],\, t \geq 0 \quad (1.23)\\ \dfrac{\partial\theta}{\partial t}\bigg|_{x=1} = \gamma\exp\left(-\dfrac{1}{\theta}\right)\bigg|_{x=1} + \mathcal{N}\dfrac{\partial\theta}{\partial x}\bigg|_{x=1+} & x = 1,\, t \geq 0 \quad (1.24)\\ \theta(L,\,t) = \theta_L & t \geq 0 \quad (1.25)\\ \theta(x,\,0) = \theta_i(x) & x \in [1,\,L] \quad (1.26)\\ \theta(x,\,t) = \theta(1,\,t) & x \in [0,\,1],\, t \geq 0. \quad (1.27)\end{cases}$$

We assume continuity of the initial/boundary conditions, which means that $\theta_i(L) = \theta_L$ related to (1.25) at the outside boundary, as well as $\theta_i(1) = \theta(1, 0)$ related to (1.27). (This is called *compatibility condition*.)

Equation (1.19) was divided into Eqs. (1.24) and (1.27), the former is the matching equation between the heat generated by reaction in the interior region and the heat conducted through the exterior region, and the latter expresses that θ is independent of x in [0, 1]. Taking this fact into account, we can perform the analysis either in [0, L] or in [1, L]. In Chapter 2, for example, it will be useful to use the domain [0, L]. On the other hand, for the study of the nonlinear PDE, it is helpful to use the restricted domain [1, L] and omit Eq. (1.27). We will always look for solutions of (1.23) that are regular in the sense of Remark 1.1.

If the internal radius b were not neglected, actually $V_{\mathcal{N}}$ in Eq. (1.7) should have been replaced by $C_{\mathcal{N}}(a^{\mathcal{N}} - b^{\mathcal{N}})$, so the term $\mathcal{N}\kappa/a$ in (1.15) would be multiplied by $a^{\mathcal{N}}/(a^{\mathcal{N}} - b^{\mathcal{N}}) > 1$. Thus, the last term in Eq. (1.19) would also be multiplied by $a^{\mathcal{N}}/(a^{\mathcal{N}} - b^{\mathcal{N}})$, which would be lead in Eq. (1.24) to the same modification. Notice that such a change in Eq. (1.24) gives rise to a similar qualitative behavior for the solution. Therefore, we do not discuss it.

Notice that it is not possible to perform a nondimensionalization that reduces $\mathcal{E}$ to 1, without changing properties in space x. As we will see, there are two types of solutions for (1.23)-(1.27) as far as $\mathcal{E}$ is concerned. The first type corresponds to $\mathcal{E} = 0$ and the second one to $\mathcal{E} > 0$. The first one corresponds to $(\rho c)_e \ll (\rho c)_i$ and is used only in Chapter 2; in the second type, the precise value of $\mathcal{E}$ is irrelevant, thus from Chapter 3 through the end of this work we will set $\mathcal{E} \equiv 1$ by assuming that the interior and exterior heat capacities for unit mass are close enough.

We will see that for any dimension $\mathcal{N} = 1, 2, 3$, the behavior of the solutions of the reactor problem is governed by θ_L and γ, the scaled prevailing temperature and the Damköhler number. Typical sizes of L, θ_L and γ are discussed in Remark 2.1.

Remark 1.2 *The standard notation for the Damköhler group IV is Da_{IV}, see [4], we have used γ given in Eq. (1.22.b) instead of Da_{IV} as a short notation. The physical meaning for this number is the ratio between the "liberated heat" by the reaction and the "conductive heat transfer". Usually the temperature used for calculating this number is a characteristic temperature, but here the characteristic temperature is E/R, which is known as the* activation temperature*. Even though this ratio is large and appears dividing γ given in Eq. (1.22.b), we will see that γ is also very large; the consequences are discussed in Appendix E.1.2.*

Chapter 2

Steady-state and quasi-steady solutions for the reactor model

This is a new world, fundamentally different
from that of real objects and real events
– the world of mental constructs,
internally ruled by laws formally stated,
the world of mathematics.
INTUITION IN SCIENCE AND MATHEMATICS,
EFRAIN FISCHBEIN.

The stationary equations for the reactor model (2.1)-(2.3) are the object of Sec. 2.1. In Sec. 2.2 the stationary solutions are studied in a general manner for any dimension $\mathcal{N}$; thus the solution formulation can be considered as a whole for further treatment.

The steady-states solutions in a semi-infinite domain, or for a finite domain with Neumann condition lead only to trivial solutions in 1D and 2D. (This is shown only for the 1D case, in Appendix D.) We will provide a unified study of solutions in a finite spherical domain in 1D, 2D and 3D.

In Sec. 2.3 we will study a reduced model, which will be proven along the work to be a nice approximation for long time behavior of the whole nonlinear problem for a wide class of initial conditions.

2.1 The stationary equations

Steady-states $\varrho(x)$ are time-independent solutions of system (1.23)-(1.24); they satisfy

$$\begin{cases} \dfrac{1}{x^{\mathcal{N}-1}}\dfrac{d}{dx}\left(x^{\mathcal{N}-1}\dfrac{d\varrho}{dx}\right) = 0 & x \in [1,\, L] \qquad (2.1) \\ \gamma \exp\left(-\dfrac{1}{\varrho}\right)\Big|_{x=1} + \mathcal{N}\dfrac{d\varrho}{dx}\Big|_{x=1+} = 0 & x \le 1, \qquad (2.2) \end{cases}$$

where the derivatives of $\varrho(x)$ are "regular" in the sense discussed in Sec. 1.2.

From Eq. (1.25), we impose the boundary condition at the right

$$\varrho(L) = \theta_L, \tag{2.3}$$

where θ_L is a non-negative temperature. Then, because of (1.27), we can impose a similar boundary condition at the left, say

$$\varrho(1) = \theta_o, \tag{2.4}$$

where θ_o needs to be determined so that $\varrho(x)$ is indeed a solution of (2.1)-(2.2). (Notice that as a matter of fact $\varrho(x) = \theta_o$ for $x \in [0,\, 1]$.)

2.2 Finding the equilibria

First we solve Eq. (2.1), leading to

$$\varrho(x) = a\, r(x) + b, \qquad \text{with} \qquad a,\, b \text{ constant}, \tag{2.5}$$

where, up to a normalization, $r(x)$ is the fundamental solution for Laplace equation or Green function:

$$r(x) := \begin{cases} \frac{L-x}{d}, & \mathcal{N} = 1, \\ 1 - \frac{\ln x}{\ln L}, & \mathcal{N} = 2, \\ \frac{1-(L/x)^{\mathcal{N}-2}}{1-L^{\mathcal{N}-2}}, & \mathcal{N} \geq 3. \end{cases} \quad \text{for} \quad x \in [1,\, L], \quad \text{with} \quad d := L - 1, \tag{2.6}$$

Notice that $r(1) = 1$ and $r(L) = 0$ for any $\mathcal{N} \geq 1$.

The constants a and b in (2.5) are determined by the Dirichlet boundary condition (2.3)-(2.4). Substituting solution (2.5), (2.6) in (2.3)-(2.4) leads to $a = \theta_o - \theta_L$, and to $b = \theta_L$, yielding the solution

$$\varrho(x) = \begin{cases} \theta_o, & x \leq 1 \\ (\theta_o - \theta_L) r(x) + \theta_L, & x \in (1,\, L]. \end{cases} \tag{2.7}$$

Equation (2.2) will determine conditions for the existence of stationary solutions. We define $s_{\mathcal{N}} := -[\mathcal{N} r'(1)]^{-1}$, which satisfies $\mathcal{N}\varrho_x(1) = (\theta_L - \theta_o)/s_{\mathcal{N}}$ as follows

$$s_{\mathcal{N}} := \begin{cases} d, & \mathcal{N} = 1 \\ \frac{1}{2}\ln L, & \mathcal{N} = 2 \\ \frac{L^{\mathcal{N}-2}-1}{\mathcal{N}(\mathcal{N}-2)L^{\mathcal{N}-2}}, & \mathcal{N} \geq 3. \end{cases} \tag{2.8}$$

From Eq. (2.2), $\gamma \exp(-1/\varrho(1)) + \mathcal{N}\varrho_x(1) = 0$ and from the boundary condition (2.4), $\varrho(1) = \theta_o$, we have

$$\gamma s_{\mathcal{N}} = \frac{\theta_o - \theta_L}{\exp(-1/\theta_o)}, \tag{2.9}$$

which expresses the fact that the heat generated in the combustion region balances the heat dissipated in the conduction region. Therefore L, θ_o, θ_L, γ and $\mathcal{N}$ are intimately

correlated for the stationary solutions. To facilitate writing the heat balance Eq. (2.9) for each given reactor temperature θ_L it is useful to define the function

$$\Xi(\theta;\,\theta_L) := \frac{\theta-\theta_L}{\exp(-1/\theta)}, \qquad \theta \geq \theta_L. \tag{2.10}$$

We are interested in the values θ_o in (2.4) that satisfy Eq. (2.9), *i.e.*, $\Xi(\theta_o;\,\theta_L) = \gamma s_{\mathcal{N}}$; this is the same expression found in [6]. We will describe soon how Ξ depends upon θ_L. However, after this discussion we will set θ_L as a fixed parameter and we will use the simplified notation

$$\Xi(\theta) := \Xi(\theta;\,\theta_L), \tag{2.11}$$

where $\Xi(\theta;\,\theta_L)$ is defined in (2.10).

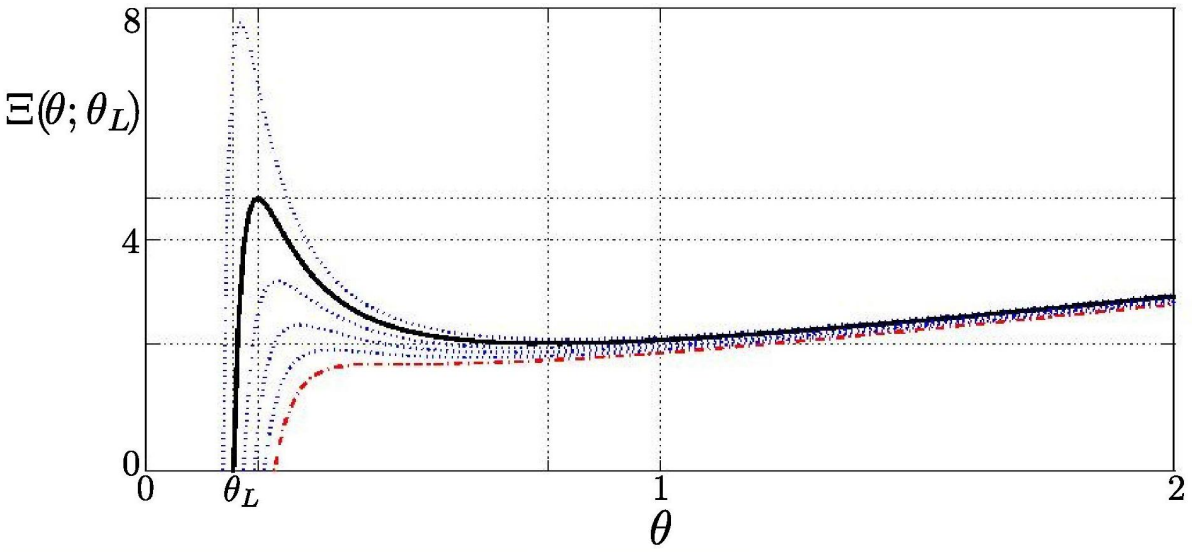

Figure 2.1: Some plots of $\Xi(\theta;\,\theta_L)$ *versus* θ. Here $\theta_L = 0.17$ for the solid curve, $\theta_L = 0.15,\, 0.19,\, 0.21,\, 0.23$ for the dotted curves (from left to right), $\theta_L = 0.25$ for the dotted-dashed curve. Notice that when θ_L is smaller, the peak becomes higher. All curves are asymptotic to $\theta - \theta_L$ when θ tends to infinity. Notice that the intersection of each curve with the θ axis occurs for the respective temperature θ_L.

Notice that $\gamma s_{\mathcal{N}} > 0$ and $\theta > \theta_L$ is such that $\Xi(\theta;\,\theta_L)$ in Eq. (2.10) is positive too. Thus the roots of Eq. (2.9) are always larger than θ_L. Looking for the extrema of the function $\Xi(\,\cdot\,;\,\theta_L)$, we see that

$$\frac{d}{d\theta}\Xi(\theta;\,\theta_L) = \frac{d}{d\theta}\left[(\theta-\theta_L)\exp\left(\frac{1}{\theta}\right)\right] = \frac{\theta^2-\theta+\theta_L}{\theta^2}\exp\left(\frac{1}{\theta}\right). \tag{2.12}$$

Then $d\Xi(\theta;\,\theta_L)/d\theta = 0$ at

$$\theta_M = \theta_M(\theta_L) = \frac{1}{2} - \frac{1}{2}\sqrt{1-4\theta_L} \qquad \text{and} \qquad \theta_m = \theta_m(\theta_L) = \frac{1}{2} + \frac{1}{2}\sqrt{1-4\theta_L}, \tag{2.13}$$

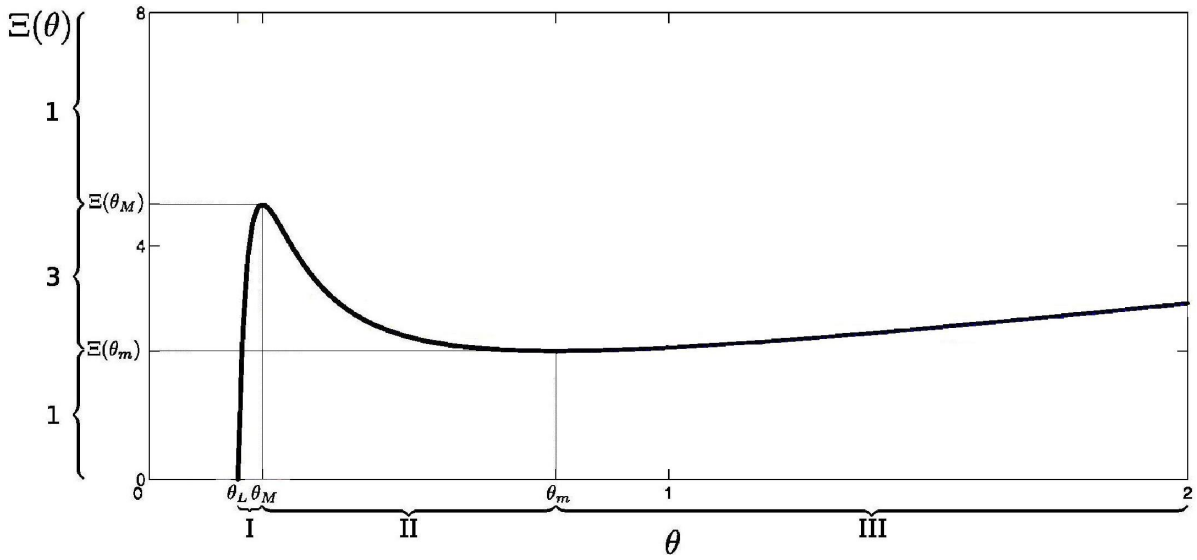

Figure 2.2: The solid curve is $\Xi(\theta)$ in (2.11) with $\theta_L = 0.17$. At the left of vertical axis we show the regions where we have one or three solutions, marked with '1' or '3' on the vertical axis. On the horizontal axis, we mark also the regions I, II, III where the corresponding θ_I, θ_{II}, θ_{III} are located.

where m stands for minimum and M for maximum, see Fig. 2.2.

Inspecting Fig. 2.1, we notice that (2.9) has always at least one root, which means that there is always a steady-state solution. (There exists one value for $\theta_o \in [\theta_L, \theta_M]$ identified with I in the horizontal axis of Fig. 2.2 for $\gamma s_{\mathcal{N}} < \Xi(\theta_m)$, and for $\gamma s_{\mathcal{N}} > \Xi(\theta_M)$ there exists one value for $\theta_o \in [\theta_m, \infty)$ related to III in Fig. 2.2 that satisfies (2.9).) For $\Xi(\theta_M) < \gamma s_{\mathcal{N}} < \Xi(\theta_m)$, there are three different roots, which define three different stationary solutions. Let us call these roots θ_I, θ_{II}, θ_{III}. Notice that

$$\theta_L < \theta_I < \theta_M < \theta_{II} < \theta_m < \theta_{III}.$$

Recall that $\theta_M = \theta_M(\theta_L)$ and $\theta_m = \theta_m(\theta_L)$. So we have that θ_I, θ_{II} and θ_{III} depend on θ_L, γ and $s_{\mathcal{N}}$.

Remark 2.1 *The standard environment temperatures are of order* 300 K, *which is equivalent to* $\theta_L \approx 0.016$, *for the activation energy* E *in Table 1 (page 87), appropriate for coke. Moreover, the system has a unique stationary solution when* $\theta_L > 0.25$, *which is approximately* 4753 K; *so for physically reasonable conditions, the model has three stationary solutions. (These conversions are made always with the ratio* $E/R \approx 2 \times 10^4$, *known as the* activation temperature, *see Appendix F.)*

We have $\theta_L = 0.016$, *then using (2.13) we see that* $\theta_M \approx 0.0163$ *and* $\theta_m \approx 0.9837$. *Introducing these values in (2.10) leads to the maximum* $\Xi(\theta_M; 0.016) \approx 1.3317 \times 10^{23}$ *and the to the minimum* $\Xi(\theta_m; 0.016) \approx 2.6744$. *In Appendix F, we provide an example calculation, which gives* $\gamma = 7.0 \times 10^8$. *For the existence of three steady-state solutions, the condition (2.9) has to be satisfied, so* $s_{\mathcal{N}}$ *must be in the range* $[\Xi(\theta_m)/\gamma, \Xi(\theta_M)/\gamma]$, *see Eq. (2.8), i.e.,* $s_{\mathcal{N}} \in [3.8206 \times 10^{-9}, 1.9025 \times 10^{14}]$.

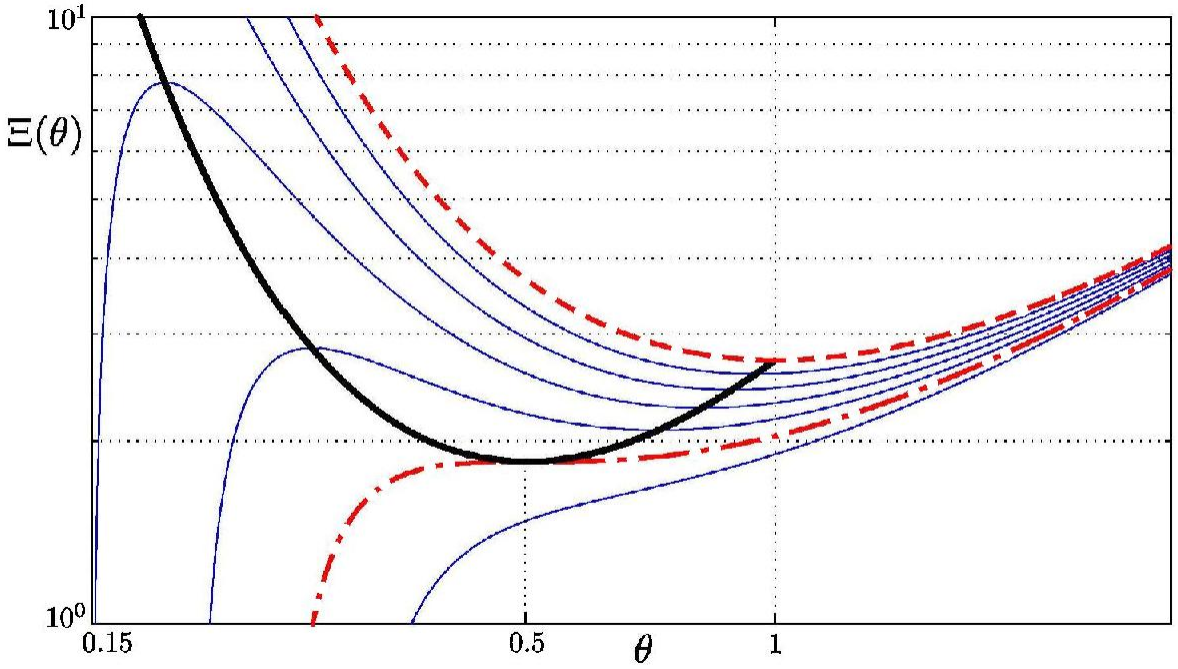

Figure 2.3: Some plots of $\Xi(\theta;\theta_L)$ *versus* θ on a log-log plot. The dashed curve corresponds to $\theta_L = 0$ and, the dotted-dashed curve to $\theta_L = 0.25$. Notice the dependence of θ_M and θ_m on θ_L defined in (2.13). The dark curve is the plot of $\theta_L \to \big(\theta_m(\theta_L), \Xi(\theta_m(\theta_L);\theta_L)\big)$ and of $\theta_L \to \big(\theta_M(\theta_L), \Xi(\theta_M(\theta_L);\theta_L)\big)$, both for $\theta_L \in [0, 0.25]$. Notice that $\theta_M(\theta_L) \leq 0.5$ and $0.5 \leq \theta_m(\theta_L)$.

Now we rescale this condition to actual physical length; recall that $a = 0.1\,\mathrm{m}$ *for porous media gives rise to the characteristic length. (This value is appropriate for the* 2D *case.) Thus, using the values of Eq. (2.8) we see that the* 1D *case has three equilibria if the dimensional radius* L *is larger than* $0.1{+}3.8206\times10^{-10}\,\mathrm{m}$ *and smaller than* $1.9025\times10^{13}\,\mathrm{m}$. *For the* 2D *case, we need* L *between approximately* $0.1\,\mathrm{m}$ *and* $\exp(3.805\times10^{14})\,\mathrm{m}$. *Finally, notice that for the* 3D *case* $s_{\mathcal{N}} \in [0,\, 1/3)$ *for nondimensional* $L \geq 1$, *so the restriction is always satisfied when the dimensional* L *is larger that* $0.1 + 10^{-8}\,\mathrm{m}$, *so that there are always three equilibria in practice.*

2.3 The reduced model: quasi-steady solutions

The idea of studying a reduced model is based on two facts. First, stationary solutions always have specific profiles for x in $[0,\, L]$ given by the functions $\varrho(x)$, Eq. (2.7), where the function $r(x)$ depends upon each dimension. Second, numerical simulations, in Appendix E, show that any solution profile of the nonlinear model will quickly approach such profiles with time-dependent values at $x = 1$. This fact also follows from analysis presented later.

Thus, in order to study solutions that have such profiles both in the initial condition and during the evolution of the solution, we make a specific kind of simplification in the original nonlinear model: we will keep (1.24), but we enforce fundamental solutions of the Laplace equation by taking $\mathcal{E} = 0$ in (1.22.a). This is the same as considering the limit of the solution when $(\rho c)_e/(\rho c)_i \to 0$.

Thus we are led to consider $R(x, t)$, the solution of the system of equations (1.23)-(1.24) with $\mathcal{E} = 0$, for $x \in [1, L]$ and $t \geq 0$. It satisfies the *reduced model*:

$$\begin{cases} 0 = \dfrac{1}{x^{\mathcal{N}-1}}\dfrac{\partial}{\partial x}\left(x^{\mathcal{N}-1}\dfrac{\partial R}{\partial x}\right) & x \in [1, L],\ t \geq 0 \qquad (2.14) \\ R_t = \gamma \exp\left(-1/R\right) + \mathcal{N}\dfrac{\partial R}{\partial x} & x = 1,\ t \geq 0, \qquad (2.15) \end{cases}$$

with the initial/boundary conditions (1.25)-(1.26), given by

$$\begin{cases} R(L, t) = \theta_L & t \geq 0 \\ R(x, 0) = (\theta_o - \theta_L)r(x) + \theta_L & x \in [1, L], \end{cases} \qquad (2.16)$$

with a fixed reactor temperature θ_L and where $r(x)$ depends upon the dimension $\mathcal{N}$, given in Eq. (2.6). Notice that $R(1, 0) = \theta_o$ in (2.16) is the initial temperature at $x = 1$. Notice that condition (1.27) extending the solution to [0, 1] can be imposed separately. Of course, the initial condition (2.16.b) must be related to the fundamental solution of the Laplace equation for $x \in [1, L]$, see (2.6).

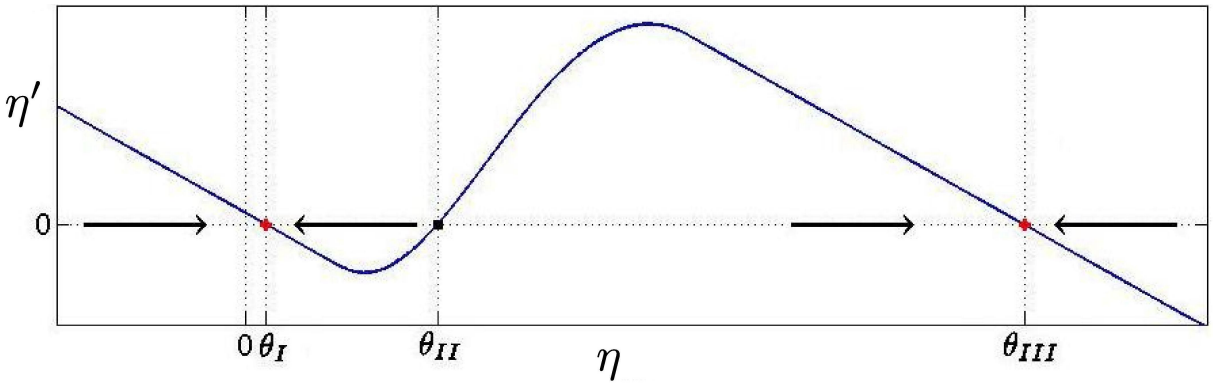

Figure 2.4: Schematic plot of the RHS of (2.18.a). The arrows denote the tendency of any condition $\eta(t)$ based on the sign of its derivative.

Inspecting Eq. (2.14) shows that the solution for any time is, in fact, a fundamental solution of Laplace equation; by analogy with Eq. (2.16.b) we see that we can write the solution as

$$R(x, t) = (\eta(t) - \theta_L)r(x) + \theta_L, \qquad (2.17)$$

which clearly satisfies the initial and boundary conditions (2.16) provided $\eta(0) := \theta_o$. Substituting (2.17) into (2.15), we see that $\eta(t)$ has to satisfy

$$\eta'(t) = \gamma \exp\left(-\frac{1}{\eta(t)}\right) - \frac{\eta(t) - \theta_L}{s_{\mathcal{N}}}, \quad \text{with} \quad \eta(0) = \theta_o. \qquad (2.18)$$

Solutions of the form (2.17) such that $\eta(t)$ satisfies Eq. (2.18) are called *quasi-steady*. See Fig. 2.4.

At equilibria, notice that $\eta' = 0$. Setting $\eta' = 0$ in (2.18), we see that stationary values η must satisfy, for Ξ given in (2.11)

$$\gamma s_{\mathcal{N}} = \Xi(\eta), \tag{2.19}$$

by recalling that now θ_L is a fixed value.

Compare (2.19) with (2.9) and notice that both are the same expression. Therefore, we see that the stationary solutions of system (2.14)-(2.16.b) and of system (1.23)-(1.25) are the same. We recall the solution (2.7), and we write the stationary solutions as

$$\varrho_I(x) := \begin{cases} \theta_I, & x \in [0,\, 1] \\ (\theta_I - \theta_L) r(x) + \theta_L, & x \in [1,\, L], \end{cases} \tag{2.20}$$

analogously for $\varrho_{II}(x)$ with $\varrho_{II}(1) = \theta_{II}$ and $\varrho_{III}(x)$ with $\varrho_{III}(1) = \theta_{III}$. In Fig. 2.5 we plot the different profiles for the 1D and 2D cases; the 3D case is very similar to the 2D case. Notice that the value of θ_{III} for $\mathcal{N} = 2$ is smaller than the value for $\mathcal{N} = 1$. Inspecting Fig. 2.1 we see that this is expected from relation (2.19) and from $s_{\mathcal{N}+1} < s_{\mathcal{N}}$ (this relationship follows easily from (2.8)).

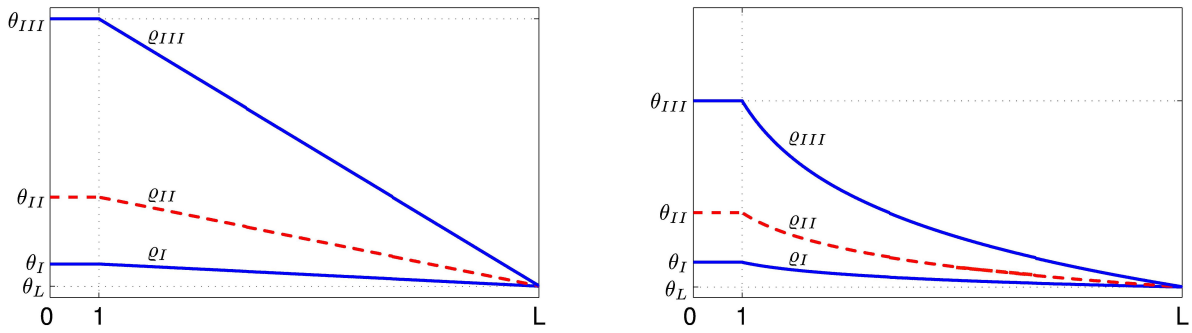

Figure 2.5: The typical plots for the stationary solutions. In the left figure, we have the profile for the 1D case, at the right for the 2D case. The solid curves are for $\varrho_I(x)$ (at the bottom) and $\varrho_{III}(x)$ (at the top), the dashed are for $\varrho_{II}(x)$.

Because $\eta'(t) > 0$ in (2.18) only if $\eta(t) \in (-\infty,\, \theta_I) \cup (\theta_{II},\, \theta_{III})$, and $\eta'(t) < 0$ only if $\eta(t) \in (\theta_I, \theta_{II}) \cup (\theta_{III},\, \infty)$, see Fig. 2.4, it follows that $\varrho_I(x)$ is an attractor for any solution of system (2.14)-(2.16) with initial condition such that $R(1,\, 0) < \theta_{II}$, so $R(x,\, t) \to \varrho_I(x)$ as $t \to \infty$. We have an analogous result for $\varrho_{III}(x)$ if $R(1,\, 0) > \theta_{II}$, because $R(x,\, t) \to \varrho_{III}(x)$ as $t \to \infty$. Clearly the steady solution $\varrho_{II}(x)$ related to θ_{II} is an unstable solution of (2.14)-(2.16), *i.e.*, a repeller.

Inspecting the plot in Figures 2.2 or 2.3 we see that the unstable equilibrium solution exists if, and only if,

$$\theta_L < 0.25 \qquad \text{and} \qquad \gamma s_{\mathcal{N}} \in \big(\Xi(\theta_m(\theta_L);\, \theta_L),\, \Xi(\theta_M(\theta_L);\, \theta_L)\big). \tag{2.21}$$

In this case all three roots of $\Xi(\,\cdot\,;\theta_L) = \gamma s_{\mathcal{N}}$ exist, and we have $\theta_I < \theta_M < \theta_{II} < \theta_m < \theta_{III}$. If at least one of the conditions (2.21) fails to be satisfied, we have a unique equilibrium, which is an attractor.

Notice that in this reduced model, the solutions form a one dimensional set of functions. We have two heteroclinic orbits in this space: one from $\varrho_{II}(x)$ to $\varrho_I(x)$ and another one from $\varrho_{II}(x)$ to $\varrho_{III}(x)$. We will show that for the nonlinear problem (1.23)-(1.27) the function space is infinite dimensional. Nevertheless, two analogous heteroclinic orbits remain, as shown in Chapter 5.

Moreover, we will be able to show that the reduced model is a very nice approximation of the complete nonlinear problem: the reduced solution captures most of the long time behavior of the nonlinear solution.

Chapter 3

Linear stability analysis around equilibria

Archangel Gabriel — Study your Math...
key to the Universe!
The Prophecy, 1995.

In this Chapter, we derive the linear equations satisfied by perturbations around any of the three equilibria found in Chapter 2. Linear analysis around each stationary solution, performed in Sec. 3.1, reveals the nature of the steady-states in Sec. 3.3.

In Sec. 3.2 a rigorous analysis is performed which shows that the evolutionary solution found in Sec. 3.3 actually describes the entire linear models of Sec. 3.1.

Recall that from this Chapter through the end of this work we will work with $\mathcal{E} \equiv 1$. In the Concluding Remarks, Chapter 6, we discuss the relevance of $\mathcal{E} \neq 1$. Also, from now on the temperature θ_L is considered as a fixed parameter for the reactor.

3.1 Linear models around equilibria

We use $\varrho(x)$ to mean any of the three equilibrium temperature distributions found in Chapter 2, namely, $\varrho_I(x)$, $\varrho_{II}(x)$ or $\varrho_{III}(x)$. Notice that for $\theta \approx \varrho$, using Taylor's formula, we can write

$$\exp\big(-1/\theta\big) \approx \exp\big(-1/\varrho\big)\big(1 + (\theta - \varrho)/\varrho^2\big). \tag{3.1}$$

Now using (3.1) on the first term of the RHS of (1.24), adding and subtracting ϱ_x and ϱ_t, recalling that $\varrho_t = 0$ and $\varrho(x = 1)$ satisfies Eq. (2.2), we have that (1.24) becomes

$$\left.\frac{\partial(\theta - \varrho)}{\partial t}\right|_{x=1} \approx \sigma(\theta - \varrho)\Big|_{x=1} + \mathcal{N}\left.\frac{\partial(\theta - \varrho)}{\partial x}\right|_{x=1+}, \tag{3.2}$$

where, with $\varrho(1) = \theta_o$, we have defined

$$\sigma = \sigma(\theta_o) := \gamma \exp(-1/\theta_o)/\theta_o^2. \tag{3.3}$$

We now examine how the solution of the evolution problem behaves when we perturb the solution around the stationary solution ϱ. To do so, we define

$$\vartheta(x,\,t) :\approx \theta(x,\,t) - \varrho(x). \tag{3.4}$$

Since we have assumed constant reactor temperature at the right boundary, we write the linear model for the perturbation from Eq. (3.2) and from the heat equation (1.23) as

$$\begin{cases} \vartheta_t &= \dfrac{1}{x^{\mathcal{N}-1}}\dfrac{\partial}{\partial x}\Big(x^{\mathcal{N}-1}\dfrac{\partial\vartheta}{\partial x}\Big) & x\in[1,\,L],\,t\geq 0 & (3.5)\\ \vartheta_t\Big|_{x=1} &= \sigma\vartheta\Big|_{x=1} + \mathcal{N}\dfrac{\partial\vartheta}{\partial x}\Big|_{x=1+} & x\leq 1,\,t\geq 0 & (3.6)\end{cases}$$

(where the spatial derivatives of $\vartheta(x,\,t)$ are "regular" in the sense discussed in Sec. 1.2,) with homogeneous Dirichlet boundary and initial conditions

$$\vartheta(L,\,t)=0,\quad t\geq 0 \qquad \text{and} \qquad \vartheta(x,\,0)=\vartheta_o(x),\quad \forall x\in[0,\,L]. \tag{3.7}$$

Notice that the initial data must be constant in the inner interval, *i.e.*, $\vartheta_o(x)=\vartheta_o(1)$ for $x\in[0,\,1]$ needs to be satisfied.

Equation (3.5) is a version of the heat equation, and a classical approach to find its solution is separation of variables. Substituting

$$\vartheta(x,\,t) := T(t)X(x) \tag{3.8}$$

into (3.5) and dividing by $X(x)T(t)$ shows that

$$\frac{\frac{1}{x^{\mathcal{N}-1}}\frac{d}{dx}\big(x^{\mathcal{N}-1}\frac{dX(x)}{dx}\big)}{X(x)} = \frac{T'(t)}{T(t)} = \lambda. \tag{3.9}$$

The constant λ arises because the first equality in (3.9) must be satisfied for all $x\in[1,\,L]$ and $t\geq 0$. Thus each of these fractions cannot depend explicitly on x neither on t.

Equating the second and the last term in Eq. (3.9), we obtain, for any λ:

$$T'(t)=\lambda T(t), \qquad \text{with solution} \qquad T(t)=A\exp(\lambda t), \tag{3.10}$$

where the constant A must be determined.

Equating the first and the last term in Eq. (3.9), we obtain

$$\frac{1}{x^{\mathcal{N}-1}}\frac{d}{dx}\left(x^{\mathcal{N}-1}\frac{dX(x)}{dx}\right) - \lambda X(x) = 0. \tag{3.11}$$

Introducing (3.8) in the boundary conditions (3.6) and (3.7.a), leads to

$$\sigma X(1) + \mathcal{N}X'(1+) = \lambda X(1) \qquad \text{and} \qquad X(L)=0; \tag{3.12}$$

these are the boundary conditions for (3.11). Equations (3.11) and (3.12) can be regarded as a nonclassical Sturm-Liouville problem. (Classical Sturm-Liouville problems have boundary conditions that do not involve λ, which is not the case of Eq. (3.12.a).)

In other words, the problem (3.5)-(3.7) for the ansatz $\vartheta(x,\,t) = T(t)X(x)$ leads to the solution (3.10.b) and to the following eigenvalue problem:

$$\begin{cases} \dfrac{1}{x^{\mathcal{N}-1}}\dfrac{d}{dx}\Big(x^{\mathcal{N}-1}\dfrac{dX(x)}{dx}\Big) &=& \lambda X(x) & x\in[1,\,L] & (3.13)\\ \sigma X(1)+\mathcal{N}X'(1+) &=& \lambda X(1) & & (3.14)\\ X(L) &=& 0 & & (3.15)\\ X(x) &=& X(1) & x\in[0,\,1). & (3.16) \end{cases}$$

In Appendix A we solve (3.13)-(3.15) for $\mathcal{N} = 1,\,2$ and 3; (3.16) can be imposed separately. We notice that the solution $X(x)$ is not necessarily unique; as a matter of fact, we will prove in Appendix A that typically there exists an unbounded countable discrete set of real eigenvalues λ_n, with associated eigenfunctions $X_n(x)$ that solve (3.11)-(3.12). In Sec. 3.2 we establish that in each dimension, the eigenfunctions form complete orthogonal bases of certain Hilbert spaces, see Appendix A.

Then, we have constructed the particular solutions

$$\vartheta_n(x,\,t) := A_n\exp(\lambda_n t)X_n(x), \tag{3.17}$$

which satisfy the boundary conditions (3.14)-(3.15) of Eq. (3.13), for the eigenvalues λ_n. The same is true for any finite linear combination of solutions of the type (3.17). We will attempt to represent the solution $\vartheta(x,\,t)$ of (3.5)-(3.7) as an infinite series on the functions $\vartheta_n(x,\,t)$:

$$\vartheta(x,\,t) = \sum A_n\exp(\lambda_n t)X_n(x). \tag{3.18}$$

Then, the constants A_n must be chosen in order to satisfy the initial condition (3.7.b). This construction is completed in Sec. 3.3.

3.2 Self-adjointness of the linear operator

We will see in Sec. 3.3 that $\vartheta(x,\,t)$ in Eq. (3.18) form a one-parameter semigroup. To prove that the operator that generates the semigroup is self-adjoint and thus its spectrum lies in the real axis, it is actually simpler to analyze $\upsilon(\mathbf{x},\,t)$ as the heat equation in the whole solid ball $B_L := B[0;\,L]$ in $\mathbb{R}^{\mathcal{N}}$ instead of $\vartheta(x,\,t)$ in the interval for $x\in[0,\,L]$. We preserve the spherical symmetry requiring

$$\upsilon(\mathbf{x},\,t) = \vartheta(\|\mathbf{x}\|,\,t),\ \text{for all } \mathbf{x}\in B_L.$$

However, we will not use explicitly spherical coordinates.

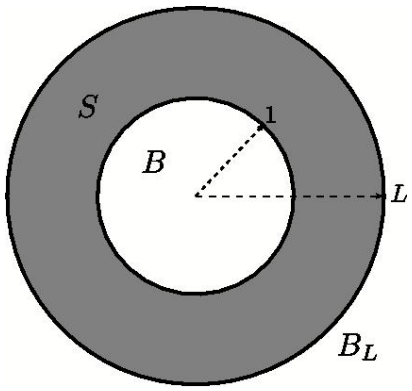

Thus, we preserve the reaction domain as the unit ball $B := B[0;\,1]$, but we will explicitly write the full Laplacian operator outside, in the solid shell $S := B_L\backslash B$. Notice that the angular derivatives simplify leading to the operator appearing in Eq. (3.5). This fact was the reason to study $\vartheta(x,\,t)$, because we are only interested in functions with radial symmetry. Thus, let us define the symmetric continuous functions in B_L that are constant in B as

$$\mathcal{C}_S[B_L] := \Big\{\phi\in\mathcal{C}[B_L]\ \Big|\ \phi(\mathbf{x}) = \phi(\mathbf{y}) \text{ if } \|\mathbf{x}\| = \|\mathbf{y}\| \text{ and } \phi(\mathbf{x}) = \phi(\mathbf{x}/\|\mathbf{x}\|) \text{ for } \|x\|\le 1\Big\}.$$

Let us define the *characteristic function* on B as

$$\mathbb{1}_B : B_L \longrightarrow \mathbb{R} \tag{3.19}$$

$$\mathbb{1}_B(\mathbf{x}) \longmapsto \begin{cases} 0, & \mathbf{x} \in S \\ 1, & \mathbf{x} \in B. \end{cases} \tag{3.20}$$

Thus, the nondimensionalization and linearization of equations (1.13), for the unit $\mathcal{N}$-dimensional ball B, the interior region, and the $\mathcal{N}$-dimensional shell S, the exterior region, lead to the problem

$$\begin{cases} \upsilon_t = \Delta\upsilon & \mathbf{x} \in S,\, t > 0 \\ \upsilon_t = \left[\sigma\upsilon + \mathcal{N}\dfrac{\partial\upsilon}{\partial r}\right]_{\partial B+} \mathbb{1}_B & \mathbf{x} \in B,\, t > 0, \end{cases} \tag{3.21}$$

where the spatial derivatives of $\upsilon(\mathbf{x},\, t)$ are "regular" in the sense of Remark 1.1 and where we notice that $\upsilon(\mathbf{x},\, t)$ has a time-dependent constant value inside B, because $T(\mathbf{x},\, t)$ is also homogeneous in B, see (1.13). Nonetheless, recall that for B we work with external limits of derivatives calculated in S and evaluated on the boundary $\partial B+$. The exterior boundary condition is

$$\upsilon(\mathbf{x},\, t) = 0, \qquad \|\mathbf{x}\| = L,\, t \geq 0, \tag{3.22}$$

as we can infer from (3.7.a). (Of course, if the initial data is constant on B and radially symmetric, the solution $\upsilon(\mathbf{x},\, t)$ is also constant on B and radially symmetric.)

Using the separation of variables $\upsilon(\mathbf{x},\, t) = \exp(\lambda t)\Phi(\mathbf{x})$ in Eqs. (3.21) and (3.22) leads to the eigenvalue problem (which is equivalent to (3.13)-(3.16))

$$\begin{cases} \Delta\Phi = \lambda\Phi & \mathbf{x} \in S \\ \left[\sigma\Phi + \mathcal{N}\dfrac{d\Phi}{dr}\right]_{\partial B+} \mathbb{1}_B = \lambda\Phi & \mathbf{x} \in B, \end{cases} \tag{3.23}$$

where the radial derivatives of $\Phi(\mathbf{x})$ are "regular" in the sense of Remark 1.1 and with $\Phi(\mathbf{x}) = \Phi(\mathbf{y})$ for all $\mathbf{x} \in B$ and any $\mathbf{y} \in \partial B+$; we also set $\Phi(\mathbf{x}) = 0$ for $\|\mathbf{x}\| = L$.

Notice that closing $\mathcal{C}_S[B_L]$ with the $L^2[B_L]$ norm defines the space $L^2_S[B_L]$ of functions $L^2[B_L]$ with spherical symmetry, defined in the closed $\mathcal{N}$-ball B_L in $\mathbb{R}^{\mathcal{N}}$ such that they are constant almost everywhere in the inner $\mathcal{N}$-ball B. For two functions $\Phi,\, \Psi \in L^2_S(B_L)$ we split the L^2_S inner product into

$$\langle \Phi,\, \Psi \rangle := \langle \Phi,\, \Psi \rangle_B + \langle \Phi,\, \Psi \rangle_S, \tag{3.24}$$

where the subscript means the region for the unit ball B or the shell S where the standard L^2 inner product in $\mathbb{R}^{\mathcal{N}}$ is taken, *i.e.*,

$$\langle \Phi,\, \Psi \rangle_B = \int_B \Phi(\mathbf{x})\Psi(\mathbf{x})\, d\mathbf{x} \qquad \text{and} \qquad \langle \Phi,\, \Psi \rangle_S = \int_S \Phi(\mathbf{x})\Psi(\mathbf{x})\, d\mathbf{x}. \tag{3.25}$$

Lemma 3.1 *The operator in the eigenvalue problem (3.23) can be expressed as*

$$\mathcal{S}[\Phi](\mathbf{x}) := \begin{cases} \Delta\Phi(\mathbf{x}) & \mathbf{x} \in S \\ \left[\sigma\Phi + \mathcal{N}\frac{d\Phi}{dr}\right]_{\partial B+} \mathbb{1}_B(\mathbf{x}) & \mathbf{x} \in B \end{cases} \tag{3.26}$$

where Φ is "regular" in the sense of Remark 1.1, i.e., the radial derivatives of $\Phi(\mathbf{x})$ have certain lateral limits at $r = 1$, L on the dense subset $D(\mathcal{S})$ of the Hilbert space $L^2_S(B_L)$ of radially symmetric functions, namely

$$D(\mathcal{S}) := \left\{ \phi \in \mathcal{C}_S[B_L] \cap \mathcal{C}^2(S) \middle| \phi(\mathbf{x}) = 0 \text{ if } \|\mathbf{x}\| = L \text{ and } \phi \text{ "regular" at } \partial S \right\}$$

with the $L^2_S[B_L]$ inner product (3.24). On $D(\mathcal{S})$ the linear operator $\mathcal{S}$ is a symmetric and upper bounded operator, with bound σ. (Notice from the very definition that $\mathcal{S}[\Phi]$ is radially symmetric in B_L and constant in B.)

Proof. The proof uses the notation for the case with $\mathcal{N} = 3$, but the proofs for other dimensions are analogous. Let Φ, Ψ be any two functions in $D(\mathcal{S})$. The normal vectors from S and B have opposite directions, so from Gauss Theorem and recalling that $\Phi(\mathbf{x}) = 0$ for $\|\mathbf{x}\| = L$, we obtain (using ds as the area element to avoid the notation conflict with the shell S)

$$\begin{aligned} \langle \Phi,\, \Delta\Psi\rangle_S \;+\; \langle \nabla\Phi,\, \nabla\Psi\rangle_S \;&=\; \int_{\partial S} \Phi(\mathbf{x}) \frac{d\Psi(\mathbf{x})}{dr}\, ds \;=\; -\int_{\partial B+} \Phi(\mathbf{x}) \frac{d\Psi(\mathbf{x})}{dr}\, ds \qquad (3.27) \\ &=\; -\left[\Phi\frac{d\Psi}{dr}\right]_{\partial B+} \int_{\partial B} ds \;=\; -\mathcal{N}|B| \left[\Phi\frac{d\Psi}{dr}\right]_{\partial B+} \;=\; -\mathcal{N}\frac{d\Psi}{dr}\bigg|_{\partial B+} \langle \Phi,\, \mathbb{1}_B\rangle_B, \end{aligned}$$

where $|B|$ is the volume of the unit ball, and because in view of relation (1.7), which implies that the surface $|\partial B|$ is equal to $\mathcal{N}|B|$. Therefore, recalling the inner product (3.24) and that Ψ is constant in B, using (3.26) and (3.27) lead to

$$\begin{aligned} \langle \Phi,\, \mathcal{S}[\Psi]\rangle \;&=\; \left[\sigma\Psi + \mathcal{N}\frac{d\Psi}{dr}\right]_{\partial B+} \langle \Phi,\, \mathbb{1}_B\rangle_B + \langle \Phi,\, \Delta\Psi\rangle_S \\ &=\; \sigma\langle \Phi,\, \Psi\rangle_B + \mathcal{N}\frac{d\Psi}{dr}\bigg|_{\partial B+} \big\langle \Phi,\, \mathbb{1}_B\big\rangle_B + \int_{\partial S} \Phi(\mathbf{x}) \frac{d\Psi(\mathbf{x})}{dr}\, ds - \langle \nabla\Phi,\, \nabla\Psi\rangle_S \\ &=\; \sigma\langle \Phi,\, \Psi\rangle_B - \langle \nabla\Phi,\, \nabla\Psi\rangle_S. \qquad (3.28) \end{aligned}$$

Now, note that Eq. (3.28) is symmetric in Φ and Ψ, so that it implies

$$\langle \Phi,\, \mathcal{S}[\Psi]\rangle = \langle \mathcal{S}[\Phi],\, \Psi\rangle. \tag{3.29}$$

We conclude that $\mathcal{S}$ is a symmetric operator. As to the upper bound, note from the relations (3.28) and (3.29) that

$$\sigma\langle \Phi,\, \Phi\rangle - \langle \mathcal{S}[\Phi],\, \Phi\rangle = \sigma\|\Phi\|^2 - \sigma\|\Phi\|^2_B + \|\nabla\Phi\|^2_S = \sigma\|\Phi\|^2_S + \|\nabla\Phi\|^2_S \geq 0. \tag{3.30}$$

So, we conclude that $\mathcal{S}$ satisfies the bound

$$\langle \mathcal{S}[\Phi],\, \Phi\rangle \leq \sigma\langle \Phi,\, \Phi\rangle, \tag{3.31}$$

and the operator has upper bound σ, which completes the proof. (Of course, $\mathcal{S}$ does not have finite norm.) □

Now we use a renowned theorem of Friedrichs applied to the operator $A := \sigma I - \mathcal{S}$ to prove the main result of this section, namely, that under these conditions, $\mathcal{S}$ can be extended to a self-adjoint operator, see [29].

Theorem 3.2 (Friedrichs extension theorem) *Let A be a positive symmetric operator and let $q(\varphi, \psi) := \langle A\varphi, \psi\rangle$ for $\varphi, \psi \in D(A)$. Then q is a closable quadratic form and its closure $\hat{q}$ is the quadratic form of a unique self-adjoint operator $\hat{A}$. $\hat{A}$ is a positive extension of A, and the lower bound of its spectrum is the lower bound of q. Further, $\hat{A}$ is the only self-adjoint extension of A whose domain is contained in the form domain of $\hat{q}$.*

Remark 3.3 *Friedrichs' theorem gives additional information: the domain of the extension of A is a subset of the form domain $\hat{q}$, therefore $D(\hat{q}) \subset L^2_S(B_L)$, because the closure of q was taken in $D(\mathcal{S}) \subset L^2_S(B_L)$ with the L^2-norm. In Appendix A we work on this space and show that the spectrum is actually discrete.*

The most important result in this section shows that (3.23) describes the spectral problem for a self-adjoint operator, therefore the spectrum of the operator lies in the real axis. In Appendix A we see that there is only point spectrum $\{\lambda_n\}$, so the eigenfunctions $\Phi_n(\mathbf{x})$ related to the eigenvalues λ_n are orthogonal to each other under the inner product (3.24).

It is important to keep in mind that we extend Φ_n as constant in B by $\Phi_n(\mathbf{x}) = \Phi_n(\mathbf{y})$ for every $\mathbf{x} \in B$ and any $\mathbf{y} \in S$ such that $\|y\| = 1$. So the eigenfunctions X_n in Appendix A are related to Φ_n via $\Phi_n(\mathbf{x}) = X_n(\|\mathbf{x}\|)$ for every $\mathbf{x} \in B_L$.

Corollary 3.4 *The first conclusion that we can extract from Theorem 3.2 is that the spectrum of $\mathcal{S}$ is restricted to the real axis in $(-\infty, \sigma]$, for any σ, L and $\mathcal{N}$.*

Moreover, we can verify that the parameter σ defined in (3.3) is bounded because

$$\frac{d\sigma(\theta)}{d\theta} = \gamma \frac{1 - 2\theta}{\theta^4} \exp\left(-\frac{1}{\theta}\right), \tag{3.32}$$

which is zero only when $\theta = 1/2$, so

$$\sigma(\theta) \leq \sigma(1/2) = 4\gamma e^{-2} \leq 4\gamma, \qquad \forall \theta \in \mathbb{R}^+. \tag{3.33}$$

Remark 3.5 *Friedrichs' theorem gives additional information: the domain of the extension of A is a subset of the form domain $\hat{q}$, therefore $D(\hat{q}) \subset L^2_S(B_L)$, because the closure of q was taken in $D(\mathcal{S}) \subset L^2_S(B_L)$ with the L^2-norm. In Appendix A we work in this space and show that the spectrum is actually discrete.*

3.3 Evolution of the linearized models

We have split the solution $\vartheta(x, t)$ by separation of variables in Eq. (3.8). We wish to find the eigenvalues λ for the modes of the solution, because we will proceed differently for eigenvalues $\lambda \leq 0$ and $\lambda > 0$.

In Appendix A we will show that there exists an eigenvalue $\lambda > 0$, and only one, when the initial temperature θ_o in the reaction region B satisfies $\theta_o \in (\theta_M, \theta_m)$, with θ_M, θ_m given by (2.13).

When it exists, let us identify the positive eigenvalue as λ_o, and its associated eigenfunction by $X_o(x)$. In Appendix A we will also verify that there exists an infinite discrete set of negative eigenvalues, say $-\lambda_n$ with associated eigenfunctions $X_n(x)$, for all $n \in \mathbb{N}$. This set of eigenvalues satisfies $-\lambda_n \to -\infty$ as n tends to ∞.

Let us define $L^2_{\mathcal{N}}[0,\, L]$ as the regular $L^2[0,\, L]$ space with weight $x^{\mathcal{N}-1}$, *i.e.*,

$$L^2_{\mathcal{N}}[0,\, L] := \big\{ f \in L^2[0,\, L] \,\big|\, \langle f,\, f\rangle_{\mathcal{N}} < \infty \big\}, \qquad \text{for} \qquad \langle f,\, g\rangle_{\mathcal{N}} := \int_0^L x^{\mathcal{N}-1} f(x) g(x) dx, \tag{3.34}$$

so $L^2_1[0,\, L] \equiv L^2[0,\, L]$. The need for the weight $x^{\mathcal{N}-1}$ on the $\mathcal{N}$ dimensional domain arises from the radial symmetry. Indeed, let f be a radially symmetric function defined in $L^2(B_L)$ (for $B_L \subset \mathbb{R}^{\mathcal{N}}$), $\|f\|$ the standard L^2 norm, thus (with some abuse of notation)

$$\|f\|^2 \;:=\; \int_{B_L} f^2(\mathbf{x})\, dV \;=\; \mathcal{N} C_{\mathcal{N}} \int_0^L r^{\mathcal{N}-1} f^2(r)\, dr \;=\; \mathcal{N} C_{\mathcal{N}} \|f\|^2_{\mathcal{N}},$$

because the area of the $\mathcal{N}$ dimensional sphere $S(r)$ with radius r is given by $\mathcal{N} C_{\mathcal{N}} r^{\mathcal{N}-1}$, see (1.7). Therefore, the standard L^2 norm is equal to the norm $\|f\|_{\mathcal{N}}$ up to the constant $\sqrt{\mathcal{N} C_{\mathcal{N}}}$, see the expression given in (1.7).

We must solve the boundary problem (3.5)-(3.7.a) for initial condition $\vartheta(x,\, 0) = \vartheta_o(x)$ in $L^2_{\mathcal{N}}[0,\, L]$ given in (3.7.b). We do this by superposition of the solutions $X_o(x)$ and $X_n(x)$, $\forall n \in \mathbb{N}$, *i.e.*,

$$\vartheta_o(x) = A_o X_o(x) + \sum_{n\in\mathbb{N}} A_n X_n(x), \tag{3.35}$$

where the first term exists when $X_o(x)$ exists. The coefficients A_o and A_n (with $n \in \mathbb{N}$) need to be determined from the initial condition. Let us assume that we have normalized the X_o and X_n eigenfunctions.

Now, by defining the semigroup operator $\mathcal{T} : [0,\, \infty) \to \mathcal{L}\big(L^2_{\mathcal{N}}[0,\, L]\big)$, the set of bounded linear operators from $L^2_{\mathcal{N}}[0,\, L]$ into itself. The semigroup operator then maps t into $\mathcal{T}(t)$ defined as

$$\mathcal{T}(t)\vartheta(x) := \langle X_o,\, \vartheta\rangle_{\mathcal{N}} \exp(\lambda_o t) X_o(x) + \sum_{n\in\mathbb{N}} \langle X_n,\, \vartheta\rangle_{\mathcal{N}} \exp(-\lambda_n t) X_n(x) \tag{3.36}$$

for all $\vartheta \in L^2_{\mathcal{N}}[0,\, L]$. Notice that $\mathcal{T}$ is a strongly continuous one-parameter semigroup, see for example [10], since

$$\mathcal{T}(0)\vartheta = \vartheta \qquad \text{and} \qquad \mathcal{T}(t)[\mathcal{T}(s)\vartheta] = \mathcal{T}(t+s)\vartheta, \tag{3.37}$$

because $\langle X_n,\, \mathcal{T}(s)\vartheta\rangle_{\mathcal{N}} = \langle X_n,\, \vartheta\rangle_{\mathcal{N}} \exp(-\lambda_n s)$, $\forall n \in \mathbb{N}$ and in an analogous manner we have $\langle X_o,\, \mathcal{T}(s)\vartheta\rangle_{\mathcal{N}} = \langle X_o,\, \vartheta\rangle_{\mathcal{N}} \exp(\lambda_o s)$, because of the orthonormality of X_o, X_1, X_2, ... Therefore, $\mathcal{T}(0) = I$ and $\mathcal{T}(t+s) = \mathcal{T}(t)\mathcal{T}(s)$ for all t, $s \geq 0$.

Therefore, following the results of the Hille-Yosida theorem, we interpret the solution (3.36) of the linearized model as

$$\upsilon(x,\, t) = \left[e^{t\mathcal{S}}\upsilon_o\right](x), \tag{3.38}$$

when $\mathcal{S}$ is defined in (3.26) or, more explicitly, we rewrite Eq. (3.36) as

$$\vartheta(x,\, t) = A_o \exp(\lambda_o t) X_o(x) + \sum_{n\in\mathbb{N}} A_n \exp(-\lambda_n t) X_n(x), \tag{3.39}$$

where the coefficients are given by

$$A_o := \langle X_o,\, \vartheta_o\rangle_{\mathcal{N}} \quad \text{and} \quad A_n := \langle X_n,\, \vartheta_o\rangle_{\mathcal{N}}, \qquad \forall n \in \mathbb{N} \tag{3.40}$$

due the completeness and orthonormality of the eigenfunctions defined in $L^2_{\mathcal{N}}[0,\, L]$.

In this Chapter we completed the linear stability analysis of the reactor problem near the equilibria. This is the local analysis. The Chapters that follow are concerned with the global analysis of the full reactor problem.

Chapter 4

Existence and uniqueness of solution for the nonlinear model

The nonlinear evolution problem can be written as a superposition of simpler auxiliary problems, as shown in Sec. 4.2. First we discuss these auxiliary problems. One of them is the reduced model of Sec. 2.3. The other is the complementary model; their solution is presented in 4.1. Once we understand the solution of these subproblems, we show how to construct the solution of the complete nonlinear problem in Sec. 4.2 as an initial data fixed point problem. This problem will be proven to have a unique solution for each initial data in Sec. 4.3.

4.1 Auxiliary linear models in $\mathcal{N}$ dimensions

To solve the nonlinear problem (1.23)-(1.27), it is useful to solve the following linear initial-boundary problem. Let $\eta \in \mathcal{C}^1[0,\,\infty)$ and let $\theta(x,\,t)$ be a function with at least two continuous derivatives in $x \in [1,\,L]$ and one continuous derivative in $t \geq 0$, satisfying

$$\begin{cases} \dfrac{\partial\theta}{\partial t} = \dfrac{1}{x^{\mathcal{N}-1}}\dfrac{\partial}{\partial x}\left(x^{\mathcal{N}-1}\dfrac{\partial\theta}{\partial x}\right) & x \in [1,\,L],\, t \geq 0 \quad (4.1) \\ \theta(1,\,t) = \eta(t) & t \geq 0 \quad (4.2) \\ \theta(L,\,t) = \theta_L & t \geq 0 \quad (4.3) \\ \theta(x,\,0) = \theta_i(x) & x \in [1,\,L]. \quad (4.4) \end{cases}$$

Here we assume continuity of the initial/boundary condition, *i.e.*,

$$\eta(0) = \theta_i(1) \qquad \text{and} \qquad \theta_i(L) = \theta_L. \tag{4.5}$$

Notice that condition $\theta(1,\,t) = \eta(t)$ replaces the original nonlinear condition (1.24) by means of the *auxiliary function* $\eta(t)$, so it must be a $\mathcal{C}^1[0,\,\infty)$ function. Thus η becomes another variable in the problem. The main advantage is that the original problem (1.23)-(1.27) is nonlinear, and since system (4.1)-(4.4) is linear we can split this problem as the sum of simpler linear problems, see *e.g.* [7]. So even if $\eta(t)$ is actually unknown, here we treat the auxiliary function as known; we will return to this issue later.

We can decompose the initial data $\theta_i(x)$ in (4.4) into two parts. The first one is $R(x,\,0)$, the initial profile for the reduced model studied in Sec. 2.3; which is the Laplace solution for nonhomogeneous Dirichlet conditions. The second part is $\theta_i(x) - R(x,\,0)$, which expresses the perturbation around the stationary-like profile $r(x)$; the second part gives rise to $\mathcal{U}(x,\,t)$ in the relationship (4.6).

We claim that any solution of (4.1)-(4.4) can be written as a sum of two solutions

$$\theta(x,\,t) \;=\; \mathcal{U}(x,\,t) + R(x,\,t). \tag{4.6}$$

where $\mathcal{U}(x,\,t)$ is the solution of the complementary model, to be studied in Sec. 4.1.1 and $R(x,\,t)$ is the solution (2.17) of the reduced problem (2.14)-(2.16), already studied in Sec. 2.3. This claim is proven in Sec. 4.1.2.

4.1.1 The complementary model

The study of a complementary model is important in order to understand the behavior of perturbations around the quasi-steady profile, which cannot be captured by the reduced model. Let $\mathcal{U}(x,\,t)$ be a function with at least two continuous derivatives in $x \in [1,\,L]$ and one continuous derivative in $t \geq 0$, satisfying the *complementary model*:

$$\left\{\begin{array}{rcll}
\mathcal{U}_t &=& \dfrac{1}{x^{\mathcal{N}-1}}\dfrac{\partial}{\partial x}\left(x^{\mathcal{N}-1}\dfrac{\partial \mathcal{U}}{\partial x}\right) - \eta'(t)r(x) \qquad x \in [1,\,L],\, t \geq 0 & (4.7)\\
\mathcal{U}(1,\,t) &=& 0 \qquad\qquad\qquad\qquad\qquad\qquad\qquad\qquad\qquad\qquad\quad t \geq 0 & (4.8)\\
\mathcal{U}(L,\,t) &=& 0 \qquad\qquad\qquad\qquad\qquad\qquad\qquad\qquad\qquad\qquad\quad t \geq 0 & (4.9)\\
\mathcal{U}(x,\,0) &=& \mathcal{U}_o(x) \qquad\qquad\qquad\qquad\qquad\qquad\qquad\qquad\quad x \in [1,\,L]. & (4.10)
\end{array}\right.$$

Here we have continuity of the initial/boundary conditions by defining

$$\mathcal{U}_o(x) := \theta_i(x) - R(x,\,0) \tag{4.11}$$

and recalling that $R(1,\,0) = \eta(0)$ and $R(L,\,0) = \theta_L$, see (2.16) and compare to (4.5).

We will use the *spectral method* to solve (4.7)-(4.10), see [18]. Recall the definition of $L^2_{\mathcal{N}}[1,\,L]$ given in (3.34); recall also the nomenclature $L^2_1[1,\,L] \equiv L^2[1,\,L]$. Let $\{X_n\}_{n\in\mathbb{N}}$ be a complete orthonormal basis of $L^2_{\mathcal{N}}[1,\,L]$ satisfying the homogeneous Dirichlet conditions $X_n(1) = X_n(L) = 0$ for all $n \in \mathbb{N}$. The eigenvalues are

$$\lambda_n \;:=\; n\pi/d, \qquad \forall n \in \mathbb{N}, \qquad \text{for } \mathcal{N} = 1,\,3, \tag{4.12}$$

$$\lambda_n \;\to\; n\pi/d, \qquad \text{as } n \to \infty, \qquad \text{for } \mathcal{N} = 2. \tag{4.13}$$

The eigenvalues for $\mathcal{N} = 2$ are given in Eq. (B.24), see Appendix B.1.2. For these eigenvalues X_n satisfy the ODE

$$\frac{1}{x^{\mathcal{N}-1}}\frac{\partial}{\partial x}\left(x^{\mathcal{N}-1}\frac{\partial X_n(x)}{\partial x}\right) = -\lambda_n^2 X_n(x), \qquad x \in [1,\,L],\, n \in \mathbb{N}. \tag{4.14}$$

In Appendix B we construct the eigenfunction bases for $\mathcal{N} = 1,\,2,\,3$.

Therefore we assume that $\mathcal{U}(\,\cdot\,,t) \in L^2_{\mathcal{N}}[1,\,L]$ for all times $t \geq 0$, a fact that will be proved soon in Claim 5.2. Thus the solution of (4.7)-(4.10) can be written as

$$\mathcal{U}(x,\,t) := \sum_{n\in\mathbb{N}} A_n(t)X_n(x), \tag{4.15}$$

where $X_n(x)$ are the eigenfunctions satisfying Eqs. (4.14) for $\mathcal{N} = 1,\,2,\,3$. Then, the boundary conditions in (4.8)-(4.9) are formally satisfied; $X_n(x) = 0$ for $x = 1,\,L$.

Substituting (4.15) into (4.7), we get formally

$$\sum_{n\in\mathbb{N}} A_n'(t)X_n(x) = \sum_{n\in\mathbb{N}} A_n(t)\,\frac{1}{x^{\mathcal{N}-1}}\frac{d}{dx}\left(x^{\mathcal{N}-1}\frac{dX_n(x)}{dx}\right) - \eta'(t)r(x). \tag{4.16}$$

Claim 4.1 *For every $X_n(x)$ satisfying (4.14) and for $r(x)$ given in Eq. (2.6), we have that $\langle X_n,\,r\rangle_{\mathcal{N}} = C/\lambda_n$ is satisfied for $\mathcal{N} = 1,\,3$ and $\langle X_n,\,r\rangle_{\mathcal{N}} = C_n/\lambda_n$ for $\mathcal{N} = 2$. (The normalizing constant is $C = \sqrt{2/d}$, see Eq. (B.9); C_n are given in Eq. (C.50).)*

Proof. Set k as a fixed natural number and fix also $\mathcal{N} = 1$, 2 or 3. Recall the definition of $r(x)$ given in (2.6) and notice that this satisfies

$$r''(x) + \frac{\mathcal{N}-1}{x}r'(x) = 0. \tag{4.17}$$

Expanding the LHS of (4.14) we notice that

$$X_n''(x) + \frac{\mathcal{N}-1}{x}X_n'(x) = -\lambda_n^2 X_n(x) \tag{4.18}$$

is also satisfied. Then, multiplying Eq. (4.17) by $x^{\mathcal{N}-1}X_n(x)$ and Eq. (4.18) by $x^{\mathcal{N}-1}r(x)$, and subtracting the results, we obtain

$$x^{\mathcal{N}-1}\big(X_n(x)r''(x) - X_n''(x)r(x)\big) + (\mathcal{N}-1)x^{\mathcal{N}-2}\big(X_n(x)r'(x) - X_n'(x)r(x)\big) = \lambda_n^2 x^{\mathcal{N}-1}X_n(x), \tag{4.19}$$

or equivalently

$$\frac{d}{dx}\big[x^{\mathcal{N}-1}\big(X_n(x)r'(x) - X_n'(x)r(x)\big)\big] = \lambda_n^2 x^{\mathcal{N}-1}X_n(x). \tag{4.20}$$

Thus, integrating the LHS from $x = 1$ to $x = L$ leads to $X_n'(1)r(1) = C\lambda_n$ for $\mathcal{N} = 1,\,3$ and $X_n'(1)r(1) = C_n\lambda_n$ for $\mathcal{N} = 2$, see Eqs. (B.41). The integration of the RHS gives rise to λ_n^2 times the inner product $\langle X_n,\,r\rangle_{\mathcal{N}}$, which proves the claim. □

Moreover, from Claim 4.1 and the orthonormality of $\{X_n\}_{n\in\mathbb{N}}$, applying the $L^2_{\mathcal{N}}[1,\,L]$ inner product with the eigenfunction $X_k(x)$ on Eq. (4.16), we obtain for $\mathcal{N} = 1,\,3$

$$A_k'(t) = -\lambda_k^2 A_k(t) - \frac{C\eta'(t)}{\lambda_k}, \qquad \forall k \in \mathbb{N}\,. \tag{4.21}$$

Applying the $L^2_{\mathcal{N}}[1,\, L]$ inner product of $X_k(x)$ on both sides of the initial data (4.10), $\mathcal{U}(x,\, 0) = \mathcal{U}_o(x)$, we see that it is necessary that

$$A_k(0) = \langle X_k,\, \mathcal{U}_o \rangle_{\mathcal{N}}, \qquad\qquad \forall k \in \mathbb{N}\,. \tag{4.22}$$

Sometimes we use the notation

$$B_n \equiv A_n(0), \qquad\qquad \forall n \in \mathbb{N}\,. \tag{4.23}$$

Assuming that the coefficients $A_n(t)$ are differentiable, Eq. (4.21) implies that they must satisfy

$$\big[A_n(t)\exp(\lambda_n^2 t)\big]' = \big[A_n'(t) + \lambda_n^2 A_n(t)\big]\exp(\lambda_n^2 t) = -C\frac{\eta'(t)}{\lambda_n}\exp(\lambda_n^2 t), \quad \forall n \in \mathbb{N}\,. \tag{4.24}$$

Renaming t as s in (4.24), integrating from time 0 to time t and using the initial condition (4.23), we see that (4.21) and (4.22) are equivalent to

$$A_n(t) = B_n\exp(-\lambda_n^2 t) - C\int_0^t \frac{\eta'(s)}{\lambda_n}\exp\big(-\lambda_n^2(t-s)\big)\,ds, \quad \forall n \in \mathbb{N}\,. \tag{4.25}$$

Let us assume that we know $\eta(t)$ for $t \geq 0$. Therefore the solution of the complementary model, Eqs. (4.7)-(4.10), is given by (4.15) with $A_n(t)$ furnished in (4.25), provided the series in (4.15) makes sense. Notice that $\lambda_n^{-2}\exp\big(-\lambda_n^2(t-s)\big)$ decays exponentially as n tends to ∞, so we will be able to verify that the series (4.15) converges under very weak hypotheses.

In further calculations, it will be useful to have a general expression for the derivative of $\mathcal{U}(x,\, t)$ at the left boundary. This requires that the expression $A_n(t)$ given in Eq. (4.25) is substituted in Eq. (4.15). We differentiate in space and evaluate at $x = 1$, leading to

$$\mathcal{N}\mathcal{U}_x(1,\, t) = U(t) + \int_0^t \eta'(s)\mathcal{R}(t-s)\,ds, \tag{4.26}$$

where we have defined, for λ_n given in Eq. (4.12) and B_n given in Eq. (4.23)

$$U(t) := \mathcal{N}C\sum_{n\in\mathbb{N}} B_n\lambda_n\exp(-\lambda_n^2 t) \quad \text{ and } \quad \mathcal{R}(t) := -\mathcal{N}C^2\sum_{n\in\mathbb{N}}\exp(-\lambda_n^2 t). \tag{4.27}$$

For $\mathcal{N} = 2$, we can easily obtain formulae analogous to (4.25), (4.27), with C_n instead of C, sometimes appearing in different locations in the formulae.

Remark 4.2 *Notice that for $\mathcal{U}_o(x) \in L^2_{\mathcal{N}}[1,\, L]$, the corresponding Fourier coefficients B_n in (4.23) belong to $l^2(\mathbb{R})$, i.e., $\sum_{n\in\mathbb{N}} B_n^2 < \infty$.*

4.1.2 Solution of the auxiliary linear model

The initial/boundary conditions of problem (4.1)-(4.4) are trivially satisfied, as we can see from the corresponding conditions for system $\mathcal{U}(x,\,t)$, namely (4.8)-(4.10), and the expression (2.17) for $R(x,\,t)$.

Now we prove that the claim given by Eq. (4.6) is in fact valid. The boundary conditions (4.2)-(4.3) for $\theta(x,\,t)$ are exactly the same as those for the reduced model (2.16.a) for $R(L,t) = \theta_L$ and (2.17) satisfying $R(1,\,t) = \eta(t)$; the complementary model has homogeneous Dirichlet boundary conditions, so indeed (4.2)-(4.3) are satisfied by the sum (4.6). The initial condition (4.4) is trivially satisfied too: from Eq. (4.10) we have that $\mathcal{U}(x,\,0) + R(x,\,0) = \theta_i(x)$. Finally, for the PDE (4.1), using (4.6), (4.7), the time derivative of $R(x,\,t)$ given in (2.17) (and again (4.7)), we see that

$$\begin{aligned}\theta_t(x,\,t) &= \mathcal{U}_t(x,\,t) + R_t(x,\,t) = \frac{1}{x^{\mathcal{N}-1}}\frac{\partial}{\partial x}\left(x^{\mathcal{N}-1}\frac{\partial \mathcal{U}(x,\,t)}{\partial x}\right) - \eta'(t)r(x) + \eta'(t)\,r(x)\\ &= \frac{1}{x^{\mathcal{N}-1}}\frac{\partial}{\partial x}\left(x^{\mathcal{N}-1}\frac{\partial \theta(x,\,t)}{\partial x}\right),\end{aligned} \tag{4.28}$$

because $\frac{1}{x^{\mathcal{N}-1}}\frac{d}{dx}\big(x^{\mathcal{N}-1}\frac{dr(x)}{dx}\big) = 0$ by noticing that $r(x)$ satisfies Eq. (2.1). Therefore, the claim given in (4.6) is indeed satisfied, the initial/boundary problem (4.1)-(4.4) is satisfied by the sum of the reduced and complementary models.

Therefore, the solution of auxiliary problem for $x \in [1,\,L]$ and $t \geq 0$, is given by the sum (4.6) of the solution of complementary model given in (4.15) by means of Eqs. (4.25), and the solution (2.17) of the reduced model:

$$\begin{aligned}\theta(x,\,t) &= \sum_{n\in\mathbb{N}} B_n \exp(-\lambda_n^2 t)X_n(x) \,-\, C\int_0^t \sum_{n\in\mathbb{N}} \frac{\eta'(s)}{\lambda_n}\exp(-\lambda_n^2(t-s))X_n(x)\,ds\\ &\quad + \big(\eta(t) - \theta_L\big)r(x) \,+\, \theta_L,\end{aligned} \tag{4.29}$$

as long as the series involved make sense (as we will soon see). For $\mathcal{N} = 2$, a formula analogous to (4.29) can be easily derived.

4.2 Formulation of the nonlinear solution

We are ready to formulate the full nonlinear problem. Let us first define the $\mathcal{C}^\infty(\mathbb{R})$ function (which depends on $\mathcal{N}$)

$$\mathcal{G}(\eta) := \begin{cases} \dfrac{\eta - \theta_L}{s_{\mathcal{N}}} - \gamma\exp\left(-\dfrac{1}{\eta}\right), & \eta > 0\\[2ex] \dfrac{\eta - \theta_L}{s_{\mathcal{N}}}, & \eta \leq 0, \end{cases} \tag{4.30}$$

with $s_{\mathcal{N}}$ given in (2.8).

Notice that $\mathcal{G}(\eta)$ has physical meaning only for positive η; we have extended $\mathcal{G}$ to the real line just for convenience of notation ahead. It is easy to prove that the derivative of

(4.30) is bounded by the quantity

$$\mathcal{G}^* \;:=\; \sup_{\eta\in\mathbb{R}}\left|\frac{d\mathcal{G}(\eta)}{d\eta}\right| \;\leq\; \frac{1}{s_{\mathcal{N}}}+4\gamma, \qquad \forall \mathcal{N}\geq 1, \tag{4.31}$$

because $\frac{d}{d\eta}\gamma\exp(-1/\eta)=\sigma(\eta)$, which is always smaller than 4γ, see Eq. (3.33).

Notice from definition (4.30) that the expression (2.18) is equivalent to $\eta'(t)=-\mathcal{G}(\eta(t))$ for $\eta>0$. In Fig. 2.4 $-\mathcal{G}(\eta)$ is plotted *versus* η. The sign is chosen in Eq. (4.30) for convenience of notation ahead.

Notice that if we set $\theta(1,\,t)=\eta(t)$, Eq. (4.2), it follows that $\theta_t(1,\,t)=\eta'(t)$. Then, a straightforward calculation shows that differentiating (4.29) and substituting it in the nonlinear boundary condition (1.24), we obtain the integro-differential equation for η

$$\eta'(t)=\int_0^t \eta'(s)\mathcal{R}(t-s)\,ds+U(t)-\mathcal{G}\big(\eta(t)\big), \tag{4.32}$$

with the aid of definitions in (4.27) and (4.30). Directly from Eq. (4.32) for $t=0$ we obtain that

$$\eta'(0)=\lim_{t\to 0}\int_0^t \eta'(s)\mathcal{R}(t-s)\,ds+U(0)-\mathcal{G}\big(\eta(0)\big)=U(0)-\mathcal{G}\big(\theta_i(1)\big) \tag{4.33}$$

must be satisfied.

Notice that solving (4.32) and substituting the resulting $\eta'(t)$ into (4.25) for each $A_n(t)$, and thus introducing these values in (4.29) provides the solution of the nonlinear problem (1.23)-(1.27).

In Eq. (4.12) we stated that the eigenvalues λ_n were exactly $n\pi/d$ for all $n\in\mathbb{N}$ for $\mathcal{N}=1,\,3$. Therefore recalling the definition (4.27.b) and using that $-n^2<-x^2$ for $x\in[n-1,\,n)$ for all $n\in\mathbb{N}$, we have

$$\begin{aligned}\int_0^t |\mathcal{R}(s)|\,ds \;&=\; \mathcal{N}C^2\int_0^t\sum_{n\in\mathbb{N}}\exp(-\lambda_n^2 s)ds \;<\; \mathcal{N}C^2\int_0^t\int_{\mathbb{R}^+}\exp\left(-\frac{x^2\pi^2 s}{d^2}\right)dxds\\ &=\; \mathcal{N}C^2 d\int_0^t\frac{ds}{\sqrt{4\pi s}} \;=\; C_{\mathcal{N}}\sqrt{t},\end{aligned} \tag{4.34}$$

where the constant $C_{\mathcal{N}}:=2\mathcal{N}C^2d/\sqrt{4\pi}=2\mathcal{N}/\sqrt{\pi}$ depends only on the dimension $\mathcal{N}$.

For $\mathcal{N}=2$, the assymptotic behavior of the λ_n given in Eq. (4.13) and also that $C_n\to C$ as $n\to\infty$, see Claim C.2, we see that a bound similar to (4.34) is valid.

Therefore, from the bound (4.34), we claim that the time integral in Eq. (4.32) is absolutely and uniformly convergent in closed time intervals starting at zero. Thus the RHS of (4.32) will be well defined. In fact, since by assumption η' is continuous, for every $t\geq 0$ there exists $M=M(t)$ such that $|\eta'(s)|\leq M$ for $s\in[0,\,t]$, and using the change of variables $s\mapsto t-\tau$, we obtain

$$\int_0^t\big|\eta'(s)\mathcal{R}(t-s)\big|\,ds \;\leq\; M\int_0^t\big|\mathcal{R}(\tau)\big|\,d\tau \;\leq\; C_{\mathcal{N}}M\sqrt{t}. \tag{4.35}$$

so, the integral in (4.35) is absolutely and uniformly convergent for $t\geq 0$, which tends to zero when $t\longrightarrow 0$, as claimed.

4.3 Existence and uniqueness of the nonlinear solution

We will show that for any two constants η_o, ζ_o there exists a unique $\eta(t) \in \mathcal{C}^1[0,\,\infty)$ that satisfies Eq. (4.29). First, we define implicitly $\zeta(t)$ in terms of $\eta(t)$ as

$$\eta(t) = \eta_o + \int_0^t \zeta(s)\,ds, \qquad \text{with} \qquad \zeta(0) := \zeta_o, \qquad t \geq 0; \tag{4.36}$$

sometimes it is useful to extend (4.36) to negative values of t, in such a way that $\eta(t)$ and $\eta'(t)$ are continuous. The extension can be defined as

$$\eta(t) = \eta_o + \zeta_o t, \qquad t \leq 0. \tag{4.37}$$

Notice that the continuity assumptions in (4.5) will be employed by the requirement $\eta_o = \theta_i(1)$ so, we also need to set $\zeta_o := U(0) - \mathcal{G}\big(\theta_i(1)\big)$, as we remarked after Eq. (4.33). Thus, for our case the two initial conditions η_o, ζ_o are well defined.

The purpose of (4.36) is to ensure the equality $\eta'(t) = \zeta(t)$. Now we rewrite (4.32) without derivatives, with the aid of Eq. (4.36), leading to the integral equation in ζ

$$\zeta(t) = \int_0^t \zeta(s)\mathcal{R}(t-s)\,ds + U(t) - \mathcal{G}\bigg(\eta_o + \int_0^t \zeta(s)\,ds\bigg), \qquad \text{with} \qquad \zeta(0) := \zeta_o. \tag{4.38}$$

This is known as a *Volterra integral equation of convolution type with a nonlinear forcing function*, see [27]. In order to show that Eq. (4.38) always has a solution, which is unique, we proceed as in the proof of Picard's Theorem, see [5].

Lemma 4.3 *Consider a Volterra integral equation of convolution type with a nonlinear forcing function given by Eq. (4.38), together with any real constants η_o, ζ_o. Assume that there exist constants $C_{\mathcal{N}}$ and $\mathcal{G}^*$ such that*

$$\int_0^t |\mathcal{R}(s)|\,ds \leq C_{\mathcal{N}}\sqrt{t} \qquad \textit{and} \qquad \sup_{\eta\in\mathbb{R}} \left|\frac{d\mathcal{G}(\eta)}{d\eta}\right| \leq \mathcal{G}^*; \tag{4.39}$$

then there exists a positive time $T := T(C_{\mathcal{N}},\,\mathcal{G}^*)$ such that (4.38) has a unique continuous solution $\zeta(t)$ for all $0 \leq t \leq T$. Such solution belongs $\mathcal{C}^0[0,\,T]$.

Proof. Given the function $\zeta(t)$, the RHS of (4.38) maps it in another function of t, $\mathcal{S}\zeta$ (we should have written $\mathcal{S}(\zeta)$ and $[\mathcal{S}(\zeta)](t)$ but we will write $\mathcal{S}\zeta$ and $[\mathcal{S}\zeta](t)$). In other words

$$[\mathcal{S}\zeta](t) := \int_0^t \zeta(s)\mathcal{R}(t-s)\,ds + U(t) - \mathcal{G}\bigg(\eta_o + \int_0^t \zeta(s)\,ds\bigg). \tag{4.40}$$

We see that (4.38) is the same as the fixed-point equation

$$\zeta(t) = [\mathcal{S}\zeta](t).$$

Our proof consists in showing that there exists a small enough T such that for $0 \leq t \leq T$, the nonlinear operator $\mathcal{S}\zeta$ is a contraction, so it possesses a unique fixed point, which turns

out to be the solution of (4.32). Define the T-norm for the Banach space $\mathcal{C}^0([0,\,T],\,\|\cdot\|_T)$ as

$$\|\zeta\|_T := \max_{t\in[0,\,T]} |\zeta(t)|, \tag{4.41}$$

where T represents a fixed value that will be defined soon.

Take any two continuous functions $\zeta,\, z : [0,\,T] \to \mathbb{R}$. Recall the definition of $\eta(t)$, Eq. (4.36), and define similarly

$$y(t) := \eta_o + \int_0^t z(s)\,ds, \qquad \text{with} \qquad z(0) = \zeta_o. \tag{4.42}$$

For $0 \le t \le T$,

$$\big|[\mathcal{S}\zeta](t) - [\mathcal{S}z](t)\big| \;\le\; \left|\int_0^t \big(\zeta(s) - z(s)\big)\mathcal{R}(t-s)ds\right| + \Big|\mathcal{G}\big(\eta(t)\big) - \mathcal{G}\big(y(t)\big)\Big|. \tag{4.43}$$

We estimate the two terms on the RHS of (4.43) separately. We use (4.39.a) in the first term and we see that it can be estimated by

$$\max_{0\le t\le T} |\zeta(t) - z(t)| \int_0^t \big|\mathcal{R}(t-s)\big|\,ds \;\le\; C_{\mathcal{N}}\sqrt{T}\|\zeta - z\|_T. \tag{4.44}$$

The second term requires some manipulation. Using the mean value theorem, the expressions (4.36) relating $\eta(t)$ and $\zeta(t)$ together with (4.42), its counterpart for $y(t)$ and $z(t)$, the hypothesis (4.39.b) and the T-norm (4.41), we have

$$\big|\mathcal{G}\big(\eta(t)\big) - \mathcal{G}\big(y(t)\big)\big| \le \mathcal{G}^*|\eta(t) - y(t)| = \mathcal{G}^*\left|\int_0^t \Big(\zeta(s) - z(s)\Big)\,ds\right| \le \mathcal{G}^*T\|\zeta - z\|_T, \tag{4.45}$$

where $\mathcal{G}^*$ was defined in Eq. (4.31) for all $\mathcal{N}$.

Using the inequalities (4.44), (4.45) in (4.43) we get

$$\big|[\mathcal{S}\zeta](t) - [\mathcal{S}z](t)\big| \le [C_{\mathcal{N}}\sqrt{T} + \mathcal{G}^*T]\|\zeta - z\|_T, \tag{4.46}$$

for all $t \in [0,\,T]$. We take T such as $\alpha := C_{\mathcal{N}}\sqrt{T} + \mathcal{G}^*T < 1$, which can be done recalling that $C_{\mathcal{N}}$ and $\mathcal{G}^*$ are constants, which depend at most on $\mathcal{N}$. Finally, if we calculate the maximum of the LHS of (4.46), we have

$$\big\|\mathcal{S}\zeta - \mathcal{S}z\big\|_T \le \alpha\|\zeta - z\|_T, \qquad \alpha < 1. \tag{4.47}$$

This means that the mapping $\mathcal{S}\zeta$ is a contraction in the space of continuous real valued functions in $[0,\,T]$ and so it has a unique fixed point, which is a continuous function. □

Notice that the hypotheses of Lemma 4.3 are satisfied, see (4.31) and (4.34), so are the conclusions. Therefore, using the fixed point solution, *i.e.*, the continuous function $\zeta(t)$, $t \in [0,\,T]$, we construct the function $\eta(t)$, which can be extended as a function in $\mathcal{C}^1[0,\,T]$ by means of Eqs. (4.36)-(4.37). We easily verify $\eta'(t) = \zeta(t)$ for $t \in [0,\,T]$. Notice that by replacing $\eta(t)$ and $\eta'(t)$ into (4.29) we obtain the unique solution of the auxiliary

linear problem (4.1)-(4.4) for all $t \in [0,\, T]$, which, as a matter of fact, solves the nonlinear problem (1.23)-(1.27).

Finally, notice that the interval $[0,\, T]$ has uniform size, therefore, we can restart the argument for a new $\zeta(0)$ defined as the last $\zeta(T)$, so we prove the existence and uniqueness of $\eta(t)$ for all $0 \leq t < \infty$.

Remark 4.4 *From the discussion in the previous paragraphs we see that $\eta' \in \mathcal{C}^0[0,\, \infty)$. Then introducing it in the RHS of Eq. (4.38) we see that the derivative of ζ is continuous too for $t > 0$; from Eqs. (4.27) and (4.30) we see that $U(t)$, $\mathcal{R}(t)$ and $\mathcal{G}(\eta)$ are $\mathcal{C}^\infty(0,\, \infty)$. We can proceed inductively to show that $\zeta(t) \in \mathcal{C}^\infty(0,\, \infty)$. From Eq. (4.36) we verify that $\eta(t) \in \mathcal{C}^\infty(0,\, \infty)$.*

From the properties of the heat equation (see e.g. [20]), we expect that $\theta(x,\, t) \in \mathcal{C}^\infty([1,\, L] \times (0,\, \infty))$. Indeed, differentiability in time and space follows from Eq. (4.29). However we cannot ensure that η has more than one continuous derivative at time $t = 0$ because $\mathcal{R}(t)$ given in Eq. (4.27) is discontinuous there, so the first derivative of the integral in Eq. (4.32) is not continuous at time $t = 0$.

4.3.1 Some *a priori* bounds

Now we will prove that when the auxiliary function $\eta(t)$ is bounded for all times, its derivative is also bounded for all times. The term $\eta(t)/s_{\mathcal{N}}$ in the definition (4.30) can be replaced by $\big[\eta(0) + \int_0^t \eta'(s)\, ds\big]/s_{\mathcal{N}}$, so we rewrite the Volterra equation (4.32) as

$$\eta'(t) = \int_0^t \eta'(s)\mathcal{R}(t-s)ds - \frac{1}{s_{\mathcal{N}}}\int_0^t \eta'(s)ds + U(t) - \frac{\eta(0) - \theta_L}{s_{\mathcal{N}}} + \gamma \exp\left(-\frac{1}{\eta(t)}\right) \quad (4.48)$$

for $\eta(t) > 0$; because of the definition of $\mathcal{G}(\eta)$ given in (4.30), the RHS of Eq. (4.48) does not contain the term $\gamma \exp(-1/\eta(t))$ for $\eta(t) \leq 0$. In any case, notice that

$$\Pi := \sup_{t \in [0,\, \infty)} \left| U(t) - \frac{\eta(0) - \theta_L}{s_{\mathcal{N}}} \right| + \gamma \quad (4.49)$$

is finite because $U(t)$ tends to zero as t tends to infinity, as it can be inferred from definition (4.27.a).

We perform the change of variables $s \mapsto t - \tau$, $ds = -d\tau$ in the two integral terms in (4.48). Since the last three terms of the RHS of (4.48) are bounded by Π, we have

$$\eta'(t) \;\leq\; \int_0^t \eta'(t-\tau)\big[\mathcal{R}(\tau) - 1/s_{\mathcal{N}}\big]d\tau + \Pi. \quad (4.50)$$

Multiplying Eq. (4.48) by -1 and using the previous change of variables, we also obtain

$$-\eta'(t) \;\leq\; \int_0^t \big(-\eta'(t-\tau)\big)\big[\mathcal{R}(\tau) - 1/s_{\mathcal{N}}\big]d\tau + \Pi. \quad (4.51)$$

These two inequalities will lead to a bound for $\eta'(t)$.

Let us inspect the convolution term $\beta(t) := \mathcal{R}(t) - 1/s_{\mathcal{N}}$. Notice that because $\mathcal{R}(t)$ is an increasing function, see (4.27.b), it is easy to verify the limits $\lim_{t\to 0+} \mathcal{R}(t) = -\infty$, $\lim_{t\to\infty} \mathcal{R}(t) = 0$ and the estimate $\mathcal{R}'(t) > 0$ for all $t > 0$. Moreover, because of (4.34) notice that

$$I(t) := \int_0^t |\beta(s)|ds = \int_0^t |\mathcal{R}(s)|ds + \int_0^t 1/s_{\mathcal{N}} ds \leq C_{\mathcal{N}}\sqrt{t} + t/s_{\mathcal{N}}; \tag{4.52}$$

in particular $I(0) = 0$. Therefore, we can choose $\tau > 0$ such that

$$I(\tau) \;=\; \alpha \;\leq\; 1/2. \tag{4.53}$$

Lemma 4.5 *Consider $\eta(t)$ satisfying (4.32). If there exists M such that $|\eta(t)| \leq M$ for all $t \geq 0$, then there exists $\mathcal{M}$ such that $|\eta'(t)| \leq \mathcal{M}$ for all $t \geq 0$.*

Proof. By contradiction let us suppose that $\mathcal{M}$ does not exist, *i.e.*, $\eta'(t)$ is not bounded. Notice from (4.50) and (4.51) that $|\eta'(0)| \leq \Pi$ and recall from Remark 4.4 that $\eta'(t)$ is a continuous function, so for every number $a \geq \Pi$ there exists $t > 0$ such that $|\eta'(t)| = a$. Therefore, let $\{t_n\}_{n\geq\Pi}$ be the sequence defined as follows. We define t_n as the first value of t such that $|\eta'(t_n)| = n$ for the natural number $n \geq \Pi$ and $t_n > \tau$ given in (4.53), so $|\eta'(t)| < n$ for all $0 \leq t < t_n$. Notice that $t_n < t_m$ for all natural numbers $\Pi \leq n < m$.

Fix $n \geq \Pi$ (notice that $t_n > \tau$). Without loss of generality, let us assume that $\eta'(t_n) = n$, otherwise (for $\eta'(t_n) = -n$) the following arguments are valid for (4.51) in lieu of (4.50). From (4.50) we have for t_n and for τ given in (4.53)

$$n = \eta'(t_n) \leq \int_0^\tau \eta'(t_n - s)\beta(s)ds + \int_\tau^{t_n} \eta'(t_n - s)\beta(s)ds + \Pi. \tag{4.54}$$

Let us inspect each of the integral terms of the RHS of (4.54) separately. The first one is bounded by:

$$\int_0^\tau \eta'(t_n - s)\beta(s)ds \leq \left| \int_0^\tau \eta'(t_n - s)\beta(s)ds \right| \leq \max_{s\in[0,\tau]} |\eta'(t_n - s)| \int_0^\tau |\beta(s)|ds \leq \frac{n}{2}, \tag{4.55}$$

because $I(\tau) = \alpha \leq 1/2$.

For the second term, notice that by integration by parts we have

$$\int_\tau^{t_n} \eta'(t_n - s)\beta(s)ds = -\eta(t_n - s)\beta(s)\Big|_\tau^{t_n} + \int_\tau^{t_n} \eta(t_n - s)\beta'(s)ds. \tag{4.56}$$

Moreover, $|\eta(t)| \leq M$ for all $t \geq 0$ and because $t_n > \tau$ and $\beta'(t) > 0$ for all $t > 0$, we have $\beta(\tau) < \beta(t_n) < -1/s_{\mathcal{N}}$, so

$$\left| \int_\tau^{t_n} \eta(t_n - s)\beta'(s)ds \right| \leq M \int_\tau^{t_n} \beta'(s)ds = M\big[\beta(t_n) - \beta(\tau)\big] \leq M|\beta(\tau)|; \tag{4.57}$$

if $t_n \leq \tau$ would be satisfied, the second integral term of (4.54) does not appear. Therefore from (4.56) and (4.57) we have that the second term of the RHS of (4.54) is bounded by

$$\left| \int_\tau^{t_n} \eta'(t_n - s)\beta(s)ds \right| \leq \big|\eta(0)\beta(t_n) - \eta(t_n - \tau)\beta(\tau)\big| + M|\beta(\tau)| \leq 3M|\beta(\tau)|. \tag{4.58}$$

Using the estimates (4.55) and (4.58) into (4.54), we have

$$n \leq n/2 + 3M|\beta(\tau)| + \Pi,$$

so subtracting $n/2$ in both sides and multiplying by 2, we obtain that

$$n \leq 2\big(3M|\beta(\tau)| + \Pi\big), \tag{4.59}$$

which leads to a contradiction: the RHS of (4.59) is a finite constant, while n in the LHS can be as large as we want. Therefore, there exists $\mathcal{M} = \mathcal{M}(M, \mathcal{N}, \Pi)$ such that the Lemma is satisfied. □

This Chapter contains the basis for the analysis of the nonlinear mode as a sum of auxiliary linear problems. In Chapter 5 we analyze the nonlinear behavior for long times.

Chapter 5

Long time behavior of the solution for the nonlinear problem in $\mathcal{N}$ dimensions

Nothing fades as fast as the future,
nothing clings like the past.
Up, Peter Gabriel.

In this Chapter we analyze the long time behavior of the auxiliary function $\eta(t)$, which represents the temperature history at the gas entrance point $x = 1$. Once $\eta(t)$ is known, the solution of the nonlinear problem is determined by solving the auxiliary linear problem studied in Sec. 4.1.

In Sec. 4.1.1 we introduce the spectral method for the resolution of the complementary model. The spectral decomposition describes the evolution of the reactor by means of an infinite number of coupled nonlinear ordinary differential equations. In Sec. 5.1 we discuss the behavior of the nonlinear solution for the complete model. Thus, in Sec. 5.2 we restrict our study to a simple example of the long time behavior, and in Sec. 5.2.1 we show evidence for the pattern of two attractor equilibria separated by a saddle point.

The notation in this Chapter is adequate for the spatial dimensions $\mathcal{N} = 1, 3$. Small modifications for the spatial dimension $\mathcal{N} = 2$ would need: the normalizing constant C must be replaced by C_n and the location of C_n in the expressions is not the same. However, because $C_n \to C$ as $n \to \infty$ as well because, for $\mathcal{N} = 2$, $\lambda_n \to n\pi/d$ as $n \to \infty$, these modifications do not alter either the behavior of the solution or its analysis.

5.1 The system with an infinite number of ODE's

Equations (4.21) form a system with infinite number of ODE's that need to be satisfied by any solution of the original nonlinear problem (1.23)-(1.26); however, we still need to impose the boundary condition (1.24):

$$\theta_t(1,\, t) = \mathcal{N}\theta_x(1+,\, t) + \gamma \exp\left(-\frac{1}{\theta(1,\, t)} \right).$$

Comparing the aforementioned condition with (4.2) we see that we can identify $\theta(1,\, t)$ with $\eta(t)$ at the left boundary, so $\theta_t(1,\, t) = \eta'(t)$; therefore we need to evaluate $\theta_x(1,\, t)$.

Recall that $X_n'(1) = C\lambda_n$ for all $n \in \mathbb{N}$, see Eq. (B.41), then we have from (4.15) that $\mathcal{U}_x(1,\, t) = C\sum_{n\in\mathbb{N}} \lambda_n A_n(t)$. Notice that $R_x(1,\, t) = (\eta(t) - \theta_L)/s_{\mathcal{N}}$, see Eqs. (2.8) and (2.17). Therefore, recalling the definition of $\mathcal{G}(\eta)$ in (4.30) and using (4.6) in (1.24) leads to

$$\eta'(t) = \mathcal{N}\sum_{n\in\mathbb{N}} C\lambda_n A_n(t) - \mathcal{G}\big(\eta(t)\big), \tag{5.1}$$

which is the spectral formulation for the original boundary condition (1.24).

We have replaced the original problem by infinitely many ODE's formed by Eq. (5.1) with an arbitrary positive number $\eta(0)$ as initial datum together with Eqs. (4.21) with initial data (4.23):

$$\eta'(t) = \mathcal{N}\sum_{k\in\mathbb{N}} C\lambda_k A_k(t) - \mathcal{G}\big(\eta(t)\big), \quad \text{with} \quad \eta(0) := \theta_i(1) \tag{5.2}$$

$$A_n'(t) = -\lambda_n^2 A_n(t) - C\frac{\eta'(t)}{\lambda_n}, \quad \text{with} \quad A_n(0) = B_n \qquad \forall n \in \mathbb{N}\,. \tag{5.3}$$

These equations may be expected to define the solution of our nonlinear problem.

Now we analyze the ordinary differential equations (5.2)-(5.3), using some of the standard notation in this area, see *e.g.* [10]. First of all, we define the Banach space

$$\mathcal{F} := \Big\{p = (\eta,\, A_1,\, A_2, \dots) \in \mathbb{R}\times\mathbb{R}^\infty \,\Big|\, \|p\| < \infty\Big\}, \text{ where } \|p\| := |\eta| + \sum_{n\in\mathbb{N}} \frac{|A_n|}{\lambda_n}, \tag{5.4}$$

recalling that $\lambda_n = n\pi/d$ for $\mathcal{N} = 1$, 3 and $\lambda_n \to n\pi/d$ for $\mathcal{N} = 2$, see Eqs. (4.12)-(4.13), and the Banach space

$$\mathcal{D} := \Big\{p \in \mathcal{F} \,\Big|\, \|p\|_D < \infty\Big\}, \text{ where } \|p\|_D := |\eta| + \sum_{n\in\mathbb{N}} \lambda_n |A_n|. \tag{5.5}$$

We notice that if $\|p\|_D < \infty$, then $\|p\| \le \max\{1,\, \lambda_1^2\}\|p\|_D$, so $\mathcal{D}$ is actually a dense subspace of $\mathcal{F}$.

We define the vector field $\mathcal{X} : \mathcal{D} \longrightarrow \mathcal{F}$:

$$\mathcal{X}(p) = \big(\mathcal{X}_o(p),\, \mathcal{X}_1(p),\, \mathcal{X}_2(p),\, \dots\big) \tag{5.6}$$

with

$$\mathcal{X}_o(p) \;:=\; C\mathcal{N}\sum_{k\in\mathbb{N}} \lambda_k A_k - \mathcal{G}(\eta) \tag{5.7}$$

from (5.2). From (5.3), (5.7)

$$\mathcal{X}_n(p) \;:=\; -\frac{C}{\lambda_n}\mathcal{X}_o(p) - \lambda_n^2 A_n \tag{5.8}$$

$$=\; \frac{C}{\lambda_n}\Big(\mathcal{G}(\eta) - C\mathcal{N}\sum_{k\in\mathbb{N}} \lambda_k A_k\Big) - \lambda_n^2 A_n, \qquad \forall n \in \mathbb{N}\,. \tag{5.9}$$

From (5.7) we observe that the following inequality holds for $p \in \mathcal{D}$:

$$|\mathcal{X}_o(p)| = \left| C\mathcal{N} \sum_{k\in\mathbb{N}} \lambda_k A_k - \mathcal{G}(\eta) \right| \leq C\mathcal{N}\|p\|_D + |\mathcal{G}(\eta)| < \infty. \tag{5.10}$$

Therefore, using the norm given in (5.4), the definition (5.9) of $\mathcal{X}_n$ and λ_n given in Eqs. (4.12)-(4.13), for every $p \in \mathcal{D}$ we have

$$\begin{aligned} \|\mathcal{X}(p)\| &\leq |\mathcal{X}_o(p)| + \sum_{n\in\mathbb{N}} \left\{ \frac{C}{\lambda_n^2} |\mathcal{X}_o(p)| + \lambda_n |A_n| \right\} = |\mathcal{X}_o(p)| \left(1 + C\frac{d^2}{\pi^2} \sum_{n\in\mathbb{N}} \frac{1}{n^2} \right) + \sum_{n\in\mathbb{N}} \lambda_n |A_n| \\ &\leq |\mathcal{X}_o(p)| \left(1 + \frac{Cd^2}{6\pi} \right) + \|p\|_D < \infty, \end{aligned} \tag{5.11}$$

because of the inequality (5.10) and because $\Sigma_{n\in\mathbb{N}} \lambda_n^{-2}$ is finite for $\mathcal{N} = 1, 2, 3$. So $\|\mathcal{X}(p)\| < \infty$, $\forall p \in \mathcal{D}$. Therefore, the vector field (5.7)-(5.9) is well defined in $\mathcal{D}$.

For the vector field $\mathcal{X}$, and a fixed $p \in \mathcal{D}$, we denote the orbit starting at p as $\varphi(t;\, p)$, where $\varphi(0;\, p) = p$. (Sometimes we use $\varphi(t) = \varphi(t;\, p)$ and $\varphi(t) := (\varphi(t)_o,\, \varphi(t)_1,\, \varphi(t)_2, \dots)$ for convenience.) In other words, $\varphi(t)$ is the solution of

$$\varphi'(t) = \mathcal{X}(\varphi(t)),\ \forall t \geq 0 \qquad \text{and} \qquad \varphi(0) = p. \tag{5.12}$$

We observe that by the definitions (5.7)-(5.9), $\eta'(t) = \mathcal{X}_o(\varphi(t))$ and $A_n'(t) = \mathcal{X}_n(\varphi(t))$.

Remark 5.1 *In Sec. 4.3 we proved that the auxiliary function $\eta(t)$ that solves the nonlinear problem is in fact a $\mathcal{C}^1[0,\, \infty) \cap \mathcal{C}^\infty(0,\, \infty)$ function. Then through Eqs. (5.3) we verify that the degree of differentiability of the functions $A_n'(t)$ is the same as that of the functions $A_n(t)$. From Eq. (4.25) we notice that $A_n(t) \in \mathcal{C}^0[0,\, \infty)$ for all $n \in \mathbb{N}$, so an inductive argument shows that $A_n(t)$ as a matter of fact belong $\mathcal{C}^1[0,\, \infty) \cap \mathcal{C}^\infty(0,\, \infty)$ for all $n \in \mathbb{N}$.*

Claim 5.2 *Given any initial datum $\eta(0) \in \mathbb{R}$ for the initial condition of the reduced model, see Eq. (2.17), and any initial condition $\mathcal{U}_o \in L^2_{\mathcal{N}}[1,\, L]$ for the complementary model, given in Eq. (4.10), we construct the initial point as $p := (\eta(0),\, A_1(0),\, A_2(0),\, \dots)$ with $A_n(0)$ given in (4.22). So, the orbit $\varphi(t;\, p)$ lies in $\mathcal{D}$ for all $t > 0$.*

Proof. From the Remark 4.4, we know that $\eta'(t) \in \mathcal{C}^0[0,\, \infty)$, so for every time $\tau > 0$ there exists a constant $M = M(\tau)$ such that $|\eta'(t)| \leq M$ for all $t \in [0,\, \tau]$. Therefore, from Eq. (4.25) we obtain

$$\begin{aligned} |A_n(t)| &\leq |A_n(0)| \exp(-\lambda_n^2 t) + \frac{CM}{\lambda_n} \int_0^t \exp\big(-\lambda_n^2 (t-s) \big) ds \\ &= |A_n(0)| \exp(-\lambda_n^2 t) + \frac{CM}{\lambda_n^3} \big[1 - \exp(-\lambda_n^2 t) \big] \\ &\leq |A_n(0)| \exp(-\lambda_n^2 t) + \frac{CM}{\lambda_n^3}. \end{aligned} \tag{5.13}$$

The first term in the RHS of (5.13) decays exponentially when $t > 0$. Notice that $\mathcal{U}_o \in L^2_{\mathcal{N}}[1, L]$ implies that all its Fourier coefficients $|A_n(0)|$ are bounded by a constant, so we see that

$$\sum_{n\in\mathbb{N}} |A_n(0)|\lambda_n \exp(-\lambda_n^2 t) < \infty, \qquad \text{for} \qquad t > 0. \tag{5.14}$$

On the other hand, from the second term on the RHS of (5.13) we see that

$$\sum_{n\in\mathbb{N}} \lambda_n \frac{CM}{\lambda_n^3} \;=\; CM \sum_{n\in\mathbb{N}} \lambda_n^{-2}, \tag{5.15}$$

converges. Therefore, we have verified that

$$\|\varphi(t)\|_D = |\eta(t)| + \sum_{n\in\mathbb{N}} \lambda_n |A_n(t)| < \infty, \qquad \text{for} \quad t \in (0, \tau], \tag{5.16}$$

is satisfied because $\eta(t)$ is continuous and the bounds (5.14) and (5.15) hold. Therefore $\varphi(t) \in \mathcal{D}$ for all $t \in (0, \tau]$; however, noticing that $\mathcal{D}$ is a subspace of $\mathcal{F}$ we can repeat the argument starting at any point in $\mathcal{D}$ for successive time intervals and show that the claim is valid for all $t > 0$. □

Remark 5.3 *We showed in Claim 5.2 that the vector field $\mathcal{X}$ is well defined from $\mathcal{D}$ to $\mathcal{F}$. From Remark 5.1 we also have the differentiability of each of the components of the vector field $\mathcal{X}$, so analogously to Claim 5.2 we can prove that the orbits (with initial data in $\mathcal{D}$) are $\mathcal{C}^0[0, \infty) \cap \mathcal{C}^\infty(0, \infty)$. Notice that the existence and uniqueness for the orbits of the vector field of the ODE's is guaranteed by the existence and uniqueness of solutions of the Cauchy problem (4.1)-(4.4) proved in Lemma 4.3.*

Remark 5.4 *From the proofs of Claim 5.2 and of Remark 5.3, we notice that actually $\mathcal{U}(\cdot\,, t)$ belongs to $L^2_{\mathcal{N}}[1, L]$ for all times $t \geq 0$, because $\mathcal{D}$ is a dense subspace of $l^2(\mathbb{R})$.*

We are interested in the equilibria of the system; they reveal an important part of the global behavior. For a point p to be an equilibrium of the vector field $\mathcal{X}$ it is necessary that $\mathcal{X}_o(p) = 0$ and $\mathcal{X}_n(p) = 0$ for all $n \in \mathbb{N}$. From the first equation in (5.9) we see that such a point p must satisfy $A_n = 0$ because $\mathcal{X}_o(p) = 0$, and so, from Eq. (5.7) we have that $\mathcal{G}(\eta) = 0$ must be satisfied.

Recalling the definition of $\mathcal{G}(\eta)$ in (4.30) and the condition $\eta'(t) = 0$ in Eq. (2.18) we notice that the three points satisfying $\mathcal{X}(p) = 0$ are

$$X_I := (\theta_I, 0, 0, \dots), \qquad X_{III} := (\theta_{III}, 0, 0, \dots) \tag{5.17}$$

and

$$X_{II} := (\theta_{II}, 0, 0, \dots). \tag{5.18}$$

We will show that X_I and X_{III} are stable equilibria and that X_{II} is a saddle point. Notice that these three equilibria correspond to the same equilibria discussed for the reduced problem, see Sec. 2.3. Indeed, by the splitting in Eq. (4.6) and the spectral decomposition (4.15) we see that X_I corresponds to $\varrho_I(x) = 0 + R(\theta_I, 0)$. (Analogously for X_{II} and X_{III}.)

5.2 Orbits from restricted initial data

A standard configuration for a reactor at starting time has stationary temperature in the shell. The reactor may be pre-heated to a certain stationary temperature distribution before the reaction starts. Thus, we study solutions such that the initial data $\mathcal{U}_o(x)$ vanishes, which from (4.16) is equivalent to $\theta_i(x)$ be a fundamental solution of the Laplace equation for x in $[1,\, L]$.

In this section we construct the domain where the orbits for such initial data are confined. This domain is a small but representative part of the Banach space $\mathcal{D}$.

Let us define the set

$$\mathcal{B} := \left\{ p \in \mathcal{F} \,\middle|\, C\mathcal{N} \sum_{n\in\mathbb{N}} \lambda_n |A_n| \le \left|\mathcal{G}(\eta)\right| \right\}; \tag{5.19}$$

notice that $\{p \in \mathcal{F} \,|\, \mathcal{X}_o(p) = 0\} \cap \mathcal{B}$ is part of the boundary of $\mathcal{B}$. Figure 5.1 shows the intersection of $\mathcal{B}$ with the linear hyperspace

$$\mathcal{F}_n := \left\{ p = (\eta,\, 0,\, \ldots,\, 0,\, A_n,\, 0,\, \ldots) \,\middle|\, \eta \in \mathbb{R},\, A_n \in \mathbb{R} \right\} \subset \mathcal{F}, \tag{5.20}$$

i.e., $\mathcal{F}_n$ is a 2D subspace of $\mathcal{F}$ for each $n \in \mathbb{N}$.

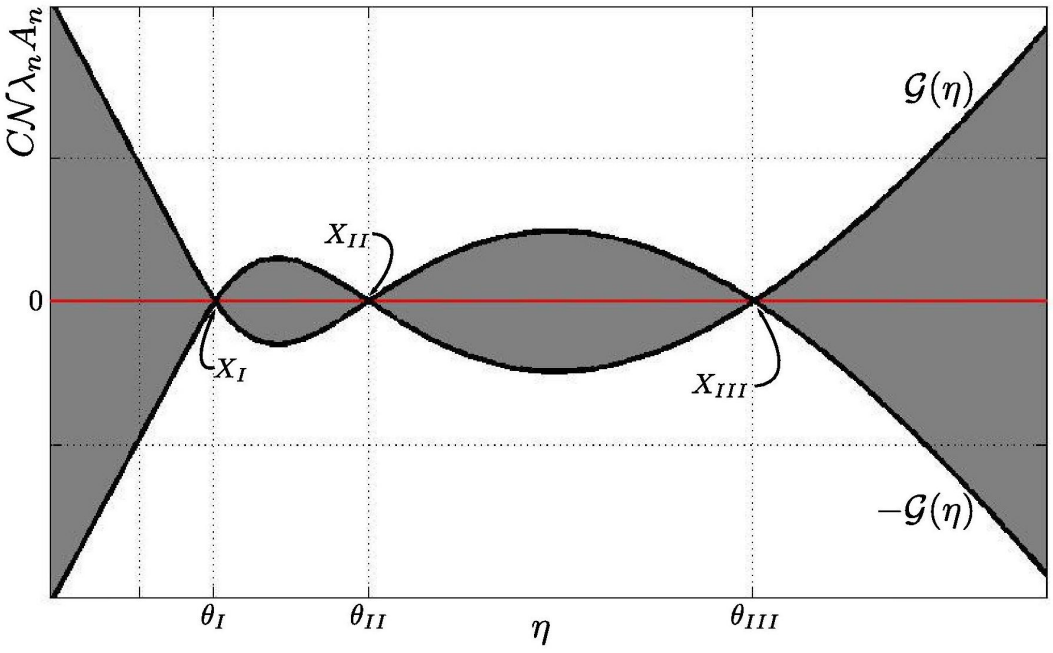

Figure 5.1: The shaded region represents the intersection of the plane $\mathcal{F}_n$ with $\mathcal{B}$, see Eq. (5.20). The solid curves are $C\mathcal{N}\lambda_n A_n = \mathcal{G}(\eta)$ where $\mathcal{X}_o(p) = 0$ and $C\mathcal{N}\lambda_n A_n = -\mathcal{G}(\eta)$.

The set $\mathcal{B}$ is a subset of subspace $\mathcal{D}$, see (5.5). Indeed, each $p \in \mathcal{B}$ satisfies

$$\sum_{n\in\mathbb{N}} \lambda_n |A_n| \le \frac{|\mathcal{G}(\eta)|}{C\mathcal{N}}, \tag{5.21}$$

and therefore

$$\|p\|_D = |\eta| + \sum_{n\in\mathbb{N}} \lambda_n |A_n| \leq |\eta| + \frac{|\mathcal{G}(\eta)|}{C\mathcal{N}} < \infty. \tag{5.22}$$

Then $p \in \mathcal{D}$, so $\mathcal{B}$ is a subset of $\mathcal{D}$. Notice that $\mathcal{B}$ is defined in terms of the norm on $\mathcal{D}$, see (5.5), so it is easy to see that it is a closed set (in the norm $\|\cdot\|_D$).

Notice that the initial condition $A_n = 0$, Eq. (5.3), leads in Eqs. (5.9) to $\mathcal{X}_n(p) \propto -\mathcal{X}_o(p)$ for all $n \in \mathbb{N}$ at the beginning of each orbit, *i.e.*, all these vector components have the same sign. This motivates the definition of the following four subregions of $\mathcal{B}$:

$$B_I^- := \big\{p \in \mathcal{B} \,\big|\, \eta \leq \theta_I,\, A_n \leq 0,\, \forall n \in \mathbb{N}\big\}, \tag{5.23}$$

$$B_I^+ := \big\{p \in \mathcal{B} \,\big|\, \eta \in [\theta_I,\, \theta_{II}],\, A_n \geq 0,\, \forall n \in \mathbb{N}\big\}, \tag{5.24}$$

$$B_{III}^- := \big\{p \in \mathcal{B} \,\big|\, \eta \in [\theta_{II},\, \theta_{III}],\, A_n \leq 0,\, \forall n \in \mathbb{N}\big\}, \tag{5.25}$$

$$B_{III}^+ := \big\{p \in \mathcal{B} \,\big|\, \eta \geq \theta_{III},\, A_n \geq 0,\, \forall n \in \mathbb{N}\big\}. \tag{5.26}$$

Notice that the superscript $\pm$ in the name of the subregion agrees with the sign of all A_n and also with the sign of $\mathcal{G}(\eta)$ in the subregion; we will show that the subscript is related with the long time behavior via the ω-limit of orbits starting in the subregion. Sometimes we use $B_{I,\,III}^{\pm}$ to denote any of the subregions in (5.23)-(5.26); we also use the definitions

$$B_I := B_I^- \cup B_I^+ \qquad \text{and} \qquad B_{III} := B_{III}^- \cup B_{III}^+. \tag{5.27}$$

Notice that in the Banach space $\mathcal{F}$, the intersection between a hyperplane with fixed η and $B_{I,\,III}^{\pm}$ is a simplex of infinite dimension. In order to visualize the subregions a graph of $\mathcal{G}(\eta)$ is helpful. Figure 5.2 shows the intersection of $B_{I,\,III}^{\pm}$ with the linear hyperspace $\mathcal{F}_n$ given in (5.20). The intersection is represented by the shaded region between the solid curve and the horizontal axis.

We can regard B_I^- and B_{III}^+ as "infinite pyramids" with an edge contained in the η axis, and X_I and X_{III} in Eq. (5.17) as the respective apices. The subregions B_I^+ and B_{III}^- have two apices each: X_I or X_{III} respectively, in Eq. (5.17), and X_{II} in (5.18).

Let us examine B_{III}^+: it is a region where $A_n \geq 0$ for every $n \in \mathbb{N}$. Its boundary ∂B_{III}^+ is formed by the apex X_{III}, Eq. (5.17.b), the *boundary faces* $P\big(B_{III}^+\big)_n$, $\forall n \in \mathbb{N}$ and the *upper boundary* U_{III}^+, where

$$P\big(B_{III}^+\big)_n := \left\{p \in B_{III}^+ \,\middle|\, \eta > \theta_{III}, A_n = 0,\, C\mathcal{N}\sum_{k\neq n} \lambda_k A_k \leq \mathcal{G}(\eta)\right\}, \tag{5.28}$$

$$U_{III}^+ := \left\{p \in B_{III}^+ \,\middle|\, \eta > \theta_{III},\, C\mathcal{N}\sum_{k\in\mathbb{N}} \lambda_k A_k = \mathcal{G}(\eta)\right\}. \tag{5.29}$$

In Fig. 5.2 notice that B_{III}^+ is bounded "below" by the boundary faces and it is bounded "above" by the upper boundary. Notice that any point in B_{III}^+ is such that $A_n \geq 0$ for $n \in \mathbb{N}$. For $\eta \geq \theta_{III}$ the points $p = (\eta,\, 0,\, 0,\, \dots)$ are in B_{III}^+, as a matter of fact, they are also included in every boundary face $P\big(B_{III}^+\big)_n$. We also remark that for every p in the upper boundary U_{III}^+ there exists at least one $A_n > 0$, because $\mathcal{G}(\eta) > 0$ in this boundary.

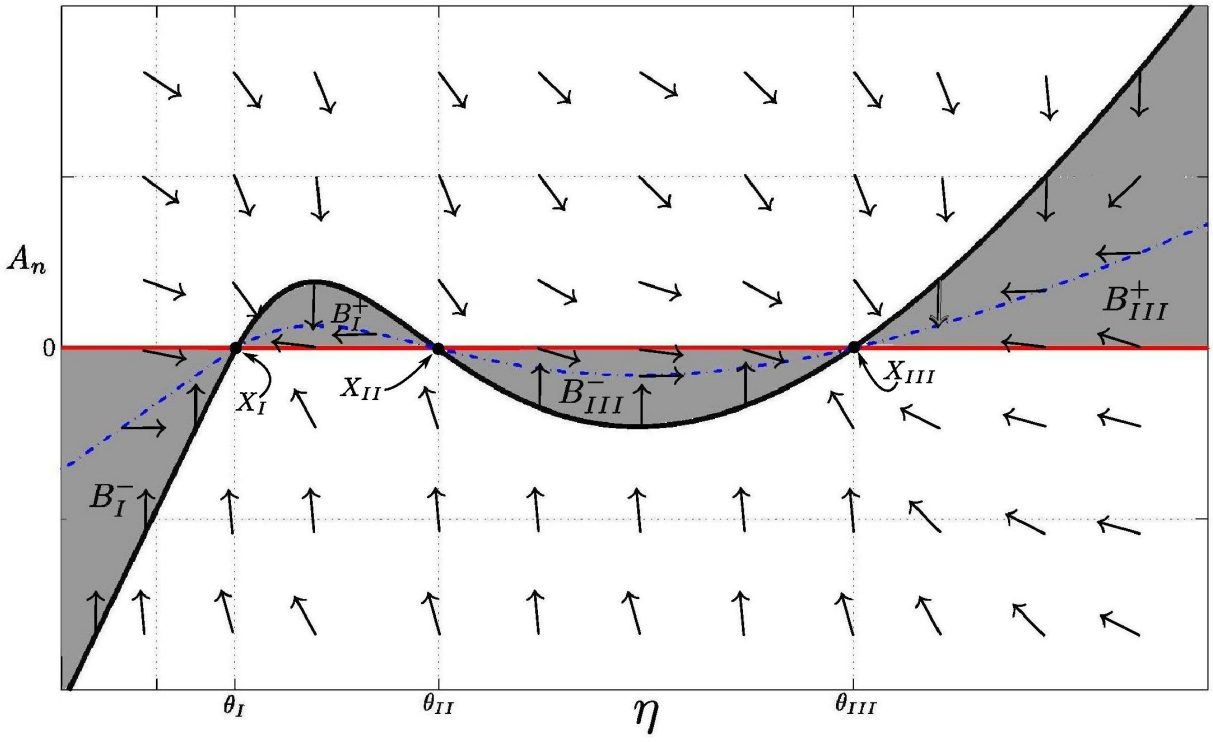

Figure 5.2: The shaded region is the intersection of plane $\mathcal{F}_n$ with $B^{\pm}_{I,III}$. On the solid curve we have $\mathcal{X}_o(p) = 0$. The vector field $\mathcal{X}(p)$ is plotted schematically, showing only directions; *e.g.*, on the curve $\mathcal{X}_o(p) = 0$ the flux is always vertical, although it is entering in the regions $B^{\pm}_{I,III}$.

Notice that the phase boundaries $P\big(B^+_{III}\big)_n$ and the upper boundary U^+_{III} have intersections. For example, a point p in $P\big(B^+_{III}\big)_n \bigcap U^+_{III}$ must satisfy $A_n = 0$ and $\mathcal{X}_o(p) = 0$. For p in $P\big(B^+_{III}\big)_n \bigcap P\big(B^+_{III}\big)_m$ the equality $A_n = A_m = 0$ is satisfied. Notice also that multiple intersection of three or more boundary faces can occur.

For the upper boundary and two or more boundary faces there are also intersections. We say that a point p in U^+_{III} is an *interior point* of the upper boundary if and only if $p \in U^+_{III}$ and $p \notin P\big(B^+_{III}\big)_n$ for all $n \in \mathbb{N}$. This mean that $p = (\eta, A_1, A_2, \dots)$ is such that $\mathcal{X}_o(p) = 0$ with $A_n > 0$ for all $n \in \mathbb{N}$.

5.2.1 Primary results

In this subsection we prove some results which identify parts of the attraction basins of the nonlinear equilibria X_I, X_{II} and X_{III}, Eqs. (5.17)-(5.18).

Definition 5.5 *A* **positively invariant** *set B for a vector field $\mathcal{X}$ is defined as a set such that:*

i) The vector field points to the interior of B at its boundary ∂B.

ii) For all $p \in B$ we have that $\varphi(t; p)$ belongs to B for all $t \geq 0$.

Lemma 5.6 *Consider an orbit such that $\varphi(0) = p$, with p in the boundary ∂B^+_{III} of B^+_{III} (respectively ∂B^-_I, ∂B^+_I or ∂B^-_{III}), then $\varphi(t) \in B^+_{III}$ for any $t \geq 0$ (resp. B^-_I, B^+_I or B^-_{III}). In other words, the subregions $B^\pm_{I,III}$ are positively invariant sets.*

Proof. We present the analysis only for B^+_{III}, because the other cases are analogous. As a *first case*, notice that $p = X_{III}$ presents no challenge, we have $\mathcal{X}_o(p) = 0$ and $\mathcal{X}_n(p) = 0$ for all $n \in \mathbb{N}$, so X_{III} is a critical point and $\varphi(t) \equiv X_{III}$ for all $t \geq 0$.

Let us consider the other boundary points by cases, noticing that for $p \in U^+_{III}$ and $p \in P(B^+_{III})_n$, $\forall n \in \mathbb{N}$, the inequality $\mathcal{G}(\eta) > 0$ is satisfied. ($\mathcal{G}(\eta) = 0$ for $p = X_{III}$.)

Second case. Let $p \in U^+_{III}$ with $A_n \neq 0$ for all $n \in \mathbb{N}$, so p is an interior point of the upper boundary. From (5.29) we have $\mathcal{X}_o(p) = 0$, then

$$\mathcal{X}_n(p) = -\frac{C}{\lambda_n}\mathcal{X}_o(p) - \lambda_n^2 A_n = -\lambda_n^2 A_n < 0, \qquad \forall n \in \mathbb{N}. \tag{5.30}$$

So, for interior p of U^+_{III}, we have that $\mathcal{X}(p)$ points to the interior of B^+_{III}.

Third case. Let p be a any point of U^+_{III}. So we know that there exists at least one $k \in \mathbb{N}$ such that $A_k > 0$, and then $\mathcal{X}_k(p) < 0$. So $\mathcal{X}(p)$ does not point out of B^+_{III}.

However, we have to notice that if for one (or several values of) $l \in \mathbb{N}$ we have $A_l = 0$, then p is also a point of $P(B^+_{III})_l$ and from an equation analogous to (5.30) we have that $\mathcal{X}_l(p) = 0$, so the vector field is tangent to $P(B^+_{III})_l$. We have to make sure that the orbit does not enter the boundary face $P(B^+_{III})_l$, rather that it enters B^+_{III}.

Notice that the derivative of the vector field component $\mathcal{X}_l(p)$ (given in (5.8)) along an orbit is

$$\frac{d\mathcal{X}_l(\varphi(t))}{dt} = -\frac{C}{\lambda_l}\frac{d\mathcal{X}_o(\varphi(t))}{dt} - \lambda_l^2 A_l'(t) = -\frac{C}{\lambda_l}\frac{d\mathcal{X}_o(\varphi(t))}{dt} - \lambda_l^2 \mathcal{X}_l(\varphi(t)). \tag{5.31}$$

Now, using (5.7) and recalling that $\mathcal{X}_o(p) = 0$, we have

$$\frac{d\mathcal{X}_o(\varphi(t))}{dt} = C\mathcal{N}\sum_{k\in\mathbb{N}} \lambda_k A_k'(t) - \mathcal{G}'(\eta)\eta'(t) = C\mathcal{N}\sum_{k\in\mathbb{N}} \lambda_k \mathcal{X}_k(\varphi(t)) - \mathcal{G}'(\eta)\mathcal{X}_o(\varphi(t)), \tag{5.32}$$

so, recalling the equivalence $p = \varphi(0)$ and $\mathcal{X}_o(p) = 0$ for $p \in U^+_{III}$, we have

$$\left.\frac{d\mathcal{X}_o(\varphi(t))}{dt}\right|_{t=0} = C\mathcal{N}\sum_{k\in\mathbb{N}} \lambda_k \mathcal{X}_k(p) \tag{5.33}$$

Thus, at a point $p \in U^+_{III}$, for the case $A_k > 0$ and $A_l = 0$ (so $\mathcal{X}_l(p) = 0$ too), substituting (5.33) into (5.31) for $t = 0$ we have that

$$\frac{d\mathcal{X}_l(p)}{dt} = -\frac{C}{\lambda_l}\frac{d\mathcal{X}_o(p)}{dt} - \lambda_l^2 \mathcal{X}_l(p) = \frac{C^2\mathcal{N}}{\lambda_l}\sum_{k\in\mathbb{N}} \lambda_k^3 A_k > 0. \tag{5.34}$$

Therefore $\mathcal{X}(p)$ points to the interior of the phase boundary $P\big(B^+_{III}\big)_l$ but the orbit $\varphi(t)$ will enter into the interior of B^+_{III}.

Fourth case. Let p be in a boundary face $P(B^+_{III})_n$ minus the upper boundary U^+_{III}: we have $A_n = 0$, $A_k \geq 0$, $\forall k \in \mathbb{N}\backslash\{n\}$ and $\mathcal{X}_o(p) < 0$, because $\mathcal{G}(\eta) > 0$ for $\eta > \theta_{III}$, therefore from (5.9)

$$\mathcal{X}_n(p) = -\frac{C}{\lambda_n}\mathcal{X}_o(p) - \lambda_n^2 A_n = -\frac{C}{\lambda_n}\mathcal{X}_o(p) > 0. \tag{5.35}$$

Notice that all other field components are unimportant; neighboring points of p with small changes of A_k keeping $A_n = 0$ fixed are still points in the boundary face $P(B^+_{III})_n$, so the field $\mathcal{X}(p)$ will point to the interior of B^+_{III}.

Notice that when more than one of the components A_n are zero, the orbit also enters B^+_{III} because the respective field coordinates satisfy $\mathcal{X}_n(p) > 0$.

Thus, from the first to the fourth case, we have covered the entire boundary of B^+_{III}. So, we have shown that for $p \in \partial B^+_{III}\backslash\{X_{III}\}$, the vector field points to the interior of B^+_{III}. Therefore $\varphi(t) \in B^+_{III}$ for all $t \geq 0$. □

Lemma 5.7 *For $-\infty < \eta^- < \eta^+ < \infty$ define the set $B[\eta^-, \eta^+] := \{p \in \mathcal{B} \,|\, \eta \in [\eta^-, \eta^+]\}$. Then its closure $K := cl(B[\eta^-, \eta^+])$ in $\mathcal{F}$ is a compact set in $\mathcal{F}$.*

Before proving Lemma 5.7, let us recall the following

Definition 5.8 *If the set A has the property that from every open covering, one can select a finite subcovering, A is said to be* **compact**. (From Definition 5.4 of [3].)

Moreover, a classical result shows that it is enough to take the open covering of A as the set of all open balls with a fixed radius centered at every point of the set.

Proof. Recall the definition of $\mathcal{G}$ given in (4.30), then take

$$M := \max_{\eta\in[\eta^-,\eta^+]} \big|\mathcal{G}(\eta)\big|, \tag{5.36}$$

and the definition (5.19) implies that for all $p \in B[\eta^-, \eta^+]$ and all $k \in \mathbb{N}$

$$|A_k| \leq \frac{M}{C\mathcal{N}\lambda_k}. \tag{5.37}$$

Define

$$S_n := \sum_{k=n}^{\infty} \lambda_k^{-2}; \tag{5.38}$$

using λ_k given in Eqs. (4.12)-(4.13) we notice that S_n is a decreasing sequence with S_1 finite and $S_n \to 0$ as $n \to \infty$. So, for every $\epsilon > 0$ there exists an integer n^* depending on ϵ such that

$$S_n < \frac{\epsilon C\mathcal{N}}{2M}, \qquad \forall n \geq n^*. \tag{5.39}$$

It is easy to see that $\mathcal{F}^* := \{p \in \mathcal{F} \,|\, A_n = 0,\, \forall n \geq n^*\}$ is isomorphic to $\mathbb{R}^{n^*}$ with the norm

$$\|\mathbf{x}\|_* := |x_o| + \sum_{k=1}^{n^*-1} \frac{|x_k|}{\lambda_k}, \qquad \text{where} \qquad \mathbf{x} := (x_o,\, x_1,\, \ldots,\, x_{n^*-1}) \in \mathbb{R}^{n^*}. \tag{5.40}$$

Because $K^* := K \cap \mathcal{F}^*$ is closed and bounded, its natural embedding in $\mathbb{R}^{n^*}$ shows that K^* is compact. Then for every $\epsilon > 0$ one can define the infinite covering for K^* given by the balls $B(p;\, \epsilon/2)$ for every $p \in K^*$; thus there exists a finite subcovering $\{B_l\}_{l=1}^m$, with $m \in \mathbb{N}$, where

$$B_l = B(p^l;\, \epsilon/2) := \{p \in \mathcal{F}^* \,|\, \|p - p^l\|_* < \epsilon/2\}, \qquad l = 1,\, 2,\, \ldots,\, m.$$

The subcovering is such that

$$K^* \subset \bigcup_{l=1}^{m} B_l. \tag{5.41}$$

Here we are using the Definition 5.4 of [3] for compactness repeated in Definition 5.8.

Thus, for K and the fixed value $\epsilon > 0$ we can define the infinite covering given by the balls $B(p;\, \epsilon)$ for every $p \in K$; now we will verify that exists a finite subcovering, by using the points p^l above.

For any $p := (\eta,\, A_1,\, A_2,\, \ldots) \in K$ set

$$p^* := (\eta,\, A_1,\, \ldots,\, A_{n^*-1},\, 0,\, \ldots) \in \mathcal{F}^* \subset \mathcal{F}.$$

Because $p^* \in K^*$ we notice from (5.41) that there exists $l \in \{1,\, \ldots,\, m\}$ such that

$$\|p^* - p^l\| = \|p^* - p^l\|_* < \epsilon/2, \tag{5.42}$$

therefore using Minkowski inequality, the bound in (5.37) for all $k \in \mathbb{N}$, the estimate in (5.39) and the expression (5.42), we have

$$\|p - p_l\| \;\leq\; \|p - p^*\| + \|p^* - p^l\| \;=\; \sum_{k=n^*}^{\infty} \frac{|A_k|}{\lambda_k} + \|p^* - p^l\|_* \tag{5.43}$$

$$<\; \frac{M}{C\mathcal{N}} \sum_{k=n^*}^{\infty} \lambda_k^{-2} + \frac{\epsilon}{2} \;<\; \frac{M}{C\mathcal{N}} \frac{\epsilon C\mathcal{N}}{2M} + \frac{\epsilon}{2} \;=\; \epsilon, \tag{5.44}$$

Therefore $\{B(p^l;\, \epsilon)\}_{l=1}^m$ is a finite cover for K. Thus the latter is a compact set. □

A classical result shows that any compact set is **sequentially compact**, see [3], which means that from every sequence in a compact set A, one can select a convergent subsequence with limit in A. Notice that $B[\eta^-,\, \eta^+]$ is only pre-compact in $\mathcal{F}$, so the limit of any convergent subsequence lies in K, not necessarily in $\mathcal{B}$.

We define, in the usual manner, the ω-limit of a point $p \in \mathcal{F}$ as the set

$$\omega(p) := \left\{ q \in \mathcal{F} \,\middle|\, \exists \{t_k\}_{k\in\mathbb{N}} \text{ such as } 0 \leq t_k \to \infty \text{ as } k \to \infty \text{ and } \lim_{t_k \to \infty} \varphi(t_k;\, p) = q \right\}. \tag{5.45}$$

Now we are able to discuss the difference between the dynamics of ODE systems in finite dimensions as compared to the dynamics of ODE systems in Banach or Hilbert spaces. Notice that in finite dimensions an invariant set always contains its ω-limit (if $\omega(p)$ exists). For our case, we proved in Claim 5.2 that the orbits $\varphi(t;\, p)$ belong to $\mathcal{D}$ for all $t > 0$; however inspecting the definition of the ω-limit given in (5.45) we see that $\omega(p)$ is given by a convergent sequence. So, the orbits belong to $\mathcal{D}$, which is a dense subspace of $\mathcal{F}$. Thus, the ω-limit belongs to the whole space $\mathcal{F}$, not necessarily to $\mathcal{D}$.

The following definition is borrowed from ideas in [2].

Definition 5.9 *A* **strictly invariant** *set B for a vector field $\mathcal{X}$ is defined as a positively invariant set, see Definition 5.5, such that for $p \in B$ all $\omega(p)$ belong to B.*

Hence, from Lemmas 4.5 and 5.6 and the definition of $B[\eta^-,\, \eta^+]$ in Lemma 5.7 we have the following.

Corollary 5.10 *The set $E := B[\eta^-,\, \eta^+] \cap B^{\pm}_{I,III}$ is strictly invariant for all fixed $\eta^-,\, \eta^+$.*

Proof. Notice from Lemma 5.7 that E is pre-compact and so it is bounded, then from Lemma 4.5 we know that exists $\mathcal{M}$ such that $|\eta'(t)| \leq \mathcal{M}$ for all $t \geq 0$.

Let p be any point in E. Assume that $\omega(p)$ is not empty. Let us take $q \in \omega(p)$. (Notice that if $\omega(p) = \emptyset \subset E$ is satisfied, then the Lemma is trivially satisfied.)

There exists a sequence $\{t_k\}_{k\in\mathbb{N}}$ satisfying (5.45), so the components of q are

$$q_o = \lim_{k\to\infty} \varphi(t_k;\, p)_o \quad \text{and} \quad q_n = \lim_{k\to\infty} \varphi(t_k;\, p)_n,\ \forall n \in \mathbb{N}\,. \tag{5.46}$$

Thus from (5.46) we obtain that

$$|q_o| \;=\; \lim_{k\to\infty} |\varphi(t_k;\, p)_o| \;=\; \lim_{k\to\infty} |\eta'(t_k)| \;\leq\; \mathcal{M},$$

and, since Eq. (5.13) is valid with $M = \mathcal{M}$, we also obtain

$$|q_n| \;=\; \lim_{k\to\infty} |\varphi(t_k;\, p)_n| \;\leq\; \frac{C\mathcal{M}}{\lambda_n^3}, \qquad \forall n \in \mathbb{N}\,.$$

Therefore, from definition (5.5) and recalling that S_1 given by Eq. (5.38) is finite, we notice that

$$\|q\|_D \;\leq\; \mathcal{M} + C\mathcal{M}\sum_{n\in\mathbb{N}} \lambda_n^{-2} \;=\; (1 + S_1)\mathcal{M} \;<\; \infty$$

is satisfied. Then, $\omega(p)$ belongs to $\mathcal{D}$, but from Lemma 5.6, E is positively invariant, so, $\omega(p)$ actually belongs to E and the result is proven. □

We have the following proposition, which is the infinite dimensional extension of a classical result in dynamical systems, see for example [33].

Proposition 5.11 *If a compact set $K \subset \mathcal{F}$ is positively invariant under the vector field $\mathcal{X}$, i.e., $\mathcal{X}(p)$ points to the interior of K, then for every $p_0 \in K$ we have:*

i) The ω-limit $\omega(p_0)$ is a nonempty of K.

ii) The ω-limit $\omega(p_0)$ is a compact subset in $\mathcal{F}$.

iii) The ω-limit $\omega(p_0)$ is positively invariant under the vector field $\mathcal{X}$, i.e., if $q \in \omega(p_0)$ the integral curve of $\mathcal{X}$ through q belongs to $\omega(p_0)$.

Proof. i) We have from the hypotheses that the orbit $\varphi(t;\, p_0)$ through a point $p_0 \in K$ will remain in K for all $t \geq 0$.

Let $t_k = k$ for all $k \in \mathbb{N}$ and define $\varphi_k := \varphi(t_k;\, p_0)$ for all $k \in \mathbb{N}$. Since the set K is compact, there exists a subsequence of $\{\varphi_k\}_{k\in\mathbb{N}}$, we call it $\{\varphi_j\}_{j\in\mathbb{N}}$, such that

$$\lim_{j\to\infty} \varphi_j = q, \qquad \text{with} \qquad q \in K, \tag{5.47}$$

thus, from the definition in (5.45), $q \in \omega(p_0)$. Therefore, the ω-limit is a nonempty subset of K.

ii) Since K is a compact set, we only need to prove that the subset $\omega(p_0)$ is closed. Let $q_n \to q$, with $q_n \in \omega(p_0)$, we will show that then $q \in \omega(p_0)$. Since $q_n \in \omega(p_0)$, then for each q_n there $\exists\{t_k^{(n)}\}_{k\in\mathbb{N}}$ such as $t_k^{(n)} \to \infty$ and $\varphi(t_k^{(n)};\, p_0) \to q_n$, as $k \to \infty$.

For every $\epsilon > 0$ there exists a natural number $n^* > 2/\epsilon$ such that $\|q_n - q\| < \epsilon/2$ for all $n \geq n^*$. Now, we choose for each sequence $\{t_k^{(n)}\}_{k\in\mathbb{N}}$, $n \geq n^*$ an element $\tau_n := t_{k(n)}^{(n)} > n$ such that $\|\varphi(\tau_n;\, p_0) - q_n\| < 1/n$. Then for all $n \geq n^*$

$$\|\varphi(\tau_n;\, p_0) - q\| \leq \|\varphi(\tau_n;\, p_0) - q_n\| + \|q_n - q\| < \frac{1}{n} + \frac{\epsilon}{2} \leq \epsilon. \tag{5.48}$$

Therefore $\varphi(\tau_n;\, p_0) \to q$, and because $\tau_n \to \infty$ when $n \to \infty$, we have that $q \in \omega(p_0)$, so the ω-limit is a closed set, and therefore a compact subset of K.

iii) Since $q \in \omega(p_0)$, there exists a sequence $\{t_j\}_{j\in\mathbb{N}}$ such as $t_j \to \infty$ and $\varphi_j \to q$ when $j \to \infty$. Let $q^s := \varphi(s;\, q)$, for fixed $s > 0$. We will show that $q^s \in \omega(p_0)$. Because φ depends continuously on the initial condition, we have

$$q^s = \varphi(s;\, q) = \varphi\Big(s;\, \lim_{j\to\infty} \varphi_j\Big) = \lim_{j\to\infty} \varphi\big(s;\, \varphi_j\big) = \lim_{j\to\infty} \varphi\big(s;\, \varphi(t_j;\, p_0)\big) = \lim_{j\to\infty} \varphi(s + t_j;\, p_0),$$

so, the sequence $\{s_j\}_{j\in\mathbb{N}}$ for $s_j := s + t_j$ is such that $s_j \to \infty$ and $\varphi(s_j;\, p_0) \to q^s$ when $j \to \infty$. Therefore $q^s \in \omega(p_0)$. □

Because of our intention to maintain the original structure of the proof by Sotomayor of the Proposition 5.11 (in [33]), we assumed that K is a compact set, which is the only modification relative to the original proof in finite dimensions. Moreover, notice that we obtain same result of Proposition 5.11 for a set K that is strictly invariant instead of compact and positively invariant, see Definition 5.9.

5.2.2 The long time behavior from restricted initial data

In this Section we present the asymptotic behavior for orbits restricted to the initial data described previously.

Theorem 5.12 *The ω-limit for any orbit starting at a point in B_I is X_I. The ω-limit for any orbit starting at a point in B_{III} is X_{III}.*

Proof. We prove the theorem only for orbits starting in B^+_{III}, the other cases are analogous. The geometrical idea is simple, see Fig. 5.2: if $p \in B^+_{III}$, then $\mathcal{X}_o(p) \leq 0$; if $\mathcal{X}_o(p) = 0$ then p is on the upper boundary U^+_{III}, so we expect that the other components of the vector field $\mathcal{X}(p)$ drive the orbit towards the interior of B^+_{III}, where the strict inequality $\mathcal{X}_o(p) < 0$ holds, so that the first component of the orbit $\varphi(t)$ always decreases. Therefore it is expected that the "pyramidal" shape of B^+_{III} implies the convergence to X_{III}.

Take $p_* = (\eta_*, a_1, a_2, \dots) \in B^+_{III}$ and define the set

$$B_* := B^+_{III}[\theta_{III}, \eta_*] = \big\{p \in B^+_{III} \,\big|\, \eta \in [\theta_{III}, \eta_*]\big\}, \tag{5.49}$$

which is pre-compact in $\mathcal{F}$, because B_* is a subset of the pre-compact set $B[\theta_{III}, \eta_*]$, see Lemma 5.7. We will prove that the ω-limit of the orbit $\varphi(t)$ through p_* is X_{III}.

First of all, we exclude the case $p_* = X_{III}$ because the proposition is true in this case. We know from Lemma 5.6 that at any $p \in \partial B^+_{III}$ the vector field $\mathcal{X}(p)$ points into B^+_{III}. The only part of the boundary of B_* that remains to be analyzed is the boundary at $\eta = \eta_*$. In this case notice that p lies also in the interior of B^+_{III}, where $\mathcal{X}_o(p) < 0$, so the vector field points inside B_* for every $p \in \partial B_*$. Therefore the orbit $\varphi(t;\, p)$ through a point $p \in B_*$ will remain in B_* for all $t \geq 0$. Thus B_* is positively invariant.

First step: For every $p_0 \in B_*$ we have that the ω-limit $\omega(p_0)$ is a nonempty, positively invariant compact subset of B_*.
From Proposition 5.11 we know that the ω-limit set is a compact subset of the compact set $K := \mathrm{cl}\,(B_*)$. From Corollary 5.10 we have that B_* is strictly invariant, see Definition 5.9, so $\omega(p_0)$ belongs to B_*.

Second step: The ω-limit of $p_0 \in B_*$ is a subset of the upper boundary U^+_{III}.
From Proposition 5.11 and the first step we know that $\omega(p_0)$ is a positively invariant subset of the pre-compact set B_*. We will show that if $q \in \omega(p_0)$ then $\mathcal{X}_o(q) = 0$, which implies $q \in U^+_{III}$, see (5.29).

Assume that $q \notin U^+_{III}$. Then $\mathcal{X}_o(q) = -c < 0$ for a positive real number c. Because of the continuity of $\varphi(t;\, q)$ and of $\mathcal{X}_o$, we know that for every $\epsilon \in (0,\, c)$ there exists $\delta > 0$ such that $\mathcal{X}_o\big(\varphi(t;\, q)\big) < -c + \epsilon/2 < -\epsilon/2$ for all $t \in [0,\, \delta]$. Then, by defining the projection

$$\pi_o : \mathcal{D} \longrightarrow \mathbb{R} \qquad \text{by} \qquad \pi_o p := \eta, \text{ where } p := (\eta, A_1, A_2, \dots), \tag{5.50}$$

we have that for $q^\delta := \varphi(\delta;\, q)$ the relation $\pi_o\varphi(\delta;\, q) < \pi_o q - \delta\epsilon/2$ is satisfied, so

$$\|q - q^\delta\| \geq |\pi_o q - \pi_o\varphi(s;\, q)| > \frac{\delta\epsilon}{2}. \tag{5.51}$$

Notice that a $t > 0$ such that $\varphi(t;\, q^\delta) = q$ does not exist, because $\mathcal{X}_o(p) \leq 0$ for all $p \in B_*$. In particular for $s < t$, we have $\pi_o\varphi(t;\, q) \leq \pi_o\varphi(s;\, q)$, so if $\varphi(s;\, p_0)$ is close to q^δ, there is no $t > s$ such that $\varphi(t;\, p_0)$ is close to q.

Clearly, q^δ lies in the orbit of q, *i.e.*, it is part of $\omega(p_0)$, so there exists an increasing sequence $\{s_l\}_{l\in\mathbb{N}}$ such that $\varphi_l := \varphi(s_l;\, p_0) \to q^\delta$ when $l \to \infty$. Moreover, $q \in \omega(p_0)$ means

that there exists an increasing sequence $\{t_j\}_{j\in\mathbb{N}}$ such that $\varphi_j := \varphi(t_j;\, p_0) \to q$ as $j \to \infty$. We see that there exist $J_o,\, L \in \mathbb{N}$ such that

$$\|\varphi_j - q\| < \frac{\delta\epsilon}{4}, \quad \forall j \geq J_o \qquad \text{and} \qquad \|\varphi_l - q^\delta\| < \frac{\delta\epsilon}{4}, \quad \forall l \geq L, \tag{5.52}$$

which means that there exist two balls of radii $\delta\epsilon/4$ centered at q and q^δ that are disjoint, and this fact will be show to lead to a contradiction.

From the second equation in (5.52) and the distance between q and q^δ, we have that for every $t > s_L$:

$$\|\varphi(t;\, p_0) - q^\delta\| < \frac{\delta\epsilon}{4} \qquad \text{and} \qquad \|\varphi(t;\, p_0) - q\| > \frac{\delta\epsilon}{4}, \tag{5.53}$$

but $t_j \to \infty$ when $j \to \infty$, then there exists $J_1 \in \mathbb{N}$ such that $t_j > s_L$ for all $j \geq J_1$. So, for $J := \max\{J_o,\, J_1\}$, we have $t_j > s_L,\, \forall j \geq J$ and then (5.52.a) and (5.53.b) can not be satisfied simultaneously, which is clearly a contradiction. Therefore $q \in U^+_{III}$ and $\omega(p_0) \subset U^+_{III}$.

Third step: From second step we conclude that the first coordinate of $q \in \omega(p_0)$ is a certain value $\tilde{\eta}$, because $\mathcal{X}_o(q) \equiv 0$. If we assume that $\tilde{\eta} \neq \theta_{III}$ we get a contradiction as follows: from Property (*iii*) of Proposition 5.11 we have that $\varphi(t;\, q) \in \omega(p_0)$ for all times t, and the second step guarantees that $\varphi(t;\, q) \subset U^+_{III}$, but on this upper boundary the vector field points inside B^+_{III} and the orbit $\varphi(t;\, q)$ escapes from U^+_{III}!

Otherwise, if $\tilde{\eta} = \theta_{III}$, then $\mathcal{X}_o(q) = 0$ and $\mathcal{X}_n(q) = 0$ for all $n \in \mathbb{N}$ and all claims are true, therefore $\omega(p_0) = X_{III}$ is the unique global attractor for $p_0 \in B^+_{III}$. □

Using Lemma 5.6 and Proposition 5.12 we note that X_I and X_{III} are (for restricted initial data) the only two attractors of the nonlinear problem (1.23)-(1.27). Indeed, if $\eta(0)$ and $\mathcal{U}_o(x)$ are such that $p = (\eta(0),\, A_1(0),\, A_2(0),\, \dots)$ belongs to $B^\pm_{I,III}$ we have proved that B_I and B_{III} lie in the attractor basins of X_I and X_{III}. Noticing also that X_I (resp. X_{III}) is related with $\varrho_I(x)$ (resp. $\varrho_{III}(x)$), we see that the long time behavior is dermined by the relative position of the initial condition $\eta(0)$ with respect to the equilibrium θ_{II}.

The previous statements can be rephrased in terms of PDE language using Eq. (4.29). We can compare the initial Cauchy data $\theta_i(x)$ directly with the unstable steady-state $\varrho_{II}(x)$. In particular, if $\theta_i(x) = R(x,\, 0)$ we observe that the spectral solution $\mathcal{U}(x,\, t)$ given in Eq. (4.15) has initial data $A_n(0) = 0,\, \forall n \in \mathbb{N}$. Therefore using Eq. (4.21), we note that any orbit with such initial condition enters into a region where all the signs of the A_n are the same; the common sign is determined by the sign of $\mathcal{G}(\eta(0))$. Thus, the orbit enters into one of the $B^\pm_{I,III}$. In summary, we see that the value of $\eta(0)$ determines which equilibrium will be the limiting solution. Indeed, we recover the same conclusions found for the reduced model in Sec. 2.3.

Remark 5.13 *As a conjecture, we expect that for the dynamics on whole domain $\mathcal{D}$ there exists a manifold $\mathcal{S}^+$ of codimension 1, the* stable manifold *of X_{II}. This manifold splits the space into two regions; each region is the basin of attraction of X_I or X_{III}. However, every point $p \in \mathcal{S}^+$ has X_{II} as its ω-limit. The basin of attraction of these three points is the whole infinite dimensional space.*

Chapter 6

Concluding remarks

If knowledge is always the product of an active mind,
one has to find in the mind itself the criteria
through which certain truth may be distinguished
for uncertain appearances.
Reneé Descartes.

The solution of the nonlinear problem can be written as the superposition of two parts, one that is very persistent while the other is ephemeral. The persistent part is a time-dependent multiple of the stationary solution in the heat conducting reactor, which solves the reduced model; this multiplier represents the history of the injection temperature. The other one consists of modes that decay linearly very fast.

Thus, we have shown that the evolution of the whole nonlinear system for a given initial state is governed essentially by the persistent solution. We are able to calculate in a very simple way the dynamics of the persistent solution by analyzing the corresponding "reduced model". In this model, depending on parameters there are either one or three equilibria. In the latter case, two of them corespond to "extinction" and "combustion", while the other equilibrium separates the two attraction domains. This picture for the solution was obtained initially by numerical simulations.

A linear stability analysis near the equilibria was performed rigorously for the complete model; they behave exactly as could be expected from the reduced model. Indeed, the reduced model is a very useful global approximation for the complete model for large times.

We were able to prove the existence and uniqueness for all times for the initial value problem through a nonlinear Volterra integral equation in time, whose unknown is the history of the injection temperature. Smoothness properties of the solution were established.

We used a spectral decomposition to rewrite the Cauchy problem as a nonlinear system with an infinite number of ODE's. We were able to prove rigorously that the complete system has the same asymptotic behavior as the reduced model, at least for a set of initial data that had to be restricted for technical reasons.

We were able to show that the two situations that lead to combustion as a final state are: initial conditions with large γ within a single steady-state equilibrium model, which is related to combustion or, for the three steady-state model, temperatures at the reaction region higher than the middle equilibrium. In summary, we require

$$\gamma s_{\mathcal{N}} > \begin{cases} \Xi(\theta_M), & \theta(1,\, t) \leq \theta_M \\ \Xi(\eta(t)), & \theta(1,\, t) \in [\theta_M,\, \theta_m] \\ \Xi(\theta_m), & \theta(1,\, t) \geq \theta_m. \end{cases}$$

By examining Fig. 6.1 we notice that for initial states $(\Xi,\, \theta)$ in the shaded region time evolution leads to ignition.

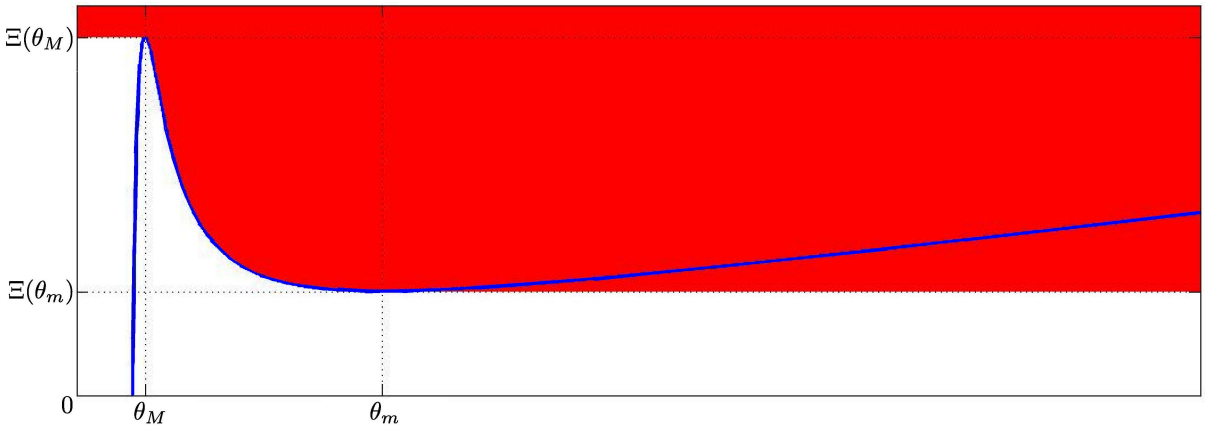

Figure 6.1: The $\Xi(\theta)$ function in Eq. (2.11) and its extrema define the global behavior; initial states in the shaded region are led to ignition, initial states in the white region are led to extinction.

Appendix A

Eigenvalues and eigenvectors for the linearized models

In this Appendix we study the eigenvalues and eigenfunction of system (3.13)-(3.16) for each geometry. From the analysis in Chapter 3, Sec. 3.2, we know that the eigenproblem (3.13)-(3.16) (for $\mathcal{N} = 1,\ 2,\ 3$) has a self-adjoint operator associated, so the spectrum lies in the real axis. Because we work in a finite domain $[0,\ L]$, we assume that the spectrum reduces to (countable) isolated eigenvalues, however, we do not prove this fact. (This fact may be proven using Sturm-Liouville theory, see *e.g.* [14].)

We work only in the interval $x \in [1,\ L]$ neglecting Eq. (3.16), because the eigenfunctions are constant in $[0,\ 1]$; its value in this interval originates from the value given by continuity at $x = 1+$. However, the orthogonality holds in $[0,\ L]$ and we write down the solution explicitly for x in $[0,\ L]$.

In the end, we will have found the eigenfunctions for $\mathcal{N} = 1,\ 2,\ 3$ for linear perturbations around each of the steady-state solutions $\varrho_I(x)$, $\varrho_{II}(x)$, $\varrho_{III}(x)$ defined in Eq. (2.20). All the eigenvalues are negative except for a positive one corresponding to the $\varrho_{II}(x)$ equilibrium. Moreover, the case of a unique stationary solution is related to $\varrho_I(x)$ or $\varrho_{III}(x)$ because all of the eigenvalues are negative. We do not discuss this case explicitly.

A.1 Eigenvalues and eigenvectors in 1D

Let us rewrite the eigenvalue problem (3.13)-(3.16) for $\mathcal{N} = 1$, in $[0,\ L]$:

$$\begin{cases} \dfrac{d^2X(x)}{dx^2} = \lambda X(x) & x \in [1,\ L] \quad \text{(A.1)} \\ \sigma X(1) + X'(1+) = \lambda X(1) & \quad \text{(A.2)} \\ X(L) = 0 & \quad \text{(A.3)} \\ X(x) = X(1) & x \in [0,\ 1]. \quad \text{(A.4)} \end{cases}$$

A.1.1 The growing mode

Take $\lambda = \beta^2$. Because β or $-\beta$ give rise to the same solution, for convenience we take $\beta \in \mathbb{R}^+$. Solving Eq. (A.1), we have for $\beta > 0$

$$X(x) = A\exp(\beta x) + B\exp(-\beta x), \tag{A.5}$$

where A and B depend on β. Substituting Eq. (A.5) in Eq. (A.3) we get $B = -A\exp(2\beta L)$. Substituting this expression in Eq. (A.2), we obtain

$$\frac{\beta^2 - \sigma}{\beta}\frac{\exp(\beta) - \exp(2\beta L - \beta)}{\exp(\beta) + \exp(2\beta L - \beta)} = 1. \tag{A.6}$$

We want to determine whether there is a $\beta \in \mathbb{R}^+$ that satisfies (A.6). We multiply the numerator and denominator of (A.6) by $\exp(-\beta L)$; using $d = L - 1$, see Eq. (2.6), we obtain

$$\frac{\sigma - \beta^2}{\beta}\frac{\sinh(\beta d)}{\cosh(\beta d)} = 1. \tag{A.7}$$

Let us define, for $\beta \geq 0$

$$F(\beta) := \frac{\sigma - \beta^2}{\beta}\tanh(\beta d). \tag{A.8}$$

So Eq. (A.7) is the same as

$$F(\beta) = 1. \tag{A.9}$$

Notice that

$$\lim_{\beta \to 0} F(\beta) = \sigma d \tag{A.10}$$

so that $F(\beta)$ is well defined from the right at $\beta = 0$.

Let us examine the derivative of $F(\beta)$,

$$F'(\beta) = \frac{\beta d}{\beta^2\cosh^2(\beta d)}\left[(\sigma - \beta^2) - (\sigma + \beta^2)\frac{\sinh(\beta d)}{\beta d}\cosh(\beta d)\right]. \tag{A.11}$$

Because $\sinh(\beta d)/(\beta d) \geq 1$, $\cosh(\beta d) \geq 1$ and $\sigma(\theta_o) > 0$, see Eq. (3.3), the term in the brackets satisfies

$$\begin{aligned}\sigma - \beta^2 - (\sigma + \beta^2)\frac{\sinh(\beta d)}{\beta d}\cosh(\beta d) &\leq (\sigma + \beta^2) - (\sigma + \beta^2)\frac{\sinh(\beta d)}{\beta d}\cosh(\beta d) \\ &= (\sigma + \beta^2)\left(1 - \frac{\sinh(\beta d)}{\beta d}\cosh(\beta d)\right) < 0,\end{aligned} \tag{A.12}$$

therefore, $F'(\beta) < 0$ for $\beta > 0$. So, taking into account (A.10), $F(\beta)$ is monotone decreasing for $\beta \in [0, \infty)$ and takes values from σd to $-\infty$. Moreover, it is clear from (A.8) that $F(\beta) \to -\infty$ as $\beta \to \infty$. Hence, for a root of $F(\beta) = 1$ to exist, it is necessary and sufficient that $\sigma d > 1$.

Notice that if $\sigma d = 1$, then $\beta = 0$ and so $\lambda = 0$, therefore the associated eigenfunction that satisfies Eq. (A.1) is $X_o(x) = a\,r(x)$ with constant a, see Eq. (2.6). Notice that the right boundary condition (A.2) is trivially satisfied. However, in order to satisfy the

left boundary condition (A.3) we must take $a = 0$. The reason why this "eigenfunction" vanishes identically is because this mode was originally removed from the initial condition for $\vartheta(x,\, t)$ in Eq. (3.4).

Using the definition of σ in (3.3) and $s(1) = d$ from Eq. (2.8), we obtain that if

$$\sigma(\theta_o)d > 1, \quad \text{then} \quad \gamma d \exp(-1/\theta_o) > \theta_o^2. \tag{A.13}$$

Manipulating (2.9) for $s(1) = d$ leads to

$$\gamma d \exp(-1/\theta_o) = \theta_o - \theta_L. \tag{A.14}$$

Comparing (A.13) and (A.14), a common root β exists if and only if

$$0 > \theta_o^2 - \theta_o + \theta_L \tag{A.15}$$

is satisfied. This requires that $\theta_o \in (\theta_M,\, \theta_m)$, given in Eqs. (2.13). In the plot of Eq. (2.11) shown in Fig. 2.1 and Fig. 2.3, we see that when we have only one stationary solution, θ_o will be either θ_I or θ_{III}; these two values lie always outside of $(\theta_M,\, \theta_m)$, so they do not satisfy (A.15), therefore the unstable mode does not exists. Thus, we have proved the following claim.

Claim A.1 *In the context of the eigenproblem given in Eqs.* (A.1)-(A.3)*, the equilibria associated to θ_I and θ_{III} have no unstable mode, while the equilibrium associated to θ_{II} has always an unstable mode.*

We use the equality

$$\exp(\beta x) - \exp\big(\beta(2L - x)\big) \;=\; -2\exp(\beta L)\sinh\big(\beta(L - x)\big) \tag{A.16}$$

in Eq. (A.5) to compute the eigenfunction associated with the eigenvalue β satisfying (A.9) as

$$X_o(x) := \begin{cases} C_o \sinh\big(\beta d\big), & x \in [0,\, 1], \\ C_o \sinh\big(\beta(L - x)\big), & x \in [1,\, L], \end{cases} \tag{A.17}$$

where C_o is a suitable positive constant to normalize this eigenfunction in the space $L^2[0,\, L]$. It is computed in Remark A.2 at the end of the section that follows.

A.1.2 Decaying modes

We now look for negative eigenvalues. Take $\lambda = -\alpha^2$ and notice that α and $-\alpha$ give rise to the same solution, so for convenience we take $\alpha \in \mathbb{R}^-$. From Eq. (A.1), we have

$$X'' + \alpha^2 X = 0.$$

It follows that $X(x)$ is a linear combination of sines and cosines with argument αx. From Eq. (A.3) we have $X(L) = 0$, so it is better to write

$$X(x) = A \sin(\alpha(L - x)), \tag{A.18}$$

where $A = A(\alpha)$ is a constant. Using (A.18) into Eq. (A.2), we get

$$(\sigma + \alpha^2)\sin(\alpha d) = \alpha\cos(\alpha d).$$

This can be rewritten as

$$F(\alpha) := \frac{\sigma + \alpha^2}{\alpha}\tan(\alpha d) = 1, \qquad \alpha < 0. \tag{A.19}$$

It will be shown soon that it can be extended smoothly to $F(0) = \sigma d$ for $\alpha = 0$.

Notice that $F(\alpha)$ is not defined for $\alpha = -n\pi/d$, $\forall n \in \mathbb{N}$, because of the tangent function asymptotes. Yet, we claim that $F(\alpha)$ is a monotone decreasing function in each interval $\alpha \in (-(n+1)\pi/d,\, -n\pi/d)$ for all $n = 0,\, 1,\, 2,\, \cdots$. Indeed

$$F'(\alpha) = \frac{\alpha d}{\alpha^2\cos^2(\alpha d)}\left[(\alpha^2 + \sigma) + (\alpha^2 - \sigma)\frac{\sin(\alpha d)}{\alpha d}\cos(\alpha d)\right]; \tag{A.20}$$

because the first fraction on the RHS of (A.20) is negative and the expression within brackets remains positive, so $F'(\alpha) < 0$ wherever it is defined; in fact, recalling that $\sigma > 0$ from (3.3)

$$\left|(\alpha^2 - \sigma)\frac{\sin(\alpha d)}{\alpha d}\cos(\alpha d)\right| < (\alpha^2 + \sigma)\left|\frac{\sin(\alpha d)}{\alpha d}\right||\cos(\alpha d)| \le \alpha^2 + \sigma, \tag{A.21}$$

from the classical result that $|\sin(x)/x| \le 1$ and also $|\cos(x)| \le 1$ for all $x \in \mathbb{R}$. Therefore, inspecting $F'(\alpha)$ in (A.20), we notice that is negative whenever $\cos(\alpha d) \neq 0$.

Therefore, comparing $F(\alpha) = 1$, both sides of (A.19), we see that there is exactly one root α_n in each interval $(-(n+1)\pi/d,\, -n\pi/d)$ with $n \in \mathbb{N}$ and when the unstable mode does not exist, there is another root in the interval $(-\pi/d,\, 0)$. The roots form a countable decreasing sequence of eigenvalues tending to $-\infty$. Each of these eigenvalues has an associated eigenfunction

$$X_n(x) := \begin{cases} C_n \sin\big(\alpha_n d\big), & x \in [0,\, 1], \\ C_n \sin\big(\alpha_n (L - x)\big), & x \in [1,\, L], \end{cases} \tag{A.22}$$

where C_n are suitable positive constants for normalizing the eigenfunctions in the space $L^2[0,\, L]$, see Remark A.2 that follows.

Remark A.2 *In Chapter 3 we showed that the eigenfunctions of the eigenproblem (3.13)-(3.16) form a complete set in $L^2[0,\, L]$. However, here we found the eigenfunctions in the domain $x \in [1,\, L]$. It is interesting to see that the problem "remembers" its physical origins; for the eigenfunctions to be orthogonal it is necessary to extend the eigenfunction as (3.16), and the extended eigenfunctions are orthogonal in the domain $x \in [0,\, L]$.*

Furthermore, we normalize the eigenfunctions in the space $L^2[0,\, L]$ by multiplying $X_o(x)$ in (A.17) by $C_o := \big(\sinh^2(\beta d) + \sinh(2\beta d)/(2\beta) - d/2\big)^{-1/2}$ and $X_n(x)$ in (A.22) by $C_n := \big(\sin^2(\alpha_n d) - \sin(2\alpha_n d)/(2\alpha_n) + d/2\big)^{-1/2}$.

A.1.3 The eigenvalue finder

We have used the negative sign for α just to emphasize that the positive eigenvalue β corresponds to the unstable mode, while the negative eigenvalues α_n correspond to the stable modes; as shown in Secs. A.1.1 and A.1.2. This arrangement is convenient because it allows us to plot all the eigenvalues in a single graph.

We can redefine the function in (A.8), (A.19) as $F(y)$ below, using positive y for β and negative y for α, as follows:

$$F(y) := \begin{cases} \dfrac{\sigma + y^2}{y} \tan\big(yd\big) & y < 0 \\ \sigma d & y = 0 \\ \dfrac{\sigma - y^2}{y} \tanh\big(yd\big) & y > 0. \end{cases} \tag{A.23}$$

Now the roots of $F(y) = 1$ define all the eigenvalues; positive y correspond to the eigenvalues $\lambda = y^2$ analyzed in Sec. A.1.1, and negative y correspond to the eigenvalues $\lambda = -y^2$ analyzed in Sec. A.1.2. Notice that $\lambda = (\operatorname{sign} y)y^2$. Moreover, $F(y)$ is a monotone decreasing function whenever it is defined, so the eigenvalues form a sequence that tends to $-\infty$.

The plot of $F(y)$ is shown in Fig. A.1. From the limit (A.10) and

$$\lim_{y \to 0-} \frac{\sigma + y^2}{y} \tan\big(yd\big) = \sigma d,$$

we see that $F(y)$ is a continuous function at $y = 0$, for any σ or L. If we let σ and L change continuously so that σd becomes less than 1, then the positive eigenvalue ceases to exist, because it becomes a negative eigenvalue. This is a very nice property, as it explains the change in nature of the spectrum of the equilibria, *i.e.*, the bifurcation properties of the equilibria.

It is possible also to show even more, the function $F(y) \in \mathcal{C}^\infty(\mathbb{R})$ and is monotone decreasing except for $y = -n\pi/d$, $n \in \mathbb{N}$, where is not defined, and at $y = 0$.

Taylor expansion shows that $F(y)$ is also $\mathcal{C}^1$ close to $y = 0$.

A.2 Eigenvalues and eigenvectors in 2D

Let us rewrite the eigenvalue problem (3.13)-(3.16) for $\mathcal{N} = 2$ in $[0,\, L]$:

$$\begin{cases} \dfrac{1}{x}\dfrac{d}{dx}\left(x\dfrac{dX(x)}{dx}\right) = \lambda X(x) & x \in [1,\, L] & \text{(A.24)} \\ \sigma X(1) + 2X'(1+) = \lambda X(1) & & \text{(A.25)} \\ X(L) = 0 & & \text{(A.26)} \\ X(x) = X(1) & x \in [0,\, 1]. & \text{(A.27)} \end{cases}$$

We need the theory of Bessel functions, which is summarized in Appendix C.

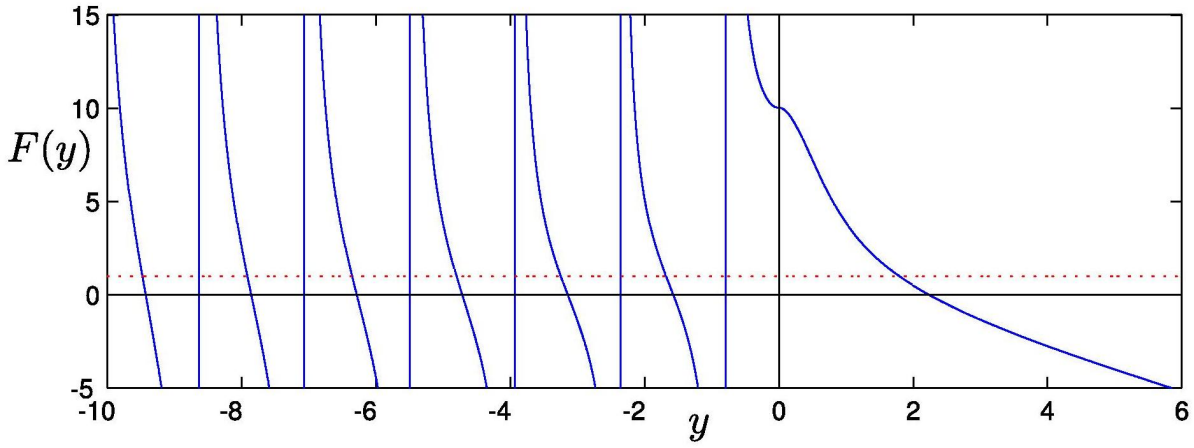

Figure A.1: Plot of the eigenvalue finder $F(y)$ for $\mathcal{N} = 1$. The positive and negative eigenvalues are determined by $F(y) = 1$. The dotted line corresponds to the constant function equal to 1. Along the positive axis we represent the condition for the existence of a positive eigenvalue β. Along the negative axis we represent the conditions that define the negative eigenvalues. Here we note that there exists at most one positive eigenvalue.

A.2.1 The growing mode

We are looking for positive eigenvalues λ, so we set $\lambda = \beta^2$ and notice that β or $-\beta$ give the same solution, so for convenience we take $\beta \in \mathbb{R}^+$. We solve the ordinary differential equation (A.24) for this value, *i.e.*,

$$X'' + \frac{1}{x}X' - \beta^2 X = 0. \tag{A.28}$$

It is known that one of the two independent solutions of (A.28) is the *modified Bessel function of the third kind with parameter* $p = 0$, $I_0(\beta x)$, see Eq. (C.23). The other solution is given by the *Macdonald function with parameter* $n = 0$, $K_0(\beta x)$, see Eq. (C.24). Then, the solution of equation (A.28) is given by

$$X_\beta(x) = AI_0(\beta x) + BK_0(\beta x), \qquad \text{for } x \in [1,\, L]. \tag{A.29}$$

Here A and B are constants to be determined from the boundary conditions. From Eq. (A.26), we see that $X_\beta(L) = 0$, so

$$BK_0(\beta L) = -AI_0(\beta L), \tag{A.30}$$

and we can write

$$X_\beta(x) = \begin{cases} C_o\big[I_0(\beta)K_0(\beta L) - I_0(\beta L)K_0(\beta)\big], & x \in [0,\, 1], \\ C_o\big[I_0(\beta x)K_0(\beta L) - I_0(\beta L)K_0(\beta x)\big], & x \in [1,\, L], \end{cases} \tag{A.31}$$

for a suitable constant C_o that normalizes the eigenfunction in the weighted space $L^2_2[0,\, L]$ defined in (3.34).

Now we use the left boundary condition, Eq. (A.25), obtaining that the values of β must be roots of

$$\frac{\beta^2-\sigma}{2\beta}\frac{I_0(\beta)K_0(\beta L)-I_0(\beta L)K_0(\beta)}{I_1(\beta)K_0(\beta L)+I_0(\beta L)K_1(\beta)}=1, \tag{A.32}$$

because $I_0'(x)=I_1(x)$ and $K_0'(x)=-K_1(x)$, see Property (5) in Appendix C and the identity (C.22).

A.2.2 Decaying modes

Now we take $\lambda=-\alpha^2$ and notice that α and $-\alpha$ give rise to the same solution, so for convenience we take $\alpha\in\mathbb{R}^-$. From Eq. (A.24) we obtain the ordinary differential equation

$$X''+\frac{1}{x}X'+\alpha^2X=0, \tag{A.33}$$

which is known as the *Bessel equation with parameter* $p=0$ (sometimes, order $p=0$). It has two independent solutions, the *Bessel functions of first- and second-kind with parameter* $p=0$, J_0 and Y_0, respectively, see Eqs. (C.2) and (C.3). Therefore the solution $X_\alpha(x)$ is written as

$$X_\alpha(x)=AJ_0(\alpha x)+BY_0(\alpha x),\qquad \text{for } x\in[1,\, L]. \tag{A.34}$$

Here A and B are constants to be determined by the boundary conditions. From Eq. (A.26), we see that $X_\alpha(L)=0$, so, as in (A.31) we obtain

$$X_\alpha(x)=\begin{cases} C_\alpha\big[J_0(\alpha)Y_0(\alpha L)-J_0(\alpha L)Y_0(\alpha)\big], & x\in[0,\,1],\\ C_\alpha\big[J_0(\alpha x)Y_0(\alpha L)-J_0(\alpha L)Y_0(\alpha x)\big], & x\in[1,\,L],\end{cases} \tag{A.35}$$

for suitable constants C_α which normalize the eigenfunctions in the $L^2_2[0,\, L]$ space.

From the left boundary condition (A.25), $2X_\alpha'(1)+(\alpha^2+\sigma)X_\alpha(1)=0$, so we search for values of α that satisfy

$$-\frac{\alpha^2+\sigma}{2\alpha}=\frac{J_0'(\alpha)Y_0(\alpha L)-J_0(\alpha L)Y_0'(\alpha)}{J_0(\alpha)Y_0(\alpha L)-J_0(\alpha L)Y_0(\alpha)}. \tag{A.36}$$

Since $J_0'(x)=-J_1(x)$ and $Y_0'(x)=-Y_1(x)$, see Property (1) in Appendix C, we simply need to find the roots α of Eq. (A.36) rewritten as:

$$\frac{\alpha^2+\sigma}{2\alpha}\frac{J_0(\alpha)Y_0(\alpha L)-J_0(\alpha L)Y_0(\alpha)}{J_1(\alpha)Y_0(\alpha L)-J_0(\alpha L)Y_1(\alpha)}=1. \tag{A.37}$$

Given a value of α satisfying (A.37), we have found an eigenvalue; its corresponding eigenvector is given by (A.35).

A.2.3 The eigenvalue finder

We can construct a function that helps in finding the eigenvalues (just as we did for the 1D case in Sec. A.1.3); from the equalities (A.32) and (A.37) we write

$$F(y) = \begin{cases} \dfrac{y^2+\sigma}{2y}\,\dfrac{J_0(y)Y_0(yL) - J_0(yL)Y_0(y)}{J_1(y)Y_0(yL) - J_0(yL)Y_1(y)} & =: \; F_-(y), \qquad y<0 \\ \dfrac{\sigma \ln L}{2} & \qquad\qquad\quad y=0 \\ \dfrac{y^2-\sigma}{2y}\,\dfrac{I_0(y)K_0(yL) - I_0(yL)K_0(y)}{I_1(y)K_0(yL) + I_0(yL)K_1(y)} & =: \; F_+(y), \qquad y>0. \end{cases} \tag{A.38}$$

The value $F(y)$ for $y = 0$ is obtained by continuity of the function $F(y)$, which will be proved soon. Now the roots of $F(y) = 1$ are all the eigenvalues; positive values of y correspond to the eigenvalues $\lambda = y^2$, analyzed in Sec. A.2.1, and negative values of y correspond to the eigenvalues $\lambda = -y^2$ analyzed in Sec. A.2.2. Notice that $\lambda = (\operatorname{sign} y)y^2$. The plot of this function is shown in Fig. A.2.

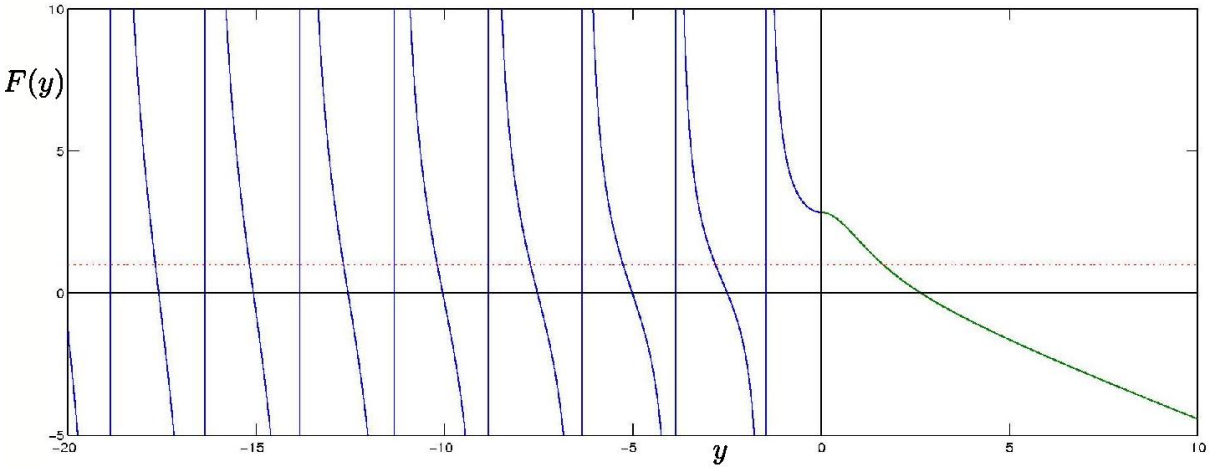

Figure A.2: Plot of the eigenvalue finder $F(y)$ for $\mathcal{N} = 2$. The positive and negative eigenvalues are determined by $F(y) = 1$. The dotted line corresponds to the constant function equal to 1. Along the positive axis we represent the condition for the existence of a positive eigenvalue β. Along the negative axis we represent the conditions that define the negative eigenvalues. Here we note that there exists at most one positive eigenvalue.

We have to verify certain properties of $F(y)$ in order to guarantee that we will find all of the eigenvalues in this way. First of all, it is easy to see that the fractions without Bessel functions, $(y^2 \pm \sigma)/(2y)$, in (A.38) are antisymmetric in y. Similarly, it is not hard to see that the quotients of Bessel functions are also antisymmetric in y, because I_0, J_0, K_0, Y_0 are even functions, but for the parameter $p = 1$, the Bessel functions I_1, J_1, K_1, Y_1 are odd functions, see Property (1) in Appendix C. So, by plotting F_- and F_+ in the appropriate half lines, we are capturing all relevant roots.

Lemma A.3 *The eigenvalue finder $F(y)$ given in Eq.* (A.38) *is continuous at $y = 0$.*

Proof. First, we check that the lower limit of (A.38.a) is given by (A.38.b). The Bessel functions involved are given by their asymptotic representations around $y = 0$, see the complete calculations in Appendix C.2, obtaining

$$F_-(y) = \frac{y^2+\sigma}{2y}\,\frac{J_0(y)Y_0(yL) - J_0(yL)Y_0(y)}{J_1(y)Y_0(yL) - J_0(yL)Y_1(y)} \tag{A.39}$$

$$= \frac{\big(y^2+\sigma\big)\big(\ln L - (y/2)^2(1+L^2)(\ln L - 1) + \mathcal{O}(y^4)\big)}{2\big(1-(y/2)^2(L^2 - 2L\ln L) + \mathcal{O}(y^4)\big)}, \tag{A.40}$$

and therefore

$$\lim_{y\to 0} F_-(y) = \frac{\sigma \ln L}{2}. \tag{A.41}$$

Thus, we see that (A.38.a) tends to (A.38.b) as $y \to 0-$.

Second, we verify that the full function $F(y)$ is continuous at $y = 0$. Let w be a complex number: from definition (C.22), notice that $I_0(w) = J_0(iw)$, $K_0(w) = Y_0(iw)$, and $I_1(w) = -iJ_1(iw)$, $K_1(w) = iY_1(iw)$, so by introducing these equalities into (A.38.a), we obtain

$$F_-(iw) = \frac{-w^2+\sigma}{2iw}\,\frac{I_0(w)K_0(wL) - I_0(wL)K_0(w)}{\frac{1}{-i}I_1(w)K_0(wL) - I_0(wL)\frac{1}{i}K_1(w)}$$

$$= \frac{w^2-\sigma}{2w}\,\frac{I_0(w)K_0(wL) - I_0(wL)K_0(w)}{I_1(w)K_0(wL) + I_0(wL)K_1(w)} = F_+(w), \tag{A.42}$$

so the limit of the analytic functions F_- and F_+ is the same for any $w \to 0$, so $F(y)$ is a continuous function. □

From the asymptotic behavior of the Bessel functions when y tends to $-\infty$, we can describe the relative size of the eigenvalues. Using Property (6) of Appendix C, when $y \ll -1$, it follows that

$$F_-(y) \approx \frac{y^2+\sigma}{2y}\,\frac{\cos(y-\pi/4)\sin(yL-\pi/4) - \cos(yL-\pi/4)\sin(y-\pi/4)}{\sin(y-\pi/4)\sin(yL-\pi/4) + \cos(yL-\pi/4)\cos(y-\pi/4)}$$

$$= \frac{y^2+\sigma}{2y}\,\frac{\sin\big(y(L-1)\big)}{\cos\big(y(L-1)\big)} = \frac{y^2+\sigma}{2y}\cot\big(y(L-1)\big). \tag{A.43}$$

In this way, the behavior of the large negative eigenvalues is very similar to the one we found for the 1D case, in Sec. A.1.2. For the behavior of the small negative eigenvalues we rely on the Bessel tools of MATLAB, see Fig. A.2, and we notice that they are very close to the eigenvalues obtained for the 1D case.

All these facts imply that the eigenvalue set is countable and it can be written as

$$\ldots < y_n < \ldots < y_2 < y_1 < 0,$$

with the property that each root y_n for $n \gg 1$ lies in the interval $(-(n+1)\pi/d,\, -n\pi/d)$. We denote each negative eigenvalue by $\alpha_n := y_n$, forming a decreasing sequence.

Similarly, we can verify that for $y \gg 1$

$$F_+(y) \approx \frac{y^2-\sigma}{2y}\coth\big(y(L-1)\big), \tag{A.44}$$

which is analogous to the result shown for the positive eigenvalue case in 1D. Then, with the MATLAB calculation for $y \geq 0$ close to origin and the behavior for large y derived analytically, we can conjecture that there is at most one positive eigenvalue. Taking into account (A.41), we see that there exists a positive eigenvalue only when

$$\frac{\sigma \ln L}{2} > 1. \tag{A.45}$$

We claim that for $y \neq 0$ that $F'(y) < 0$ is satisfied wherever it is defined. The verification is based on the following: (i) the analysis of $F(y)$ for $y \ll -1$, see (A.43), (ii) the analysis of $F(y)$ for $y \gg 1$, see (A.44) and (iii) numerical evaluation done with MATLAB close to the origin.

We have found the eigenvalues that belong to the real axis. In Sec. 3.2, we used the Friedrichs extension theorem to prove that they form a complete set (so there are no other eigenvalues).

A.3 Eigenvalues and eigenvectors in 3D

Let us rewrite the eigenvalue problem (3.13)-(3.16) for $\mathcal{N} = 3$ in $[0,\, L]$:

$$\begin{cases} \dfrac{1}{x^2}\dfrac{d}{dx}\left(x^2\dfrac{dX(x)}{dx}\right) = \lambda X(x) & x \in [1,\, L] & \text{(A.46)} \\ \sigma X(1) + 3X'(1+) = \lambda X(1) & & \text{(A.47)} \\ X(L) = 0 & & \text{(A.48)} \\ X(x) = X(1) & x \in [0,\, 1]. & \text{(A.49)} \end{cases}$$

Due to the similarities with two previous sections, we will be terse.

A.3.1 The growing mode

Take $\lambda = \beta^2$, again with $\beta \in \mathbb{R}^+$ to recover the eigenvalue. Solving Eq. (A.46), we have

$$X(x) = A\frac{\exp(\beta x)}{x} + B\frac{\exp(-\beta x)}{x}, \tag{A.50}$$

with A, B dependent on β. Substituting Eq. (A.50) in Eq. (A.48) we get $B = -A\exp(2\beta L)$. Substituting this expression in Eq. (A.47), we obtain

$$\frac{\sigma - 3 - \beta^2}{3\beta}\frac{\sinh(\beta d)}{\cosh(\beta d)} = 1. \tag{A.51}$$

Thus, we define

$$F(\beta) := \frac{\sigma - 3 - \beta^2}{3\beta} \tanh(\beta d), \qquad \beta > 0. \tag{A.52}$$

So Eq. (A.51) is the same as

$$F(\beta) = 1. \tag{A.53}$$

The eigenfunction associated to the eigenvalue β is

$$X_o(x) := \begin{cases} C_o \sinh\big(\beta d\big), & x \in [0,\, 1], \\ C_o \dfrac{\sinh\big(\beta(L-x)\big)}{x}, & x \in [1,\, L], \end{cases} \tag{A.54}$$

where C_o is a suitable constant to normalize the eigenfunction on the weighted space $L^2_3[0,\, L]$ defined in (3.34).

A.3.2 Decaying modes

We now look for negative eigenvalues. Take $\lambda = -\alpha^2$ and notice that α and $-\alpha$ give rise to the same solution, so for convenience we take $\alpha \in \mathbb{R}^-$. From Eq. (A.46), we have

$$X(x) = A\frac{\cos(\alpha x)}{x} + B\frac{\sin(\alpha x)}{x},$$

but from Eq. (A.48), we have $X(L) = 0$, so it is better to choose

$$X_\alpha(x) = C\frac{\sin(\alpha(L-x))}{x}, \tag{A.55}$$

where the constant C depends on α. Using (A.55) into Eq. (A.47), we get

$$\frac{\sigma - 3 + \alpha^2}{3\alpha} \tan(\alpha d) = 1. \tag{A.56}$$

Thus we define

$$F(\alpha) := \frac{\sigma - 3 + \alpha^2}{3\alpha} \tan(\alpha d), \qquad \alpha < 0. \tag{A.57}$$

The eigenvalues are the roots of $F(\alpha) = 1$, by comparison with Eq. (A.56).

Inspecting $F(\alpha) = 1$ we see that there is a unique root α_n for $n \in \mathbb{N}$ in each interval $(-(n+1)\pi/d,\, -n\pi/d)$. The roots form a countable decreasing sequence of eigenvalues for our model. Each of these eigenvalues has an associated eigenfunction

$$X_n(x) := \begin{cases} C_n \sin\big(\alpha_n d\big), & x \in [0,\, 1], \\ C_n \dfrac{\sin\big(\alpha_n(L-x)\big)}{x}, & x \in [1,\, L], \end{cases} \tag{A.58}$$

where C_n are suitable positive normalizing constants for the eigenfunctions in the space $L^2_3[0,\, L]$.

A.3.3 The eigenvalue finder

We have used the negative sign for α because it allows us to plot all the conditions in a single graph. We can redefine the function in (A.52), (A.57) as $F(y)$ below, using positive y for β and negative y for α, in this way:

$$F(y) := \begin{cases} \dfrac{\sigma - 3 + y^2}{3y} \tan\big(yd\big) & y < 0 \\ \dfrac{\sigma - 3}{3} d & y = 0 \\ \dfrac{\sigma - 3 - y^2}{3y} \tanh\big(yd\big) & y > 0. \end{cases} \tag{A.59}$$

Now the roots of $F(y) = 1$ are all the eigenvalues; positive y correspond to the eigenvalues $\lambda = y^2$, analyzed in Sec. A.3.1, and negative y correspond to the eigenvalues $\lambda = -y^2$ analyzed in Sec. A.3.2. Notice that $\lambda = (\operatorname{sign} y)y^2$.

Notice that $3 \times F(y)$ in Eq. (A.59) is the same as $F(y)$ in Eq. (A.23) for $\sigma - 3$ in lieu of σ. Thus, it is easy to verify that $F(y)$ in (A.52) is monotone decreasing for $y \in (0, \infty)$ taking values from $(\sigma - 3)d/3$ to $-\infty$. Thus, a rescaled plot of this function is shown in Fig. A.1.

Notice the similarities between Eqs. (A.59) and (A.23). All the statements in Sec. A.1.3 are also true for the 3D case, changing the inner product. We remark that for $y \neq 0$, $F'(y) < 0$ wherever is defined, so the eigenvalue finder has a unique root $F(y) = 1$ in each interval $(-(n+1)\pi/d, -n\pi/d)$ for all $n \in \mathbb{N}$ and there is at most a single eigenvalue for $y > 0$, because there is one root in the interval $(-\pi/d, \sigma)$. (Notice that $F'(y) < 0$ for $0 \neq y \in (-\pi/d, \sigma)$ and that the limits $\lim_{y \to -\pi/d+} F(y) = +\infty$ and $\lim_{y \to +\infty} F(y) = -\infty$ are satisfied.)

Remark A.4 *We mentioned that the functions $F(y)$ in Eqs. (A.23), (A.38) and in Eq. (A.59) are at least continuous around $y = 0$ and that for $y \neq 0$ it is monotone decreasing in each interval where it is defined. Notice that the eigenvalue for the growing mode is dependent of σ and L. However, from (3.3), we notice that*

$$\sigma(\theta) = \gamma \exp(-1/\theta)/\theta^2 \leq 4\gamma \tag{A.60}$$

for all values of $\theta \geq 0$, and moreover, if $\gamma s_{\mathcal{N}} \geq \Xi(\theta_M)$ the unstable mode does not exists, see Eq. (2.9) and Fig. 2.1 or Fig. 2.2. Thus, when σd grows to infinity the associated eigenvalue β grows also to infinity! However, since σ is bounded, the product σd only grows if d does, inspecting Fig. 2.1 we see that then the unstable equilibria θ_{II} no longer exists, which restrict the growing of the eigenvalue β.

Therefore, the value of the growing mode is always bounded by the positive root of $F(y) = 1$ when $\sigma = 4\gamma$ and γ is taken as $\Xi(\theta_M)/s_{\mathcal{N}}$. In Sec. 3.2 we showed as a corollary of Friedrichs' Theorem that this limit is just $\sigma = 4\gamma$. Thus the eigenvalue β and so the rate of growth of the unstable mode is always bounded by 4γ.

Appendix B

Eigenvalues and eigenvector for the spectral decomposition

The basis for the spectral decomposition is constructed by means of the classical separation of variables method. In Sec. B.1, we solve first a transient model because the similarities between the separation of variables for this model and the spectral decomposition are the guide for the construction of the orthonormal basis. In Sec. B.2 we summarize the results.

We proceed as follows. In each subsection of Sec. B.1 we focus on the spatial dimensions $\mathcal{N} = 1, 2, 3$; we study the solution of the transient model providing its solution.

B.1 Solution for the transient model

In order to find the solution of a transient model in a bounded domain it is convenient to apply the method of separation of variables. The solution for a general case as a forced model with a spectral decomposition will be found as a consequence.

B.1.1 Orthonormal basis for 1D

Let us write the transient problem for the heat equation for $\mathcal{N} = 1$:

$$\begin{cases} u_t = u_{xx} & x \in [1,\, L],\, t \geq 0 & \text{(B.1)} \\ u(1,\, t) = 0 & t \geq 0 & \text{(B.2)} \\ u(L,\, t) = 0 & t \geq 0 & \text{(B.3)} \\ u(x,\, 0) = u_o(x) & x \in [1,\, L]. & \text{(B.4)} \end{cases}$$

Let us use separation of variables. We consider solutions of the form

$$u(x,\, t) = T(t)X(x). \tag{B.5}$$

Introducing (B.5) in Eq. (B.1) and dividing by $X(x)T(t)$ shows that

$$\frac{X''(x)}{X(x)} = \frac{T'(t)}{T(t)} = -\lambda^2. \tag{B.6}$$

The constant $-\lambda^2$ arises because the first equality in (B.6) must be satisfied for all $t \geq 0$ and $x \in [1,\, L]$. Thus each of these fractions cannot depend explicitly on x or t. The sign of $-\lambda^2$ is consistent with decay for the heat equation solution for long times, see [20].

Equating the first fraction and the last term in Eq. (B.6), we obtain the following boundary eigenvalue problem with $X(1) = X(L) = 0$

$$X''(x) + \lambda^2 X(x) = 0, \qquad \text{so} \qquad X(x) = \alpha \cos(\lambda x) + \beta \sin(\lambda x), \tag{B.7}$$

where α, β are constant. Introducing (B.7) in the boundary conditions (B.2)-(B.3) leads to the boundary conditions for (B.7):

$$X(1) = 0 \qquad \text{and} \qquad X(L) = 0. \tag{B.8}$$

We see that the solution $X(x)$ is not unique; the set of solutions $X_n(x)$ and λ_n given by

$$X_n(x) := C \sin\big(\lambda_n(x-1)\big), \qquad \text{with} \qquad \lambda_n := n\pi/d,\, n \in \mathbb{N}\,, \tag{B.9}$$

solve (B.7), (B.8); here $d = L - 1$ as in (2.6). We have chosen the constant $C := \sqrt{2/d}$ for convenience as we will show soon.

Equating the second fraction and the last term in Eq. (B.6), we obtain, for each λ_n:

$$T_n'(t) = -\lambda_n^2 T_n(t), \qquad \text{or} \qquad T_n(t) = B_n \exp(-\lambda_n^2 t) \tag{B.10}$$

where B_n must be determined.

Thus, we have constructed the particular solutions

$$u_n(x,\, t) = B_n \exp(-\lambda_n^2 t) X_n(x), \tag{B.11}$$

which satisfy all the homogeneous boundary conditions in (B.8). The same is true for any finite linear combination of solutions of type (B.11). We attempt to represent the solution $u(x,\, t)$ of (B.1)-(B.4) as an infinite series in the functions $u_n(x,\, t)$:

$$u(x,\, t) = \sum_{n \in \mathbb{N}} B_n \exp(-\lambda_n^2 t) X_n(x), \qquad \text{with} \tag{B.12}$$

$$u_o(x) = \sum_{n \in \mathbb{N}} B_n X_n(x), \tag{B.13}$$

under the assumption that u_o belongs to $L^2[1,\, L]$. The constant C in $X_n(x)$, Eq. (B.9), is chosen so $\{X_n\}_{n \in \mathbb{N}}$ satisfy the relation

$$\langle X_n,\, X_k \rangle = \delta_{n,\,k}, \qquad \forall n,\, k \in \mathbb{N}\,, \tag{B.14}$$

in the $L^2[1,\, L]$ inner product. Therefore, calculating the $L^2[1,\, L]$ inner product with the eigenfunction $X_k(x)$ for both sides of (B.13), we see that the coefficients B_k must be taken as

$$B_k := \langle X_k,\, u_o \rangle. \tag{B.15}$$

Notice that $\{X_n\}_{n \in \mathbb{N}}$ form a complete orthonormal set of eigenfunctions in the space $L^2[1,\, L]$ for the operator $-d^2/dx^2$ with homogeneous Dirichlet boundary conditions; then

there is a unique decomposition for every $u_o \in L^2[1,\, L]$ given by (B.13), with B_n given in (B.15). Therefore, we write the solution of (B.1)-(B.4) in the form (B.12) with B_n given by (B.15) and $X_n(x)$ by (B.9).

On the other hand, from definition of $X_n(x)$ in (B.9) and a simple calculation we have that

$$X_n'(1) := C\lambda_n \cos\big(\lambda_n(x-1)\big)\big|_{x=1} = C\lambda_n, \qquad \forall n \in \mathbb{N}\,, \tag{B.16}$$

is satisfied.

B.1.2 Orthonormal basis for 2D

Let us write the transient problem for the heat equation for $\mathcal{N} = 2$:

$$\begin{cases} u_t &=& \dfrac{1}{x}\dfrac{\partial}{\partial x}\left(x\dfrac{\partial u}{\partial x}\right) & x \in [1,\, L],\, t \geq 0 & \text{(B.17)} \\ u(1,\, t) &=& 0 & t \geq 0 & \text{(B.18)} \\ u(L,\, t) &=& 0 & t \geq 0 & \text{(B.19)} \\ u(x,\, 0) &=& u_o(x) & x \in [1,\, L]. & \text{(B.20)} \end{cases}$$

We use separation of variables obtaining

$$u(x,\, t) = \exp(-\lambda^2 t)X(x). \tag{B.21}$$

We use only negative eigenvalues $-\lambda^2$. The reason arise from the boundedness of the Dirichlet boundary conditions at $x = 1$ and $x = L$, see Eqs. (B.18) and (B.19). Indeed, if we imagine the shell domain in $\mathbb{R}^2$ and expect a positive mode λ^2 we see a contradiction by the maximum principle, see *e.g.* [20].

We obtain from (B.21) the boundary eigenvalue problem

$$\begin{cases} \dfrac{1}{x}\dfrac{d}{dx}\left(x\dfrac{dX}{dx}\right) &=& -\lambda^2 X & & x \in (1,\, L) \\ X(1) &=& X(L) &=& 0. \end{cases} \tag{B.22}$$

This ODE is the Bessel equation for parameter $p = 0$ with Dirichlet boundary conditions, see [25]. As explained in Appendix C, we know that for each λ the solution for the first equation in (B.22) is

$$X_\lambda(x) = AJ_0(\lambda x) + BY_0(\lambda x), \tag{B.23}$$

with constant A and B. From the boundary condition $X(1) = 0$, the solution must satisfy $A = Y_0(\lambda)$ and $B = -J_0(\lambda)$. Using the boundary condition $X(L) = 0$, λ must be a root of

$$Z(\lambda) = 0, \qquad \text{where} \qquad Z(\lambda) := Y_0(\lambda)J_0(\lambda L) - J_0(\lambda)Y_0(\lambda L). \tag{B.24}$$

A plot of $Z(\lambda)$ is shown in Fig. B.1, from which we can find the roots by inspection; we denote such roots by λ_n in increasing order. Because of the parity of the Bessel function with parameter $p = 0$, we know that the negative roots would yield the same

eigenvalues and eigenvectors, so they are unnecessary. Moreover, as shown in Property (6) of Appendix C, we have that for $\lambda \to \infty$

$$Y_0(\lambda) \approx \sqrt{\frac{2}{\pi\lambda}} \sin\left(\lambda - \frac{\pi}{4}\right) \qquad \text{and} \qquad J_0(\lambda) \approx \sqrt{\frac{2}{\pi\lambda}} \cos\left(\lambda - \frac{\pi}{4}\right), \tag{B.25}$$

so

$$Z(\lambda) \approx \frac{2}{\pi\lambda\sqrt{L}} \sin\big(\lambda(L-1)\big), \tag{B.26}$$

this fact is a partial justification for the asymptotic behavior $\lambda_n \approx n\pi/d$ for $n \to \infty$.

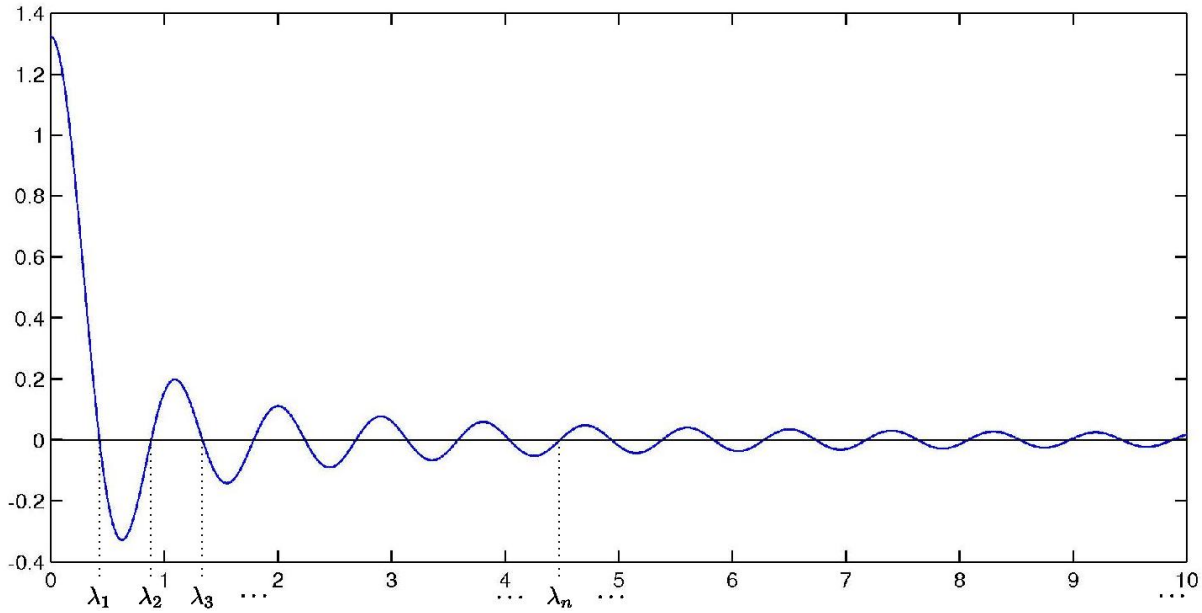

Figure B.1: Plot of $Z(\lambda)$ for $\lambda \geq 0$. This is a MATLAB plot using Bessel tools.

The eigenfunctions are

$$X_n(x) := E_n\big(J_0(\lambda_n)Y_0(\lambda_n x) - Y_0(\lambda_n)J_0(\lambda_n x)\big), \tag{B.27}$$

where λ_n are roots of $Z(\lambda) = 0$ and E_n are constants. Using the weighted Hilbert space $L^2_2[1, L]$ defined in (3.34), we show in Appendix C.3 that the eigenfunctions are orthonormal for suitable normalizing constants E_n defined in Eq. (C.41). Recalling the radial symmetry, it can also be proven that these eigenfunctions define a complete basis for the space $L^2_2[1, L]$, but we will not do it here.

In Appendix C.3 we prove the orthonormality of the eigenfunctions X_n given in (B.27). In Appendix C.4, we show in Claim C.1 that $X_n'(1) = C_n\lambda_n$ for all $n \in \mathbb{N}$ and in Claim C.2 it is proved that C_n tends to $\sqrt{2/d}$ as n tends to ∞.

B.1.3 Orthonormal basis for 3D

Let us write the transient problem for the heat equation for $\mathcal{N} = 3$:

$$\begin{cases} u_t &= \dfrac{1}{x^2}\dfrac{\partial}{\partial x}\left(x^2\dfrac{\partial u}{\partial x}\right) & x \in [1,\, L],\, t \geq 0 & \text{(B.28)} \\ u(1,\, t) &= 0 & t \geq 0 & \text{(B.29)} \\ u(L,\, t) &= 0 & t \geq 0 & \text{(B.30)} \\ u(x,\, 0) &= u_o(x) & x \in [1,\, L]. & \text{(B.31)} \end{cases}$$

As in the case for $\mathcal{N} = 1$, we use separation of variables and obtain

$$u(x,\, t) = \exp(-\lambda^2 t)X(x). \tag{B.32}$$

We use again only negative eigenvalues $-\lambda^2$. The boundary eigenvalue problem

$$\begin{cases} \dfrac{1}{x^2}\dfrac{d}{dx}\left(x^2\dfrac{dX}{dx}\right) &= -\lambda^2 X & x \in [1,\, L] \\ X(1) &= X(L) = 0, \end{cases} \tag{B.33}$$

obtained from (B.32), (B.29)-(B.30), has solution

$$X(x) = C\frac{\sin\big(\lambda(x-1)\big)}{x} \tag{B.34}$$

satisfying the left boundary condition $X(1) = 0$. The (normalizing) constant C in principle depends upon the value of λ. In order to apply the right boundary condition $X(L) = 0$ we must have $\lambda_n = n\pi/d$, $\forall n \in \mathbb{N}$. Therefore, we define

$$X_n(x) := C\frac{\sin\big(\lambda_n(x-1)\big)}{x}, \qquad \lambda_n = \frac{n\pi}{d}, \qquad \forall n \in \mathbb{N}. \tag{B.35}$$

By choosing $C := \sqrt{2/d}$ for all $n \in \mathbb{N}$, the eigenfunctions $\{X_n\}_{n\in\mathbb{N}}$ are orthonormal in the weighted inner product of the space $L^2_3[1,\, L]$, see (3.34).

Moreover, from definition (B.35) we have

$$X_n'(1) := \left[C\frac{\lambda_n\cos\big(\lambda_n(x-1)\big)}{x} - C\frac{\sin\big(\lambda_n(x-1)\big)}{x^2}\right]_{x=1} = C\lambda_n, \qquad \forall n \in \mathbb{N}. \tag{B.36}$$

B.2 Summary for the bases in $\mathcal{N}$ dimensions

In order to summarize the results of this Appendix that are important for Chapters 4 and 5, we emphasize the similarities the results among $\mathcal{N} = 1,\, 2,\, 3$. From Eqs. (B.9), (B.27) and (B.35), we see that $\{X_n\}_{n\in\mathbb{N}}$ form a complete orthonormal basis in $L^2_{\mathcal{N}}[1,\, L]$ that satisfy Eqs. (4.14), where we recall that $L^2_1[1,\, L] \equiv L^2[1,\, L]$.

Notice that $X_n(x)$ are the eigenfunctions, defined in Eq. (B.9) for $\mathcal{N} = 1$:

$$X_n(x) := C\sin\big(\lambda_n(x-1)\big), \qquad \lambda_n = n\pi/d, \qquad \text{for } n \in \mathbb{N}, \tag{B.37}$$

where $C := \sqrt{2/d}$.

For $\mathcal{N}=2$ we notice that $C_n := E_n\big(Y_0(\lambda_n)J_1(\lambda_n) - J_0(\lambda_n)Y_1(\lambda_n)\big)$ for $n \in \mathbb{N}$, see Eq. (C.50). Thus the eigenfunctions given in Eq. (B.27) can be rewritten as:

$$X_n(x) := C_n \frac{J_0(\lambda_n)Y_0(\lambda_n x) - Y_0(\lambda_n)J_0(\lambda_n x)}{Y_0(\lambda_n)J_1(\lambda_n) - J_0(\lambda_n)Y_1(\lambda_n)}, \qquad \text{for } n \in \mathbb{N}, \tag{B.38}$$

where λ_n, $n \in \mathbb{N}$ are the roots of $Z(\lambda) = 0$ given in Eq. (B.24). From Eq. (C.50) and then from Claim C.2 and the approximations in Eq. (B.25) we notice that

$$X_n'(1) = C_n\lambda_n, \quad \forall n \in \mathbb{N} \qquad \text{and} \qquad C_n\lambda_n \approx C\frac{n\pi}{d}, \quad \text{for} \quad n \gg 1. \tag{B.39}$$

For $\mathcal{N}=3$, we defined in Eq. (B.35):

$$X_n(x) := C\frac{\sin\big(\lambda_n(x-1)\big)}{x}, \qquad \lambda_n = n\pi/d, \qquad \text{for } n \in \mathbb{N}. \tag{B.40}$$

Moreover, from Eqs. (B.16), (B.36) and Eq. (B.39.a), we have

$$\begin{array}{rcll} X_n'(1) & = & C\lambda_n, & \forall n \in \mathbb{N}, \quad \text{for } \mathcal{N}=1,\,3, \\ X_n'(1) & = & C_n\lambda_n, & \forall n \in \mathbb{N}, \quad \text{for } \mathcal{N}=2. \end{array} \tag{B.41}$$

Appendix C

Properties of Bessel functions and bases

We compile here all the properties that are used in this work, especially in the Appendixes A.2 and B.1.2. Some of them are classical, but is nice to list them all here. All the information can be recovered from the books [39], [25] or from the book of Tolstov, [36].

First of all, we recall that Bessel functions arise from solving the ODE for $x \in \mathbb{C}$

$$x^2X''(x) + xX'(x) + (x^2 - p^2)X(x) = 0, \tag{C.1}$$

called the Bessel equation with parameter p.

Using some manipulations by change of variables and looking $x \in \mathbb{C}$ for a solution in the form of a series, we arrive at the solutions

$$J_p(x) = \sum_{k=0}^{\infty} \frac{(-1)^k (x/2)^{2k+p}}{\Gamma(k+1)\Gamma(k+p+1)}. \tag{C.2}$$

Is easy to prove that $J_p(x)$ and $J_{-p}(x)$ are two linearly independent solutions of Eq. (C.1) if, and only if, $p \notin \mathbb{Z}$. Otherwise we have a difficulty, because $J_{-n}(x) = (-1)^n J_n(x)$ for all $n \in \mathbb{N}$. To obtain a second linearly independent solution for the situations where $p \in \mathbb{Z}$, we define

$$Y_n(x) := \lim_{p \to n} \frac{J_p(x)(-1)^p - J_{-p}(x)}{\sin(p\pi)}, \tag{C.3}$$

when $n \in \mathbb{N}$. To compute this limit we use the L'Hôpital rule and some properties of the Gamma function, and we conclude that

$$Y_n(x) = \frac{2}{\pi} J_n(x) \left(\ln \frac{x}{2} + \mathcal{C} \right) - \frac{1}{\pi} \sum_{k=0}^{n-1} \frac{(n-k-1)!}{k!} \left(\frac{x}{2} \right)^{2k-n} \tag{C.4}$$

$$- \frac{1}{\pi} \sum_{k=0}^{\infty} \left[\frac{(-1)^k (x/2)^{n+2k}}{k!(n+k)!} \left(\sum_{j=1}^{n+k} \frac{1}{j} + \sum_{j=1}^{k} \frac{1}{j} \right) \right], \tag{C.5}$$

where $\mathcal{C}$ is the *Euler's constant*, and we have

$$\mathcal{C} = \lim_{x \to \infty} \left[x - \Gamma\left(\frac{1}{x} \right) \right] = \lim_{n \to \infty} \left[\frac{\Gamma(1/n)\Gamma(n+1) n^{1+1/n}}{\Gamma(1+n+1/n)} - \frac{n^2}{n+1} \right], \tag{C.6}$$

or $\mathcal{C} = 0.577215664901532 \cdots$.

In particular, we have the expressions

$$\begin{aligned} Y_0(x) &= \frac{2}{\pi}J_0(x)\left(\ln\frac{x}{2}+\mathcal{C}\right)-\frac{2}{\pi}\sum_{k=1}^{\infty}\frac{(-1)^k}{(k!)^2}\left(\frac{x}{2}\right)^{2k}\left(1+\frac{1}{2}+\frac{1}{3}+\cdots+\frac{1}{k}\right) \\ &=: \frac{2}{\pi}J_0(x)\left(\ln\frac{x}{2}+\mathcal{C}\right)-\frac{2}{\pi}\Sigma(x), \end{aligned} \tag{C.7}$$

here $\Sigma(x)$ is an auxiliary notation for the remainder series; $\hat{\Sigma}(x)$ and $\tilde{\Sigma}(x)$ ahead are also remainder series

$$\begin{aligned} Y_1(x) &= \frac{2}{\pi}J_1(x)\left(\ln\frac{x}{2}+\mathcal{C}\right)-\frac{2}{\pi x}-\frac{2}{\pi}\sum_{k=1}^{\infty}\frac{(-1)^k(x/2)^{2k+1}}{2\big[(k+1)!\big]^2} \\ &\quad -\frac{2}{\pi}\sum_{k=1}^{\infty}\left(\frac{(-1)^k(x/2)^{2k+1}}{k!(k+1)}\right)\left(1+\frac{1}{2}+\cdots+\frac{1}{k}\right) \\ &=: \frac{2}{\pi}J_1(x)\left(\ln\frac{x}{2}+\mathcal{C}\right)-\frac{2}{\pi x}-\frac{2}{\pi}\hat{\Sigma}(x)-\frac{2}{\pi}\tilde{\Sigma}(x). \end{aligned} \tag{C.8}$$

We compile some useful properties of Bessel functions; we write them down only for J_p functions, but they are also valid for Y_p functions. All the calculations are found in [36].

1. By direct differentiation, for any p, we have

$$\frac{d}{dx}\big[x^pJ_p(x)\big] = x^pJ_{p-1}(x), \quad \frac{d}{dx}\big[x^{-p}J_p(x)\big] = -x^{-p}J_{p+1}(x), \quad \text{therefore:}$$

$$xJ_p'(x)+pJ_p(x) = xJ_{p-1}(x), \tag{C.9}$$

$$xJ_p'(x)-pJ_p(x) = -xJ_{p+1}(x). \tag{C.10}$$

2. Adding or subtracting (C.9) and (C.10), we obtain

$$2J_p'(x) = J_{p-1}(x)-J_{p+1}(x), \qquad \frac{2p}{x}J_p(x) = J_{p-1}(x)+J_{p+1}(x).$$

3. It is proven asymptotically in [36] (Eq. (9.17) in page 213) that for large $x\in\mathbb{R}^+$

$$\begin{aligned} J_p(x) &= \sqrt{\frac{2}{\pi x}}\sin\left(x-\frac{\pi}{2}\Big(p-\frac{1}{2}\Big)\right)+\frac{r_p(x)}{x\sqrt{x}}, \\ Y_p(x) &= \sqrt{\frac{2}{\pi x}}\sin\left(x-\frac{\pi}{2}\Big(p+\frac{1}{2}\Big)\right)+\frac{\rho_p(x)}{x\sqrt{x}}, \end{aligned}$$

where $r_p(x)$ e $\rho_p(x)$ are bounded functions when x goes to $+\infty$.

4. From (1), or even from (3), we see that the zeros of $J_p(x)$ and $Y_p(x)$ are alternating, moreover, they form a countable infinite set. Also we notice that, when $x\gg 1$ the zeros are close to the zeros of a sine translated by $\frac{\pi}{2}(p\pm\frac{1}{2})$.

5. Other useful properties that arise from equality (C.10) are

$$J_0'(x) = -J_1(x), \qquad \text{also} \qquad Y_0'(x) = -Y_1(x).$$

6. From Property (3), we have for $x \in \mathbb{R}^+$

$$J_p(x) \approx \sqrt{\frac{2}{\pi x}} \cos\left(x - \frac{\pi}{4}(1+2p)\right), \tag{C.11}$$

$$Y_p(x) \approx \sqrt{\frac{2}{\pi x}} \sin\left(x - \frac{\pi}{4}(1+2p)\right), \tag{C.12}$$

$$I_p(x) \approx \frac{1}{\sqrt{2\pi x}}\, e^x, \tag{C.13}$$

$$K_p(x) \approx \sqrt{\frac{\pi}{2x}}\, e^{-x}, \tag{C.14}$$

when $x \gg 1$. The last two will be clear after Appendix C.1. (The argument is also valid for $z \in \mathbb{C}$, when $|z| \gg 1$, see [39].)

7. In [39], p. 31, it is stated that for $x \in \mathbb{R}$,

$$|J_0(x)| \leq 1 \qquad \text{and} \qquad |J_n(x)| \leq 1/\sqrt{2} \qquad \text{for} \qquad n = 1, 2, \ldots.$$

To see that $Y_0(x)$ and $Y_1(x)$ are bounded for $x \geq 1$, notice that they are continuous functions for $x > 0$. Then, from Property (6) they tend to zero as $x \to \infty$; the boundedness is clear. As a matter of fact, these bounds are smaller that 1.

C.1 The Macdonald function and the modified Bessel function of the third kind

In Appendix A.2.1 we need the solution for the equation

$$X''(x) + \frac{1}{x}X'(x) - \beta^2 X(x) = 0. \tag{C.15}$$

Using the traditional power series only one solution can be found; this could imply that the other solution is not analytic at the origin.

We had the same problem with the Bessel equation, therefore, we take instead of (C.15) the equation

$$X''(x) + \frac{1}{x}X'(x) - \left(\frac{p^2}{x^2} + \beta^2\right)X(x) = 0, \tag{C.16}$$

for any parameter p, imitating the construction of the solution for the Bessel equation.

We make the change of variables $y := i\beta x$, so that

$$\frac{d}{dx}X(y) = i\beta X'(y) \qquad \text{and} \qquad \frac{d^2}{dx^2}X(y) = (i\beta)^2 X''(y), \tag{C.17}$$

and substitute these two relations in equation (C.16), obtaining

$$-\beta^2 X''(y) + \frac{i\beta}{x} X'(y) - \left(\frac{p^2}{x^2} + \beta^2\right) X(y) = 0 \tag{C.18}$$

$$\text{or} \qquad -\beta^2 X''(y) - \frac{\beta^2}{y} X'(y) - \left(\beta^2 - \frac{\beta^2 p^2}{y^2}\right) X(y) = 0. \tag{C.19}$$

We multiply (C.19) by $-y^2/\beta^2$, obtaining

$$y^2 X''(y) + yX'(y) + \left(y^2 - p^2\right) X(y) = 0, \tag{C.20}$$

which is the Bessel equation with parameter p in Eq. (C.1): the solutions for this equation were given in Eqs. (C.2) and (C.3)

$$\begin{cases} J_p(y),\, J_{-p}(y), & \text{with } p \notin \mathbb{Z}\,, \\ J_p(y),\, Y_p(y), & \text{with } p \in \mathbb{Z}\,. \end{cases} \tag{C.21}$$

In this case, using the inverse change of variables $x = -iy/\beta$ we have that the solutions are $J_0(i\beta x)$ and $Y_0(i\beta x)$; usually we denote $I_0(\beta x) = J_0(i\beta x)$ and $K_0(\beta x) = Y_0(i\beta x)$, the solutions we used before.

It is common to define the modified Bessel function of the third kind and Macdonald function in the same way, just by multiplying by a convenient constant, as

$$I_p(x) := i^{-p} J_p(ix) \quad \text{and} \quad K_p(x) := i^p Y_p(ix), \tag{C.22}$$

respectively. Notice that applying Eq. (C.22) into (C.11) and (C.12), and after some manipulation we recover (C.13) and (C.14) respectively. Therefore, we can write

$$I_0(x) = \sum_{k=0}^{\infty} \frac{(x/2)^{2k}}{(k!)^2}, \tag{C.23}$$

$$K_0(x) = \lim_{p \to 0} \frac{I_{-p}(x) - I_p(x)}{2p}, \tag{C.24}$$

because the limit in Eq. (C.3) satisfies $\sin(p\pi) \approx p$ as $p \to 0$. Hence, it is not difficult to see that $I_p(x)$, $K_p(x) \geq 0$ for all $x \geq 0$. The Macdonald function $I_p(x)$ is also known as the modified Bessel function of the first kind; we follow the terminology in [25] and [39].

C.2 Behavior of the eigenvalue finder function near zero

We can express the Bessel functions as a truncated power series, in order to show that the eigenfinder $F_-(z)$ is precisely the expression written in Eq. (A.40). Directly from (C.2), (C.7) and (C.8) we write the approximations of order $\mathcal{O}(z^3)$ for $z \in \mathbb{C}$, z near zero, as

$$J_0(z) = 1 - \left(\frac{z}{2}\right)^2 + \mathcal{O}(z^4), \qquad J_1(z) = \frac{z}{2} - \frac{1}{2}\left(\frac{z}{2}\right)^3 + \mathcal{O}(z^5), \tag{C.25}$$

$$\Sigma(z) = -\left(\frac{z}{2}\right)^2 + \mathcal{O}(z^4), \quad \tilde{\Sigma}(z) = -\frac{1}{2}\left(\frac{z}{2}\right)^3 + \mathcal{O}(z^5), \quad \hat{\Sigma}(z) = -\frac{1}{2^3}\left(\frac{z}{2}\right)^3 + \mathcal{O}(z^5). \tag{C.26}$$

Using expression (C.7) for Y_0, we notice that

$$J_0(z)Y_0(zL) = \frac{2}{\pi}\left[J_0(z)J_0(zL)\left(\ln\frac{zL}{2} + \mathcal{C}\right) - J_0(z)\Sigma(zL)\right], \tag{C.27}$$

$$J_0(zL)Y_0(z) = \frac{2}{\pi}\left[J_0(zL)J_0(z)\left(\ln\frac{z}{2} + \mathcal{C}\right) - J_0(zL)\Sigma(z)\right], \tag{C.28}$$

so, using the approximations (C.25)-(C.26) for these products, we have

$$\begin{aligned} T(z) &:= J_0(z)Y_0(zL) - J_0(zL)Y_0(z) = \frac{2}{\pi}\Big[J_0(z)J_0(zL)\ln L - J_0(z)\Sigma(zL) + J_0(zL)\Sigma(z)\Big] \\ &= \frac{2}{\pi}\left[\left(1 - (1+L^2)\left(\frac{z}{2}\right)^2 + \mathcal{O}(z^4)\right)\ln L + L^2\left(\frac{z}{2}\right)^2 + \mathcal{O}(z^4) - \left(\frac{z}{2}\right)^2 + \mathcal{O}(z^4)\right] \\ &= \frac{2}{\pi}\left[\ln L - (1+L^2)(\ln L - 1)\left(\frac{z}{2}\right)^2 + \mathcal{O}(z^4)\right]. \end{aligned} \tag{C.29}$$

Analogously, using expressions (C.7) for Y_0 and (C.8) for Y_1, we have

$$J_1(z)Y_0(zL) = \frac{2}{\pi}\left[J_1(z)J_0(zL)\left(\ln\frac{zL}{2} + \mathcal{C}\right) - J_1(z)\Sigma(zL)\right], \tag{C.30}$$

$$J_0(zL)Y_1(z) = \frac{2}{\pi}\left[J_0(zL)J_1(z)\left(\ln\frac{z}{2} + \mathcal{C}\right) - \frac{J_0(zL)}{z} - J_0(zL)\tilde{\Sigma}(z) - J_0(zL)\hat{\Sigma}(z)\right],$$

so, using the approximations (C.25)-(C.26) for these products, we have

$$B(z) := 2z\big(J_1(z)Y_0(zL) - J_0(zL)Y_1(z)\big) \tag{C.31}$$

$$\begin{aligned} &= \frac{4}{\pi}\Big[zJ_1(z)J_0(zL)\ln L - zJ_1(z)\Sigma(zL) + J_0(zL) + zJ_0(zL)\big(\tilde{\Sigma}(z) + \hat{\Sigma}(z)\big)\Big] \\ &= \frac{4}{\pi}\left[\left(2L\left(\frac{z}{2}\right)^2 + \mathcal{O}(z^4)\right)\ln L + \mathcal{O}(z^4) + 1 - \left(\frac{z}{2}\right)^2 + \mathcal{O}(z^4) + \mathcal{O}(z^4)\right] \\ &= \frac{2}{\pi}\Big[2 - 2\big(L^2 - 2L\ln L\big)\left(\frac{z}{2}\right)^2 + \mathcal{O}(z^4)\Big]. \end{aligned} \tag{C.32}$$

Therefore $F_-(y)$ in (A.40) satisfies

$$F_-(z) = \frac{\big(z^2+\sigma\big)T(z)}{B(z)} = \frac{\big(z^2+\sigma\big)\big(\ln L - (z/2)^2(1+L^2)(\ln L - 1) + \mathcal{O}(z^4)\big)}{2\big(1 - (z/2)^2(L^2 - 2L\ln L) + \mathcal{O}(z^4)\big)}, \tag{C.33}$$

and taking the limit when $z \to 0$, we obtain simply

$$\lim_{z\to 0} F_\alpha(z) = \frac{\sigma \ln L}{2}. \tag{C.34}$$

C.3 Orthonormality for the Bessel basis

We need to verify that $\{X_n\}_{n\in\mathbb{N}}$ given in (B.27) is an orthogonal basis in $L_2^2[1,\, L]$, defined in (3.34). Take $y(x) := X_k(x)$ and $z(x) := X_m(x)$ for two natural numbers k, m, for X_n defined in Eq. (B.27). From Eq. (B.22.a) they satisfy:

$$xy'' + y' = -\lambda_k^2 xy \qquad \text{and} \qquad xz'' + z' = -\lambda_m^2 xz.$$

Multiply the former equation by $z(x)$ and the latter by $y(x)$ and by subtraction, we obtain

$$x(zy'' - z''y) + (zy' - z'y) = (\lambda_m^2 - \lambda_k^2)xyz, \quad \text{or} \quad [x(zy' - z'y)]' = (\lambda_m^2 - \lambda_k^2)xyz. \tag{C.35}$$

Integrating from 1 to L and recalling that $X_k(1) = X_k(L) = 0$, for k as well as for m, we get

$$(\lambda_m^2 - \lambda_k^2)\int_1^L xy(x)z(x)\,dx = [x(zy' - z'y)]_{x=1}^L = 0. \tag{C.36}$$

Therefore if $k \neq m$ we have $\lambda_k^2 \neq \lambda_m^2$. In the weighted space $L_2^2[1,\, L]$ we obtain that $\{X_k\}_{k\in\mathbb{N}}$ form an orthogonal basis.

Let us calculate $\langle X_n,\, X_n\rangle_2$. We cannot use directly Eq. (C.36) because the LHS also vanish. Following [25], instead of $X_m(x)$ we use $X_\mu(x)$ for $\mu \in \mathbb{R}$, which satisfies (B.22.a), so notice that

$$\langle X_n,\, X_n\rangle_2 \;=\; \lim_{\mu\to\lambda_n} \frac{\lambda_n L X_\mu(L)X_n'(L) - \lambda_n X_\mu(1)X_n'(1)}{\mu^2 - \lambda_n^2}, \tag{C.37}$$

where we have used the property $X_n(1) = X_n(L) = 0$. Notice that in the limit both numerator and denominator vanish, so using L'Hôpital leads to

$$\langle X_n,\, X_n\rangle_2 = \lim_{\mu\to\lambda_n} \frac{\lambda_n L \frac{d}{d\mu}X_\mu(L)X_n'(L) - \lambda_n \frac{d}{d\mu}X_\mu(1)X_n'(1)}{2\mu}. \tag{C.38}$$

However, differentiating $X_\mu(L) = E_\mu\big(J_0(\mu)Y_0(\mu L) - Y_0(\mu)J_0(\mu L)\big)$, see Eq. (B.27)

$$\frac{dX_\mu(L)}{d\mu} = -E_n\big(Y_1(\mu)J_0(\mu L) - J_1(\mu)Y_0(\mu L) + L\big[Y_0(\mu)J_1(\mu L) - J_0(\mu)Y_1(\mu L)\big]\big) \neq 0, \tag{C.39}$$

and $dX_\mu(1)/d\mu = 0$. Then substituting (C.39) into (C.38) and taking the limit $\mu \to \lambda_n$, we obtain

$$\begin{aligned}\langle X_n,\, X_n\rangle_2 \;=\; & \frac{E_n^2 L}{2}\big(Y_0(\lambda_n)J_1(\lambda_n L) - J_0(\lambda_n)Y_1(\lambda_n L)\big) \\ & \times\big(Y_1(\lambda_n)J_0(\lambda_n L) - J_1(\lambda_n)Y_0(\lambda_n L) + L\big[Y_0(\lambda_n)J_1(\lambda_n L) - J_0(\lambda_n)Y_1(\lambda_n L)\big]\big).\end{aligned} \tag{C.40}$$

Therefore, we have $\langle X_n,\, X_n\rangle_1 = 1$ for all $n \in \mathbb{N}$, by defining E_n as

$$E_n := \left(\frac{2\big(Y_1(\lambda_n)J_0(\lambda_n L) - J_1(\lambda_n)Y_0(\lambda_n L) + L\big[Y_0(\lambda_n)J_1(\lambda_n L) - J_0(\lambda_n)Y_1(\lambda_n L)\big]\big)^{-1}}{L\big(Y_0(\lambda_n)J_1(\lambda_n L) - J_0(\lambda_n)Y_1(\lambda_n L)\big)}\right)^{\frac{1}{2}}. \tag{C.41}$$

C.4 Estimates for constants in the Bessel basis

For $n \gg 1$ we can find nice estimates. In the following proofs, we will use the auxiliary notation

$$a := \lambda_n - \pi/4, \qquad a_L := \lambda_n L - \pi/4, \tag{C.42}$$

$$b := \lambda_n - 3\pi/4, \quad b_L := \lambda_n L - 3\pi/4, \quad \text{and} \quad b_x := \lambda_n x - 3\pi/4, \tag{C.43}$$

which depend on n, but for the sake of simplicity we will omit such dependence because it does not lead to confusion.

Claim C.1 *For $n \gg 1$ we have that $E_n \approx \pi\lambda_n/\sqrt{2d}$.*

Proof. Recalling the formula (C.41) for E_n, using the Property (6) of this Appendix and the auxiliary definitions (C.42)-(C.43), we have that for $n \to \infty$ the eigenvalues satisfy $\lambda_n \approx n\pi/d$, see Eq. (B.26), so

$$\begin{aligned}
E_n^{-2} &\approx \frac{L}{2}\frac{4}{\pi^2\lambda_n^2 L}\big(\sin a\cos b_L - \cos a\sin b_L\big) && \text{(C.44)}\\
&\quad \times\big[\sin b\cos a_L + L\sin a\cos b_L - \sin b\cos a_L - L\cos a\sin b_L\big] && \text{(C.45)}\\
&= \frac{2}{\pi^2\lambda_n^2}\sin(a-b_L)\big[\sin(b-a_L) + L\sin(a-b_L)\big] && \text{(C.46)}\\
&\approx \frac{2}{\pi^2\lambda_n^2}\sin(\pi/2-n\pi)\big[\sin(-\pi/2-n\pi) + L\sin(\pi/2-n\pi)\big] && \text{(C.47)}\\
&= \frac{2}{\pi^2\lambda_n^2}(-1)^{n+1}[(-1)^n + (-1)^{n+1}L] \;=\; \frac{2d}{\pi^2\lambda_n^2}. && \text{(C.48)}
\end{aligned}$$

Therefore the claim is proved. □

A simple differentiation of the eigenfunctions X_n, given in (B.27), shows that

$$X_n'(1) = \lambda_n E_n(Y_0(\lambda_n)J_1(\lambda_n) - J_0(\lambda_n)Y_1(\lambda_n)), \qquad \forall n \in \mathbb{N}\,, \tag{C.49}$$

with the normalizing constant E_n given in (C.41). So, let us define the constants C_n as

$$C_n := E_n(Y_0(\lambda_n)J_1(\lambda_n) - J_0(\lambda_n)Y_1(\lambda_n)), \qquad \forall n \in \mathbb{N}\,. \tag{C.50}$$

in order to express $X_n'(1) = \lambda_n C_n$.

Claim C.2 *For $n \gg 1$ we have that $Y_0(\lambda_n)J_1(\lambda_n) - J_0(\lambda_n)Y_1(\lambda_n) \approx 2/(\pi\lambda_n)$. Also $C_n \approx \sqrt{2/d}$.*

Proof. First notice, from differentiating Eq. (B.27), that

$$X_n'(x) = -\lambda_n E_n\big(J_0(\lambda_n)Y_1(\lambda_n x) - Y_0(\lambda_n)J_1(\lambda_n x)\big), \tag{C.51}$$

and that $|J_k(x)| \le 1$ for $x \in \mathbb{R}$ and $k = 0, 1, 2, \ldots$ and $|Y_m(x)| \le 1$ for values $x > 1$ when $m = 0, 1$, see Property (7) in this Appendix; therefore $|X_n'(x)| \le 2\lambda_n E_n$. However, we can do better as follows.

Using the expression (C.51) at $x = 1$, the Property (6) and the auxiliary numbers (C.42)-(C.43), we have that for $n \gg 1$

$$\begin{aligned} Y_0(\lambda_n)J_1(\lambda_n) - J_0(\lambda_n)Y_1(\lambda_n) &\approx -E_n\lambda_n\left(\frac{2}{\pi\lambda_n}\right)\big(\sin b\cos a - \sin a\cos b\big) \\ &= \frac{2}{\pi\lambda_n}\sin\frac{\pi}{2} = \frac{2}{\pi\lambda_n} \end{aligned} \tag{C.52}$$

Thus we have proved the first part of the claim. The second part follows from Claim C.1 by recalling that $C_n := E_n\big(Y_0(\lambda_n)J_1(\lambda_n) - J_0(\lambda_n)Y_1(\lambda_n)\big)$, in Eq. (C.50). □

Appendix D

Boundary conditions and stationary solutions

In this Appendix we study all possible boundary conditions that can be used for problem (2.1)-(2.2), for $\mathcal{N} = 1$:

$$\begin{cases} \dfrac{d^2\varrho}{dx^2} = 0 & x \in [1,\, L] \\ \gamma \exp\left(-\dfrac{1}{\varrho}\right)\Big|_{x=1} + \dfrac{d\varrho}{dx}\Big|_{x=1+} = 0 & x = 1, \end{cases} \tag{D.1}$$

namely, one of the boundary conditions at the right

$$\begin{array}{rcll} \varrho_x(x) & = & -q, & \text{if} \quad x = L < \infty \\ \varrho(x) & \to & \theta_\infty, & \text{if} \quad x \to L = \infty. \end{array} \tag{D.2}$$

With $q > 0$, $-q$ is an outgoing flux, and θ_∞ is a non-negative temperature.

We start by analyzing the case when $L = \infty$. To define a solution for the system (D.1), the solution

$$\varrho(x) = ax + b, \qquad \text{(with } a,\, b \text{ constants)} \tag{D.3}$$

needs $a = 0$ and $b = \theta_\infty$. In order to satisfy the right boundary condition (D.2.b), it is necessary that $\varrho(1) = \theta_\infty$. Using the solution (D.3) in (D.1.b), we get

$$\frac{d\varrho}{dx}\Big|_{x=1} = 0, \quad \text{then} \quad \exp\left(-\frac{1}{\varrho}\right)\Big|_{x=1} = 0. \tag{D.4}$$

This is only possible if $-1/\theta_\infty \to -\infty$, which means that $\varrho \equiv 0$, thus for $L = \infty$ the only solution is uninteresting.

Now we restrict to some finite L. Using a finite interval $[1,\, L]$ for x allows for more possibilities, depending on the boundary condition used at $x = L$. The two most common boundary conditions are Dirichlet's and Neumann's. The first one, applied to this case, fixes the temperature of the exterior of our domain, while the second one prescribes the heat flux at the boundary of our domain.

The stationary system for the Neumann conditions is very simple. We start again from system (D.1), and impose a heat flux condition at the right boundary on $x = L$. This situation does not correspond to what happens in the field: we never have an isolated reservoir. However, it may be obtained in the laboratory, and it is a nice scenario to test the model.

For the homogeneous Neumann problem, we have the stationary system (D.1) with boundary condition (D.2)

$$\varrho_x(L) = 0. \tag{D.5}$$

Again, the solution is given by $\varrho(x) = ax+b$. Since we have $\varrho_x \equiv a$, from the boundary condition (D.5), we obtain that $a = 0$. From the left boundary we have $\varrho(1) = b$. Using these values in the second equation of (D.1), we recover the limit in (D.4). Once again, we only get a trivial and uninteresting solution. This fact is in agreement with intuition; if at $x = 1$ we have a positive source of heat and the reservoir is isolated at $x = L$, then the temperature never stabilizes.

However, if we specify a nonzero heat flow at $x = L$, *i.e.*

$$\varrho_x(L) = -q, \tag{D.6}$$

then from solution (D.3)

$$\varrho'(x) \;=\; a \qquad \text{or} \qquad a \;=\; -q. \tag{D.7}$$

Using this result in the second Eq. of (D.1), we get:

$$\gamma \exp\left(-\frac{1}{-q+b}\right) - q \;=\; 0 \tag{D.8}$$

$$\text{therefore} \qquad b \;=\; q - \frac{1}{\log(q/\gamma)}. \tag{D.9}$$

In this case we have a stationary solution only if $\varrho(1) = -(\log(q/\gamma))^{-1}$. Note that when $q \to 0+$ we return to the case where the flux is zero; we recover the trivial solution.

For the case $q \geq \gamma$, the resulting steady temperature is negative at $x = 1$, which does not make physical sense, so we restrict the flux q to the range $[0,\, \gamma)$; we disregard fluxes such that energy goes out too fast and fluxes that inject energy into the system, as these cases cannot yield stationary solutions.

However, this case gives rise to only one interesting situation, because

$$\varrho(1) = b + a = -\frac{1}{\log(q/\gamma)}, \tag{D.10}$$

has to be satisfied. The linear analysis of stability is easy, and this steady-state solution is stable.

Appendix E

Numerical simulations

We left for this Appendix all the numerical methods and simulations, and each section describes facts specific to each dimension.

E.1 Numerical method for the 1D case

In this section we discuss the finite difference scheme we use for the nonlinear problem (1.23)-(1.27) with spatial dimension one. This scheme and others can be found in [34]. We implement the Crank-Nicolson method (CN) for the heat equation (1.23), thus for

$$\theta_t \;=\; \theta_{xx}, \qquad x \in [1,\, L],$$

the CN scheme with $n = 0,\, 1,\, \ldots$ and $m = 0,\, 1,\, \ldots,\, M$ is:

$$-\frac{\mu}{2}v_{m-1}^{n+1} + (1+\mu)v_m^{n+1} - \frac{\mu}{2}v_{m+1}^{n+1} = \frac{\mu}{2}v_{m-1}^{n} + (1-\mu)v_m^{n} + \frac{\mu}{2}v_{m+1}^{n}, \tag{E.1}$$

where $v_m^n = v(mh+1,\, nk)$ is the discrete approximation solution (notice that we set $(mh+1,\, nk)$ because it is convenient to represent $v_0^n = v(1,\, nk)$ as the first spatial point for the domain starting at $x = 1$), $\mu := k/h^2$, h is the grid spacing and k is the time interval. Here $M := (L-1)/h$, so $v_M^n = v(L,\, nk)$.

The CN method is of order $\mathcal{O}(h^2,\, k^2)$, and it is unconditionally stable for appropriate discrete boundary conditions. However, in our original nonlinear problem, one of the boundary conditions is nonlinear. There is no general theory for the stability of nonlinear schemes. Nevertheless, we expect that for small parameters h and k the scheme have a nice behavior.

The complete nonlinear problem (1.23)-(1.27), in the domain $x \in [1,\, L]$, for $\mathcal{N} = 1$ has for $t > 0$ the boundary conditions:

$$\theta_t(1,\, t) \;=\; \gamma \exp(-1/\theta(1,\, t)) + \theta_x(1,\, t), \tag{E.2}$$

$$\theta(L,\, t) \;=\; \theta_L. \tag{E.3}$$

Then, the right boundary condition is governed by $v_M^{n+1} = v_M^n$, where we set $v_M^0 = \theta_L$. In order to discretize the left boundary (E.2), we recall that one way of deriving the

discretization of CN method utilizes an auxiliary grid point between two step times, namely $\big(1+mh,\,(n+\frac{1}{2})k\big)$. For the sake of consistency we have to expand the time derivatives at the boundary around the auxiliary point $\big(1,\,(n+\frac{1}{2})k\big)$. Notice that

$$\begin{aligned}\theta\big(1,\,(n+1/2\pm 1/2)k\big) &= \theta\big(1,\,(n+1/2)k\big) \pm 1/2\theta_t\big(1,\,(n+1/2)k\big)\\ &\quad + (k^2/8)\theta_{tt}\big(1,\,(n+1/2)k\big) + \mathcal{O}(k^3). \end{aligned}\tag{E.4}$$

By subtracting the $(-)$ equation from the $(+)$ equation in (E.4) and dividing by k we find

$$\theta_t\big(1,\,(n+1/2)k\big) = \frac{\theta\big(1,\,(n+1)k\big)-\theta(1,\,nk)}{k}+\mathcal{O}(k^2).\tag{E.5}$$

We do something similar for the spatial derivative, but in this case, we use spatial average at two neighboring grid points by adding both the $(-)$ and the $(+)$ versions of an equation similar to (E.4) for θ_x instead of θ. Notice that $\theta_x(1,\,\cdot\,) = [\theta(1+h,\,\cdot\,) - \theta(1,\,\cdot\,)]/h + \mathcal{O}(h)$, then

$$\begin{aligned}\theta_x\big(1,\,(n+1/2)k\big) &= \frac{1}{2}\bigg[\frac{\theta\big(1+h,\,(n+1)k\big)-\theta\big(1,\,(n+1)k\big)}{h}\\ &\quad + \frac{\theta(1+h,\,nk)-\theta(1,\,nk)}{h}\bigg] + \mathcal{O}(h,\,k^2).\end{aligned}\tag{E.6}$$

Finally we can write

$$\exp\left(\frac{-1}{\theta\big(1,\,(n+1/2)k\big)}\right)=\frac{1}{2}\left[\exp\left(\frac{-1}{\theta\big(1,\,(n+1)k\big)}\right)+\exp\left(\frac{-1}{\theta(1,\,nk)}\right)\right]+\mathcal{O}(k^2).\tag{E.7}$$

From these approximations, we get the final form for the boundary condition (E.2)

$$\left(1+\frac{\lambda}{2}\right)v_0^{n+1}-\frac{\lambda}{2}v_1^{n+1}-\frac{k\gamma}{2}\exp\left(\frac{-1}{v_0^{n+1}}\right)=\left(1-\frac{\lambda}{2}\right)v_0^{n}+\frac{\lambda}{2}v_1^{n}+\frac{k\gamma}{2}\exp\left(\frac{-1}{v_0^{n}}\right),\tag{E.8}$$

here λ stands for k/h.

Although this boundary scheme is of first order in space in comparison to the former base scheme of second order, using it locally does not reduce the order of accuracy of the overall scheme. Thus, the accuracy of the scheme is second order in space and time.

E.1.1 Implementation of the numerical method

Let $h=(L-1)/M$ be the size of the spatial grid and $M+1$ the number of spatial nodes of the numerical domain. Let $v^n := (v_0^n,\,v_1^n,\ldots,\,v_M^n)^T$. We write the CN method as

$$Av^{n+1}-U(v^{n+1}) = Bv^n+U(v^n),\ \text{ where }\ U(v^n):=\left(\frac{k\gamma}{2}\exp\Big(-\frac{1}{v_0^n}\Big),\,0,\ldots,\,0\right)^T\tag{E.9}$$

and

$$A:=\begin{pmatrix} 1+\frac{\lambda}{2} & -\frac{\lambda}{2} & 0 & & \\ -\frac{\mu}{2} & 1+\mu & -\frac{\mu}{2} & & \\ & \ddots & \ddots & \ddots & \\ & & -\frac{\mu}{2} & 1+\mu & -\frac{\mu}{2}\\ & & 0 & 0 & 1 \end{pmatrix},\quad B:=\begin{pmatrix} 1-\frac{\lambda}{2} & \frac{\lambda}{2} & 0 & & \\ \frac{\mu}{2} & 1-\mu & \frac{\mu}{2} & & \\ & \ddots & \ddots & \ddots & \\ & & \frac{\mu}{2} & 1-\mu & \frac{\mu}{2}\\ & & 0 & 0 & 1 \end{pmatrix}.$$

We want to solve each nonlinear step of the implementation of (E.9) by Newton's method. Let us define a vector $\omega^0 := v^n$; we will iterate with $\omega^{l+1} := \omega^l + d^l$, where d^l is a vector that corrects the previous prediction ω^l. Now we describe how v^{n+1} is obtained from ω^l.

We are looking for d^l such that ω^{l+1} instead of v^{n+1} solves (E.9.a) approximately. Set $K := Bv^n + U(v^n)$; K will remain fixed for a given n. Assuming that d_0^l is small, we use Taylor's formula to express

$$\exp\left(\frac{-1}{\omega_0^{l+1}}\right) = \exp\left(\frac{-1}{\omega_0^l + d_0^l}\right) = \exp\left(\frac{-1}{\omega_0^l}\right)\left(1 + \frac{d_0^l}{(\omega_0^l)^2}\right) + \mathcal{O}\big((d_0^l)^2\big), \tag{E.10}$$

so, we have the iterative equation

$$Ad^l - U(\omega^l)\frac{d_0^l}{(\omega_0^l)^2} = K - A\omega^l + U(\omega^l). \tag{E.11}$$

To solve this equation, let $M_l := -A\omega^l + U(\omega^l)$ and

$$\Lambda(l) := \begin{pmatrix} \alpha_l & -\frac{\lambda}{2} & 0 & & \\ -\frac{\mu}{2} & 1+\mu & -\frac{\mu}{2} & & \\ & \ddots & \ddots & \ddots & \\ & & -\frac{\mu}{2} & 1+\mu & -\frac{\mu}{2} \\ & & 0 & 0 & 1 \end{pmatrix}, \tag{E.12}$$

where $\alpha_l = 1 + \frac{\lambda}{2} - \frac{k\gamma}{2(\omega_0^l)^2}\exp\big(-\frac{1}{\omega_0^l}\big)$. Then, Eq. (E.11) is $d^l = \Lambda^{-1}(K + M_l)$. At the start of each iteration, we take $\omega^{l+1} = \omega^l + d^l$ and update M_l. However, we need to solve a linear system for $\Lambda(l)$ in each iteration, which is somewhat expensive.

Notice that the matrices A and $\Lambda(l)$ differ only in the first diagonal entry, which changes at each step l of the iterative solver. A Gaussian elimination can be implemented from the bottom row upwards in (E.12), *i.e.*, the opposite of the standard direction. In this way, the U part of the decomposition is always the same and can be precomputed once and for all. The L part is the same except for the first entry. This algorithm reduces the operation count for the linear algebra by almost 50%.

E.1.2 Numerical results

In Appendix F we set a typical value of $\gamma = 7\times10^8$. Using large values of γ in the numerical method leads to slow convergence: the nonlinear part in Eq. (E.8) and consequently the α_l coefficient in the solver increases and the solver requires a small step time parameter k in order to guarantee convergence. Nevertheless, we are interested in simulating situations with three steady-state solutions and in seeing the qualitative behavior of its solutions. So, we use a small value γ in the simulations to control the machine time by reasonable parameter k, then we ensure the presence of the three steady-states through d, see the Eq. (2.9).

Even using a coarse mesh, we obtain good convergence to both stable stationary solutions. For $k = 0.2$ and $h = 0.01$ we get an error no larger than 10^{-2} in comparison to the actual θ_I and θ_{III} values.

A good example of this behavior is the following. We set $\gamma = 1/4$, the reservoir temperature $\theta_L = 0.2$ and $L = 10$. For these parameters, the stationary left temperatures are $\theta_I \approx 0.22803135$, $\theta_{II} \approx 0.47920158$ and $\theta_{III} \approx 1.12500985$. Furthermore, we set the grid numbers $h = 0.05$ and $k = 0.2$, and the initial condition

$$u_o(x) = \frac{(\theta_L - \theta_i)x + \theta_i L - \theta_L}{L-1} + 0.4095 \sin\big(0.6(L-x)\big) + 0.5905 \sin\big(0.4(L-x)\big), \quad \text{(E.13)}$$

where $\theta_i = 0.4792015876$. The results of the simulation for the unstable stationary solution agree with our intuition: the evolution of the numerical solution approaches the unstable equilibria solution in a very short time, $t \approx 30$. It remains close to that solution for quite a long time: it diverges only for $t > 800$, and approaches a stable stationary solution around $t \approx 1850$. Notice that using a bisection method we can find initial conditions that remain close to the unstable solution for times as long as we please. The profiles of this simulation are plotted at certain times on Fig. E.1 for CN. In this figure we also show results for the Backward Euler method with central differentiation (BE). Refining the grid numbers shows that the convergence is to $\varrho_I(x)$ in both cases.

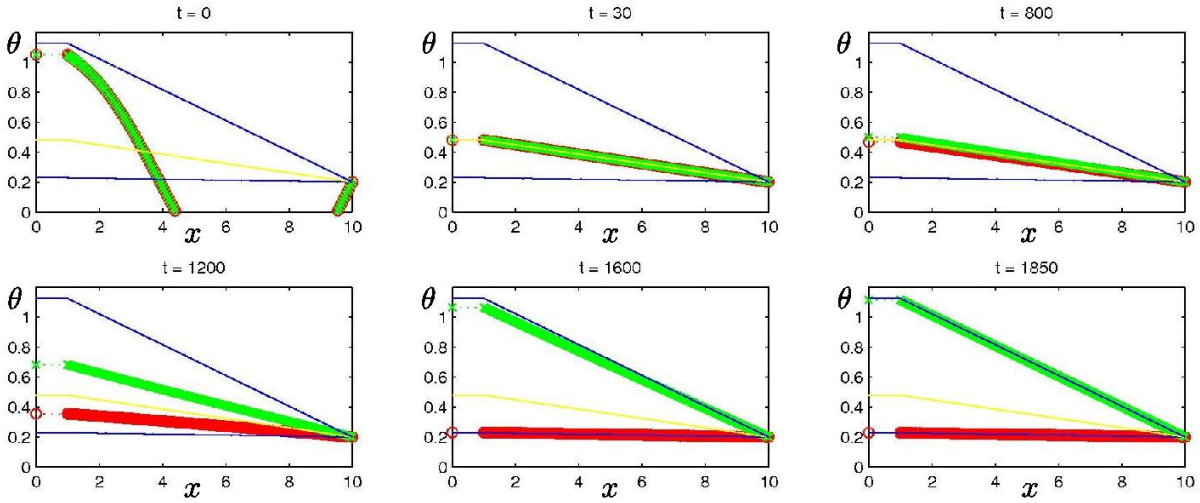

Figure E.1: The initial condition, for time $t = 0$, given in (E.13) is plotted on the top left. We plot with dark circles the CN method and with light crosses the BE method, the three "linear" plots are the three stationary solutions. For times closer to $t = 30$ the solution obtained by both methods approximate the unstable solution. Both solutions remain close to it until $t = 800$. The bifurcation starts leading CN to $\varrho_I(x)$ at $t = 1600$ and BE to $\varrho_{III}(x)$ at $t = 1850$.

Several simulations show that the behavior of any solution of the nonlinear model always has a fast convergence to an almost linear profile, from which the solution will be driven to one of the stable stationary solutions. The separation between trajectories that converge to $\varrho_I(x)$ from those converging to $\varrho_{III}(x)$ appears to occur at a value $\theta(1, t)$ comparable to θ_{II} in our simulations.

In order to verify this convergence to the quasi-steady solutions of the reduced model, we made several simulations for many values of γ. We observe that for small values of γ the convergence to quasi-steady solutions is slow, while for large values of γ the convergence is fast.

It would be interesting to analyze the dependence on γ of the rate of convergence.

E.2 Numerical method for 2D and 3D cases

We implement the Crank-Nicolson scheme (CN), as for the 1D case, because we have seen that is accurate and stable. The partial differential equation (1.23), for $\mathcal{N} = 2$ or 3, to be solved is

$$\theta_t \;=\; \frac{1}{x^{\mathcal{N}-1}}\big(x^{\mathcal{N}-1}\theta_x\big)_x \qquad x \in [1,\, L]. \tag{E.14}$$

Which has the CN scheme based on six points written as

$$-\alpha_m v_{m-1}^{n+1} + (1+\beta_m)v_m^{n+1} - \gamma_m v_{m+1}^{n+1} = \alpha_m v_{m-1}^{n} + (1-\beta_m)v_m^{n} + \gamma_m v_{m+1}^{n}, \tag{E.15}$$

for $x \in (1,\, L)$, where $\mu = k/h^2$, $x = 1 + mh$ and $0 \le m \le M := (L-1)/h$. Here for $\mathcal{N} = 2$:

$$\alpha_m := (1 + (m-1/2)h)\mu/(1+mh),\; \gamma_m := (1 + (m+1/2)h)\mu/(1+mh)$$

and $\beta_m = \alpha_m + \gamma_m \equiv 2\mu$. For $\mathcal{N} = 3$:

$$\alpha_m := [(1 + (m-1/2)h)/(1+mh)]^2\mu,\; \gamma_m := [(1 + (m+1/2)h)/(1+mh)]^2\mu$$

and $\beta_m := \alpha_m + \gamma_m$.

Note that $(m \pm 1/2)h$ appears in some terms: this is because even though the scheme only uses grid points with n, $m \in \mathbb{N}$, for the construction of the scheme we used auxiliary points at points with step time coordinate corresponding to $n + 1/2$, as in the standard CN for the heat equation in 1D. Yet, there also appear points with spatial coordinate corresponding to $m \pm 1/2$ for controlling the two concatenated spatial derivative on the RHS of equation (E.14).

Recall the boundary condition for $\mathcal{N} = 2$, 3:

$$\theta_t(1,\, t) \;=\; \gamma \exp(-1/\theta(1,\, t)) + \mathcal{N}\theta_x(1,\, t), \tag{E.16}$$

$$\theta(L,\, t) \;=\; \theta_L. \tag{E.17}$$

For the left boundary condition given in (E.16), we obtain a formula analogous to the one for the 1D case in Eq. (E.8). The only real difference is a factor of $\mathcal{N}$ that appears in front of $\lambda := k/h$:

$$\left(1+\frac{\mathcal{N}\lambda}{2}\right)v_0^{n+1} - \frac{\mathcal{N}\lambda}{2}v_1^{n+1} - \frac{k\gamma}{2}\exp\left(-\frac{1}{v_0^{n+1}}\right) = \left(1-\frac{\mathcal{N}\lambda}{2}\right)v_0^{n} + \frac{\mathcal{N}\lambda}{2}v_1^{n} + \frac{k\gamma}{2}\exp\left(-\frac{1}{v_0^{n}}\right). \tag{E.18}$$

As to the boundary condition on the right, we simply take $v_M^{n+1} = v_M^n$.

Using the vector form, $v^n := (v_0^n, \ldots, v_M^n)^T$, we write the scheme as

$$Av^{n+1} - U(v^{n+1}) = Bv^n + U(v^n), \tag{E.19}$$

where

$$A = \begin{pmatrix} 1+\frac{\mathcal{N}\lambda}{2} & -\frac{\mathcal{N}\lambda}{2} & & & & \\ -\alpha_1 & 1+\beta_1 & -\gamma_2 & & & \\ & -\alpha_2 & 1+\beta_2 & -\gamma_3 & & \\ & & \ddots & \ddots & \ddots & \\ & & & -\alpha_{M-1} & 1+\beta_{M-1} & -\gamma_M \\ & & & & & 1 \end{pmatrix}. \tag{E.20}$$

The other matrix is very similar

$$B = \begin{pmatrix} 1-\frac{\mathcal{N}\lambda}{2} & \frac{\mathcal{N}\lambda}{2} & & & & \\ \alpha_1 & 1-\beta_1 & \gamma_2 & & & \\ & \alpha_2 & 1-\beta_2 & \gamma_3 & & \\ & & \ddots & \ddots & \ddots & \\ & & & \alpha_{M-1} & 1-\beta_{M-1} & \gamma_{M-1} \\ & & & & & 1 \end{pmatrix} \tag{E.21}$$

Finally, we take $U(v^n) := \left(\frac{k\gamma}{2}\exp(-1/v_0^n),\, 0, \ldots, 0\right)^T$. Recall that the matrix Λ in (E.12) arose from the Newton's method, here it is the same, all the entries of Λ are exactly the entries of A in (E.20) except for the first entry, which is:

$$\Lambda_{11}(l) = 1 + \frac{\mathcal{N}\lambda}{2} - \frac{k\gamma}{2(\omega_0^l)^2}\exp\left(-\frac{1}{\omega_0^l}\right). \tag{E.22}$$

Therefore, we notice that the notation used in Sec. E.1.1 is analogous to the one written down in Eq. (E.19), so we implement these schemes in a way very similar to that for the 1D case.

Appendix F

Estimate of the dimensionless group γ

This Appendix presents the evaluation of the value of the chemical *Damköhler Number* γ that we use in the reactor model treated in this work. Actually the standard notation for such number is Da_{IV} (see [40, Table B, Serial No. D4, page F-331], in Table B the Serial No. D4 of page F-331), we have used γ as a short notation. This Appendix is due to J. Bruining, the co-adviser of this work. His concern is combustion *in-situ* for oil recovery. This is the reason why coke originating from pyrolysis of oil is used as fuel in this evaluation.

We would like to obtain a realistic value for the

$$\gamma = \frac{\Delta H c_o c_c A a^2 R}{\kappa E}. \tag{F.1}$$

The models in this work accept any kind of fuel. So, we use c_c for Coke concentration for its applicability of chemical reactors as the beginning of combustion in porous media.

Notice that γ is actually a Damköhler number of the group IV. Indeed, by defining the "liberated heat" Q_l and the "conductive heat transfer" Q_{tr} as

$$Q_l := \Delta H c_o c_c A a^3 \qquad \text{and} \qquad Q_{tr} := a\kappa \frac{E}{R}, \tag{F.2}$$

we see that $\gamma = Q_l/Q_{tr}$. (We prove soon that the units of $(c_o\, A)$ are actually $[\mathrm{s}^{-1}]$.) For the dimensional analysis following the respective units from Table 1, page 87, we have

$$\left[\Delta H c_c (c_o A) a^3\right] \;=\; (\mathrm{J}\,/\,\mathrm{mol}) \times (\mathrm{mol}\,/\,\mathrm{m}^3) \times \mathrm{s}^{-1} \times \mathrm{m}^3 \;=\; \mathrm{J}\,/\,\mathrm{s} \tag{F.3}$$

and

$$\left[a\kappa \frac{E}{R}\right] \;=\; \mathrm{m} \times \big(\,\mathrm{J}\,/(\mathrm{m}\times\mathrm{s}\times\mathrm{K})\big) \times \frac{\mathrm{J}\,/\,\mathrm{mol}}{\mathrm{J}\,/(\mathrm{mol}\times\mathrm{K})} \;=\; \mathrm{J}\,/\,\mathrm{s}\,. \tag{F.4}$$

Notice that Q_l and Q_{tr} can be taken as fluxes per unit area.

It is not trivial to obtain an approximate value for the reaction rate prefactor A, where the reaction rate parameter k follows the usual Arrhenius form $k = A\exp(-E/RT)$. This value is found for petroleum coke from the literature ([37]) as follows. The intrinsic reactivity $\widetilde{\rho}_i$ of petroleum coke at atmospheric air pressure, thus at a oxygen pressure for 21.3 kPa, can be written as

$$\widetilde{\rho}_i = 133 \times 10^6 \exp(-158 \times 10^3/RT). \tag{F.5}$$

The intrinsic reactivity is expressed in [g-Coke/($m^2\times$ min $\times$ bar-air)]. The reactive surface area S_m of coke depends on the particle size, *i.e.*, is $0.9, 1.0$ and 1.6 m^2/g for particle diameters of $2.9, 0.9$ and 0.22 mm respectively. We assume that for the quoted equation in Eq. (F.5) the surface area is 1 m^2/g. This appears to be a reasonable average given the fact that Eq. (F.5) is derived from plotting a large number of literature data from various sources. Another source of inaccuracy is that the equation is found from a least square fit of the logarithm of $\widetilde{\rho}_i$ versus $1/T$ and thus we find the geometric average as opposed to the arithmetic average, thus underestimating its value. We will disregard this aspect in the following. Using that $R = 8.31$ [J/(mol $\times$ K)], we can thus write

$$\widehat{\rho}_i = 2.22 \times 10^6 \exp(-19013/T), \tag{F.6}$$

where the intrinsic reactivity $\widehat{\rho}_i$ is now expressed in terms of [g-Coke/(g-Coke $\times$ s $\times$ bar-air)] = [mol-Coke/(mol-Coke $\times$ s $\times$ bar-air)]. The value 19013 can be considered as the activation temperature T_E.

The intrinsic reactivity should include a term involving the oxygen concentration. Assuming a linear relationship with pressure we would obtain

$$\rho_i = 2.22 \times 10^6 \frac{P_{O_2}}{P^o_{O_2}} \exp(-T_E/T), \tag{F.7}$$

where P_{O_2} is the pressure of oxygen and $P^o_{O_2}$ is the oxygen pressure in atmospheric air. We will come back how ρ_i can be converted to find A in Eq. (F.1).

The concentration of fuel requires an estimate of the coke saturation S_C in the pore and the porosity $\varphi \approx 0.3$. Following reference [1] we find that the value for S_C by using that the fraction of coke to initial oil ranges between 11% and 17%. Assuming that the initial oil saturation is 80% we arrive at $S_C = 0.12$. In the estimate that follows we will assume that the molar weight of coke $M_C \approx 0.012$ [kg/mol] and that the density of coke $\rho_C \approx 1000$ [kg/m^3]. The concentration of coke will then be $c_c = \varphi\rho_C S_C = 36$ [kg/m^3] $= 3000.0$ [mol/m^3]. The enthalpy ΔH in Eq.. (F.1) will be expressed in terms of the energy per mole of carbon and we take $\Delta H \approx 4 \times 10^5$ [J/mol$-C$].

We assume that the concentration of oxygen corresponds to the concentration of oxygen in air of one bar. Let us now see which units we must assign to (Ac_o) to make it dimensionless. We find that

$$\left[\frac{\Delta H\,(Ac_o)\,c_c a^2 R}{\kappa E}\right] = \frac{(\mathrm{J\,/\,mol}) \times [U] \times (\mathrm{mol\,/\,m^3}) \times \mathrm{m^2} \times \big(\mathrm{J\,/(mol \times K)}\big)}{\big(\mathrm{W\,/(m \times K)}\big) \times (\mathrm{J\,/\,mol})} = \frac{\mathrm{J}}{\mathrm{W}}\ [\mathrm{U}],$$

meaning that the unit of (Ac_o) must have units [s^{-1}]. Considering the situation that the coal is subjected to atmospheric oxygen in the atmosphere and considering Eq. (F.7), we conclude that $(Ac_o) = 2.22 \times 10^6 \exp(-T_E/T)$ [s^{-1}]. Hence we obtain for γ

$$\gamma = \frac{\Delta H\,(Ac_o)\,c_c a^2 R}{\kappa E} = \frac{4 \times 10^5 \times 2.22 \times 10^6 \times 3000 \times 0.01 \times 8.31}{2 \times 1.58 \times 10^5} = 7.0 \times 10^8.$$

Other data may lead to values that are a factor of 100 smaller or larger. The main uncertainty for estimating γ is in the value for the intrinsic reactivity.

The temperature elevation is defined as the temperature that would be attained if the coke in place is burnt and heats up the rock in which it was deposited. This temperature is given as

$$\Delta T = \frac{c_c \Delta H}{(\rho c)_m} = 600 \text{ [K]}.$$

In the combustion process the temperature becomes always higher as the upstream part of the heated zone is transported by convection of gases, whereas the downstream part velocity is determined by the fuel consumption rate. Adding nitrogen to the injected oxygen increases the velocity of the upstream heat wave, but leaves the combustion rate unchanged. If the velocity of the heat wave and the combustion wave become close the temperature can rise to very high values.

Table 1. Typical field data for combustion

Physical quantity	*Symbol*	*Value*	*Unit*
Atmospheric oxygen pressure	$P^o_{O_2}$	21300	[Pa]
Oxygen pressure	P_{O_2}	21300	[Pa]
Porosity	φ	0.3	[-]
Coke saturation	S_C	0.12	[-]
Concentration coke	c_c	3000	[mol-Coke/m^3]
Gas constant	R	8.31	[J/(mol $\times$ K)]
Density coke	ρ_C	1000	[kg/m^3]
Molecular weight of coke	M_C	0.012	[kg/mol]
Pre-exponential factor	(Ac_o)	2.22×10^6	[s^{-1}]
Heat of combustion	ΔH	4×10^5	[J/mol-Coke]
Radius heated zone	a	0.1	[m]
Activation energy	E	1.58×10^5	[J/mol]
Thermal conductivity	κ	2	[W/(m $\times$ K)]
Initial temperature	T_{ini}	320	[K]
Heat capacity rock	$(\rho c)_m$	2×10^6	[J/(m$^3\times$ K]
Heat generated	$\Delta H c_c$	1.2×10^9	[J/(mol $\times$ K)]
Temperature elevation	ΔT	600	[K]

Bibliography

[1] Abu-Khamsin, S. A., Brigham, W. E. and Ramey, H. J. (1988) "Reaction kinetics of fuel formation for in-situ combustion", *SPE Reservoir Engineering* **No. 3:4**, pp. 1308-1316.

[2] Babin, A. V. and Vishik, M. I. (1992) *Attractors of evolution equations.* Elsevier Science, North Holland.

[3] Bachman, G. and Narici, L. (2000) *Functional Analysis.* New York, Dover.

[4] Boucher, D. F. and Alves, G. E. (1959) "Dimensionless analysis", *Chem. Eng. Progr.* **Vol. 59**, No. 9, pp. 55-64.

[5] Burton, T. A. (1983) *Volterra integral and differential equations.* New York, Academic Press.

[6] Bruining, J. and Marchesin, D. (2008) "Spontaneous ignition in porous media at long times", ECMOR XI. 8-11 Sept., 11th European Conference on the Mathematics of Oil Recovery. Bergen, Norway.

[7] Cannon, J. R. (1984) *The one dimensional heat equation.* Reading, Mass., Addison-Wesley.

[8] Da Prato, G. (2006) *An introduction to infinite-dimensional analysis.* Springer.

[9] Davies, B. (2001) *Integral transforms and their applications.* New York, Springer-Verlag.

[10] Deimling, K. (1977) *Ordinary differential equations in Banach spaces.* Berlin, Springer-Verlag.

[11] Favini, A., Goldstein, G. R., Goldstein, J. A. and Romanelli, S. (2006) "The heat equation with nonlinear general Wentzell boundary condition", *Adv. Diff. Eqs.* **Vol. 11**, No. 5, pp. 481-510.

[12] Fife, P. C. (1979) *Mathematical aspects of reacting and diffusing systems.* Berlin, Springer-Verlag.

[13] Friedrichs, K. O. (1939) "On differential operators in Hilbert spaces", *American Journal of Mathematics* **Vol. 61**, No. 2, pp. 523-544.

[14] Gal, G. C. (2005) "Strum-Liouville operator with general boundary conditions", *Electronic J. Diff. Eqs.* **Vol. 2005**, No. 120, pp. 1-17. [http://ejde.math.txstate.edu/]

[15] Genrich, J. F. and Pope, G. A. (1988) "A simplified performance-predictive model for in-situ combustion processes", *SPE Reservoir Engineering*, pp. 410-418.

[16] Godunov, S. K. (1997) *Ordinary differential equations with constant coefficient.* Translations of Mathematical Monographs, **Vol. 169**. Rhode Island, AMS.

[17] Goldstein, G. R. (2006) "Derivation and physical interpretation of general boundary conditions", *Adv. Diff. Eqs.* **Vol. 11**, No. 4, pp. 457-480.

[18] Gottlieb, D. and Orszag S. A. (1977) *Numerical analysis of spectral methods: Theory and applications.* CBMS-NSF, **Vol. 26**. Philadelphia, SIAM.

[19] Hale, J. K. (1969) *Ordinary differential equations.* New York, Wiley-Interscience.

[20] John, F. (1981) *Partial differential equations, 4^{th} Ed.* New York, Springer-Verlag.

[21] Kato, T. (1980) *Perturbation theory for linear operators.* Berlin, Springer.

[22] Kharrat, R. and Vossoughi, S. (1985) "Feasibility study of the in-situ combustion process using TGA/DSC techniques", *Journal of Petroleum Techniques*, pp. 1441-1445.

[23] Kramers, H. A. (1940) "Brownian motion in a field of force and diffusion model of chemical reactions", *Physica* **7**, pp. 284-304.

[24] Lax, P. D. (2002) *Functional analysis.* New York, Wiley.

[25] Lebedev, N. N. (1972) *Special functions and their applications.* New York, Dover.

[26] Matkowsky, B. J., Schuss, K. and Ben-Jacob, E. (1982) "A singular perturbation approach to Kramers' diffusion problem", *SIAM J. Appl. Math.* **Vol. 42**, No. 4, pp. 833-849.

[27] Miller, R. K. (1971) *Nonlinear Volterra integral equations.* Menlo Park, California, W. A. Benjamin.

[28] Park, J. H., Bayliss, A., Matkowsky, B. J. and Nepomnyashchy, A. A. (2006) "On the route to extinction in nonadiabatic solid flames", *SIAM J. Appl. Math.* **Vol. 66**, No. 3, pp. 873-895.

[29] Reed, M. and Simon, B. (1975) *Methods of modern mathematical physics.* New York, Academic Press.

[30] Rybak, W. (1988) "Intrinsic reactivity of petroleum coke under ignition conditions", *Fuel* **Vol. 67**, pp. 1696-1702.

[31] Sagan, H. (1961) *Boundary and eigenvalue problems in mathematical physics.* New York, Wiley.

[32] SMOLLER, J. (1994) *Shock waves and reaction-diffusion equations.* New York, Springer-Verlag.

[33] SOTOMAYOR, J. (1979) *Lições de equações diferenciais ordinárias.* Projeto Euclides, IMPA, Brasil.

[34] STRIKWERDA, J. C. (1989) *Finite difference schemes and partial differential equations.* Wadsworth & Brooks, California.

[35] TADEMA, H. J. AND WEIJDEMA, J. (1970) "Spontaneous ignition of oil sands", *Oil Gas J.* **Vol. 68**, No. 50, pp. 77-80.

[36] TOLSTOV, G. P. (1962) *Fourier series.* New York, Dover.

[37] TYLER, R. J. (1985) "Intrinsic reactivity of petroleum coke to oxygen", *Fuel* **Vol. 65**, pp. 235-240.

[38] VITILLARO, E. (2005) "Global existence for the heat equation with nonlinear dynamical boundary conditions", *Proc. Roy. Soc. Edinburgh* **Vol. 135A**, pp. 175-207.

[39] WATSON, G. N. (1958) *A treatise on the theory of Bessel functions.* University Press.

[40] WEAST, R. C. (ed.) (1978) *Handbook of chemistry and physics, 58th Ed.* CRC Press.